

Review of lattice results concerning low energy particle physics

FLAG working group* of FLAVIANET

July 26, 2013

* G. Colangelo^a, S. Dürr^{b,c}, A. Jüttner^d, L. Lellouch^e, H. Leutwyler^a, V. Lubicz^f,
S. Necco^d, C. T. Sachrajda^g, S. Simula^h, A. Vladikasⁱ, U. Wenger^a, H. Wittig^j

^a Albert Einstein Center for Fundamental Physics, Institut für Theoretische Physik,
Universität Bern, Sidlerstr. 5, CH-3012 Bern, Switzerland

^b Bergische Universität Wuppertal, Gausstr. 20, D-42119 Wuppertal, Germany

^c Jülich Supercomputing Centre, Forschungszentrum Jülich, D-52425 Jülich, Germany

^d CERN, Physics Department, TH Unit, CH-1211 Geneva 23, Switzerland

^e Centre de Physique Théorique¹, Case 907, Campus de Luminy, F-13288 Marseille, France

^f Dipartimento di Fisica, Università Roma Tre, and INFN, Via della Vasca Navale 84, I-00146 Roma, Italy

^g School of Physics and Astronomy, University of Southampton, Southampton SO17 1BJ, UK

^h INFN, Sezione di Roma Tre, Via della Vasca Navale 84, I-00146 Roma, Italy

ⁱ INFN, Sezione di Tor Vergata, c/o Dipartimento di Fisica, Università di Roma Tor Vergata,
Via della Ricerca Scientifica 1, I-00133 Rome, Italy

^j Institut für Kernphysik and Helmholtz Institute Mainz, University of Mainz,
Becher Weg 45, 55099 Mainz, Germany

Abstract

We review lattice results relevant for pion and kaon physics with the aim of making them easily accessible to the particle physics community. Specifically, we review the determination of the light-quark masses, the form factor $f_+(0)$, relevant for the semileptonic $K \rightarrow \pi$ transition at zero momentum transfer as well as the ratio f_K/f_π of decay constants and discuss the consequences for the elements V_{us} and V_{ud} of the CKM matrix. Furthermore, we describe the results obtained on the lattice for some of the low-energy constants of $SU(2)_L \times SU(2)_R$ and $SU(3)_L \times SU(3)_R$ Chiral Perturbation Theory and review the determination of the B_K parameter of neutral kaon mixing. We introduce quality criteria and use these when forming averages. Although subjective and imperfect, these criteria may help the reader to judge different aspects of current lattice computations. Our main results are summarized in section 1.2, but we stress the importance of the detailed discussion that underlies these results and constitutes the bulk of the present review.

¹CPT is research unit UMR 6207 of the CNRS and of the universities Aix-Marseille I, Aix-Marseille II and Sud Toulon-Var, and is affiliated with the FRUMAM.

Contents

1	Introduction	4
1.1	Scope of the present review	4
1.2	Summary of the main results	7
1.3	Plan of the paper	9
2	Quality criteria	9
2.1	Colour code	9
2.2	Averages and estimates	12
3	Quark masses	14
3.1	Contributions from the electromagnetic interaction	15
3.2	Pion and kaon masses in the isospin limit	18
3.3	Lattice determination of m_s and m_{ud}	19
3.3.1	$N_f = 2$ lattice calculations	19
3.3.2	$N_f = 2 + 1$ lattice calculations	21
3.4	Lattice determination of m_u and m_d	28
3.5	Estimates for R and Q	30
4	V_{ud} and V_{us}	33
4.1	Experimental information concerning $ V_{ud} $, $ V_{us} $, $f_+(0)$ and f_K/f_π	33
4.2	Lattice results for $f_+(0)$ and f_K/f_π	34
4.3	Direct determination of $f_+(0)$ and f_K/f_π	36
4.4	Testing the Standard Model	39
4.5	Analysis within the Standard Model	41
5	Low-energy constants	42
5.1	SU(2) Low-Energy Constants	44
5.1.1	Quark-mass dependence of pseudoscalar masses and decay constants	44
5.1.2	Two-point correlation functions in the ϵ -regime	45
5.1.3	Energy levels of the QCD Hamiltonian in a box, δ -regime	47
5.1.4	Other methods for the extraction of the Low-Energy Constants	47
5.1.5	Pion form factors	48
5.1.6	Results	49
5.2	SU(3) Low-Energy Constants	59
5.2.1	Quark-mass dependence of pseudoscalar masses and decay constants	59
5.2.2	Charge radius	59
5.2.3	Partially quenched formulae	59
5.2.4	Recent lattice determinations	60
6	Kaon B-parameter B_K	64
6.1	Indirect CP-violation and ϵ_K	64
6.2	Lattice computation of B_K	66

A	Glossary	71
A.1	Lattice actions	71
A.1.1	Gauge actions	71
A.1.2	Quark actions	73
A.2	Setting the scale	75
A.3	Matching and running	77
A.4	Chiral extrapolation	78
A.5	Summary of simulated lattice actions	79
B	Notes	82
B.1	Notes to section 3 on quark masses	82
B.2	Notes to section 4 on $ V_{ud} $ and $ V_{us} $	90
B.3	Notes to section 5 on Low-Energy Constants	95
B.4	Notes to section 6 on Kaon B -parameter B_K	102

1 Introduction

Flavour physics provides an important opportunity for exploring the limits of the Standard Model of particle physics and in constraining possible extensions of theories “Beyond the Standard Model”. As the LHC explores a new energy frontier, the importance of flavour physics will grow still further, in searches for signatures of new physics through precision measurements and/or in helping to unravel the theoretical framework behind direct discoveries of new particles. The major theoretical limitation arises from the precision with which strong interaction effects can be quantified and large-scale numerical simulations of lattice QCD provide the opportunity of computing these effects from first principles. In this paper we review the current status of lattice results for a variety of physical quantities in low-energy physics; our aim is to provide the answer to the frequently posed question “What is currently the best lattice value for a particular quantity?” in a way which is readily accessible to non-lattice-experts. This is generally not an easy question to answer; different collaborations use different lattice actions (discretizations of QCD) with a variety of lattice spacings and volumes, and with a range of masses for the u and d quarks. Not only are the systematic errors therefore different, but also the methodology used to estimate these uncertainties vary between collaborations. Below we summarize the main features of each of the calculations and provide a framework for judging and combining the different results. Sometimes it is a single result which provides the “best” value; more often it is a combination of results from different collaborations. Indeed, the consistency of values obtained using different formulations adds significantly to our confidence in the results.

1.1 Scope of the present review

The Flavianet Lattice Averaging Group (FLAG) was constituted in November 2007, at a general meeting of the European Network on Flavour Physics (Flavianet), with the remit of providing the current lattice results to the network’s working groups and to the wider community. In this paper we focus on physically important quantities in kaon and pion physics, specifically the masses of the light quarks, the CKM matrix element V_{us} determined from leptonic and semileptonic kaon decays, the B_K parameter of $K^0 - \bar{K}^0$ mixing and the low-energy constants of the $SU(2)_L \times SU(2)_R$ and $SU(3)_L \times SU(3)_R$ chiral Lagrangians. In the future, we plan to extend the range of topics covered and to update the material regularly. Below, we review papers which appeared before the closing date of the present edition, 28 February 2011. The averages are based on the results quoted in the tables, which exclusively list articles that appeared before this date. Most of the data concern simulations for which the masses of the two lightest quarks are set equal. This is indicated by the notation: $N_f = 2 + 1 + 1$, for instance, denotes a lattice calculation with four dynamical quark flavours and $m_u = m_d \neq m_s \neq m_c$. Our review is also available on the FLAG webpage [1], which will be updated as new lattice results appear. A compilation of some of the results discussed below can also be found on the web page of Laiho, Lunghi and Van de Water [2, 3]. These authors restrict themselves to simulations with $N_f = 2 + 1$ dynamical flavours, but in addition cover lattice results for bound states containing charmed or beauty quarks, which are beyond the scope of the present review. Our analysis does include simulations with $N_f = 2$. The significance of these data for the physics conclusions to be drawn from the work done on the lattice is discussed in section 2.2.

It is by now generally accepted that, taken together, QCD and QED provide a very

accurate approximation for the laws governing the low energy properties of nature – other degrees of freedom, such as those of the W and Z bosons, appear to be frozen at low energies. Moreover, since QED is infrared stable, the electromagnetic interaction can be dealt with perturbatively at low energy, but for QCD, this is not the case. The present review deals with the information obtained about the low energy structure of that theory by simulating it on a lattice.

Lattice QCD is a mature field today as a result of a 30-year history of theoretical and computational developments, many of which were tested on quenched simulations. Indeed the remarkable recent progress in the precision of lattice calculations is due to improved algorithms, better computing resources and, last but not least, conceptual developments, such as improved actions that reduce lattice artifacts, regularizations which preserve (remnants of) chiral symmetry, understanding the finite size effects, non-perturbative renormalization, etc. For recent discussions of these developments, we refer to [4, 5]. A concise characterization of the various discretizations that underlie the results reported in the present review is given in appendix A.1.2 (cf. [6] for a more extended overview). The recent developments in the domain of computer algorithms were triggered by [7–10]. For an outline of the progress in computer architecture, we refer to [11], which also contains an overview of recent developments in simulation-algorithms.

Each discretization has its merits, but also its shortcomings. One of the main points emerging from this review is that the large variety of discretizations employed by the various collaborations lead to consistent results, confirming universality within the accuracy reached. In our opinion, only the eventual convergence of the various lattice results, obtained with different discretizations and methods, can lead to a reliable determination, for which all systematic errors can be claimed to be fully under control.

The lattice spacings reached in recent simulations go down to 0.05 fm or even smaller. In that region, growing autocorrelation times may slow down the sampling of the configurations [12–16]. Many groups check for autocorrelations in a number of observables, including the topological charge, for which a rapid growth of the autocorrelation time is observed if the lattice spacing becomes small. In the following, we assume that the continuum limit can be reached by extrapolating the existing simulations.

Lattice simulations of QCD currently involve at most four dynamical quark flavours. To connect these with the QCD sector of the Standard Model, which is characterized by $N_f = 6$, one considers a sequence of effective theories, obtained from full QCD by sending one of the quark masses after the other to infinity: QCD_5 , QCD_4 , ... The series terminates with gluodynamics, QCD_0 . The physical value of the coupling constant is conventionally specified in terms of the value in QCD_5 , in the $\overline{\text{MS}}$ scheme at scale $\mu = M_Z$. We characterize the masses of the light quarks by their running $\overline{\text{MS}}$ values in QCD_4 at scale $\mu = 2 \text{ GeV}$.²

In this language, lattice calculations with $N_f = 3$ concern QCD_3 . This theory deviates from full QCD by Zweig-suppressed corrections of $O(1/m_c^2)$. Note that calculations with $N_f = 2$ dynamical flavours often include strange valence quarks interacting with gluons, so that bound states with the quantum numbers of the kaons can be studied – what these simulations share with QCD_2 is that strange sea quark fluctuations are neglected. Likewise, calculations done in the quenched approximation, in which sea quark effects are treated as a

²Note that this convention is not universally adopted – the scale at which QCD_3 is matched to QCD_4 is not always taken below 2 GeV. The difference between the numerical values in QCD_3 and QCD_4 is small, but with the increase of precision on the lattice, it does become necessary to specify which one of these effective theories the quoted running masses refer to (see section 3).

mean field, can be made to involve light valence quarks and mesons as well as baryons, while in QCD₀, the spectrum exclusively contains glueballs.

For $N_f \leq 3$, the connection between the observables and the running coupling constant and quark masses of the effective theory is now understood at the non-perturbative level. In the case of QCD₃, for instance, which is obtained from the QCD sector of the Standard Model by sending m_t, m_b and m_c to infinity, the running quark masses $m_u(\mu)$, $m_d(\mu)$, $m_s(\mu)$ and the running coupling constant $g(\mu)$ can unambiguously be related to the masses M_{π^+} , M_{K^+} , M_{K^0} and the mass of one of the baryons that occur in the spectrum, so that the simulation yields parameter free results for all of the observables of the effective theory in terms of these masses. The lattice results obtained so far, which concern the isospin limit of QCD₃, agree with experiment, within the accuracy of the calculation. The results reported for the masses of the long-lived baryons in BMW 08 [17], for instance, have a precision of better than 4%. In particular, if the scale is fixed with M_{Ξ} , the mass of the Ω can be calculated to an accuracy of 1.5%. The fact that the result agrees with experiment indicates that the residual effects generated by the neglected heavy degrees of freedom are small.

We concentrate on pion and kaon observables and assume that, at the precision indicated, simulations which do not account for the heavy degrees of freedom represent a sufficiently accurate approximation to full QCD. In particular, for f_K/f_π and $f_+(0)$, where flavour symmetry suppresses the dynamics, we expect the effects generated by the presence of heavy sea quarks to be too small to be seen, despite the fact that the level of accuracy reached is impressive indeed. We emphasize that the estimates quoted below and labeled $N_f = 2$ or $N_f = 2 + 1$ concern the values of the relevant quantities in full QCD – the label merely indicates the method by means of which these estimates are obtained.

At low energies, the fact that QCD has an approximate, spontaneously broken *chiral symmetry* plays a crucial role. In the limit where the masses of the three lightest quarks are set to zero, this symmetry becomes exact, so that the spectrum contains a massless octet of Nambu-Goldstone bosons. There are lattice formulations of the theory that preserve this symmetry and we refer to appendix A.1.2 for an overview. We rely on the understanding of the dependence on the lattice spacing reached with Symanzik’s effective theory [18, 19]. This framework can be combined with Chiral Perturbation Theory (χ PT), to cope with the Nambu-Goldstone nature of the lowest excitations that occur in the presence of light quarks [20–40]. The form of the effective theory depends on the discretization used – see appendix A.4 for a brief characterization of the different variants in use.

As the calculations become more precise, it is important to emphasize the need for continued close collaboration between the lattice and χ PT communities. Lattice computations are generally performed at u and d quark masses which are heavier than the physical ones and the results are then extrapolated to the physical point. Although these masses are decreasing very significantly with time (see, in particular, the most recent calculations by BMW [41] and PACS-CS [42]), it remains true that this extrapolation is one of the most significant sources of systematic error. Indeed several lattice collaborations have found that the expansion of M_π^2 , M_K^2 , f_π , f_K to first non-leading order in the quark masses m_u, m_d, m_s [SU(3) χ PT to NLO] does not yield an adequate parametrization of the data, and so cannot reliably be used for guiding the chiral extrapolation. In part, the problem may be due to the fact that in the simulations, the mean mass of u and d is usually significantly heavier than in nature, while m_s is taken in the vicinity of the physical mass of the strange quark, so that the kaon mass is then too heavy for χ PT to be of use, but it may also indicate that contributions of NNLO need to be accounted for to have sufficient accuracy (an analytic approximation for the latter

that goes beyond the double-log approximation [43] is proposed in [44, 45]). One method to circumvent the impasse is to (a) work at a smaller value of m_s , so that the data taken concern the region where the kaon mass does not exceed its physical value [46, 47] and (b) use NNLO χ PT for the extrapolation to the quark masses of physical interest. Alternatively, one may try to apply brute force, lower the mean mass of u and d to the physical value and avoid using an extrapolation altogether [41, 42]. Which one of these approaches yields better results yet remains to be seen, but all of them can teach us something about the low-energy regime of QCD and can contribute to a better determination of the low-energy constants of χ PT.

1.2 Summary of the main results

We end this introduction with a summary of our main results, but we stress that they should be considered together with the many comments and observations which accompany their determination. The lattice results for the running masses of the three lightest quarks are discussed in detail in section 3. Using the $\overline{\text{MS}}$ scheme and fixing the running scale at 2 GeV, the lattice data with $N_f = 2 + 1$ dynamical flavours lead to

$$m_{ud} = 3.43 \pm 0.11 \text{ MeV}, \quad m_s = 94 \pm 3 \text{ MeV}, \quad \frac{m_s}{m_{ud}} = 27.4 \pm 0.4, \quad (1)$$

with $m_{ud} \equiv \frac{1}{2}(m_u + m_d)$. We emphasize that these results represent a very significant improvement of our knowledge: as compared to the estimates for the light quark masses given by the Particle Data Group [48], the uncertainties in the above estimates for m_s , m_{ud} and m_s/m_{ud} are reduced by about an order of magnitude, in all three cases! Note also that the estimates (1) agree with the only $N_f = 2$ determination that satisfies our quality criteria [49]:

$$m_{ud} = 3.6 \pm 0.2 \text{ MeV}, \quad m_s = 95 \pm 6 \text{ MeV}, \quad \frac{m_s}{m_{ud}} = 27.4 \pm 0.4. \quad (2)$$

The lattice simulations are performed with $m_u = m_d$, so some additional input is required to obtain m_u and m_d separately (see the discussion in section 3.4). We quote

$$m_u = 2.19 \pm 0.15 \text{ MeV}, \quad m_d = 4.67 \pm 0.20 \text{ MeV}, \quad \frac{m_u}{m_d} = 0.47 \pm 0.04. \quad (3)$$

In the determination of the CKM matrix elements V_{us} and V_{ud} , the term $f_+(0)$ (form factor relevant for the semileptonic transition $K^0 \rightarrow \pi^-$, evaluated at zero momentum transfer) and the ratio f_K/f_π of the kaon and pion decay constants play a central role. Both of these quantities can now be determined rather precisely on the lattice. Adding statistical and systematic errors in quadrature, the results for $f_+(0)$ read

$$\begin{aligned} f_+(0) &= 0.959 \pm 0.005, & (\text{direct}, N_f = 2 + 1), \\ f_+(0) &= 0.956 \pm 0.008, & (\text{direct}, N_f = 2). \end{aligned} \quad (4)$$

On the basis of the detailed discussion in section 4.3, we conclude that the value

$$f_+(0) = 0.956 \pm 0.008 \quad (\text{direct}) \quad (5)$$

represents a conservative estimate for the range permitted by the presently available direct determinations of $f_+(0)$ in lattice QCD.

For f_K/f_π , the results are

$$\begin{aligned} f_K/f_\pi &= 1.193 \pm 0.005, & (\text{direct}, N_f = 2 + 1), \\ f_K/f_\pi &= 1.210 \pm 0.018, & (\text{direct}, N_f = 2), \end{aligned} \quad (6)$$

where the first number is the average of three calculations whereas the second stems from a single one. We refer to these results, which do not rely on the Standard Model, as *direct* determinations.

Two precise experimental results constrain the determination of V_{us} and V_{ud} : the observed rate for the semileptonic $K^0 \rightarrow \pi^-$ decay determines the product $|V_{us}|f_+(0)$, while the ratios of the kaon's and pion's leptonic widths determine the ratio $|V_{us}|f_K/|V_{ud}|f_\pi$. In section 4.4, these results are combined with the lattice determinations of f_K/f_π and $f_+(0)$ to test the unitarity of the CKM matrix. We find that the first row obeys this property within errors: $|V_{ud}|^2 + |V_{us}|^2 + |V_{ub}|^2 = 1.002 \pm 0.015$ and 1.036 ± 0.037 for $N_f = 2 + 1$ and $N_f = 2$, respectively.³ In obtaining these results, we have not made use of the recent determinations of $|V_{ud}|$ from super-allowed nuclear β -decays [50], but these are perfectly consistent with the outcome of the lattice calculations. In fact, the unitarity test sharpens considerably if the results obtained on the lattice are combined with those found in β -decay: the interval allowed for the sum $|V_{ud}|^2 + |V_{us}|^2 + |V_{ub}|^2$ then shrinks by more than an order of magnitude. Since this interval includes unity, CKM unitarity passes the test.

Within the Standard Model of particle physics, the CKM matrix is unitary. As explained in section 4.5, this condition and the experimental results for $|V_{us}|f_+(0)$, $|V_{us}|f_K/|V_{ud}|f_\pi$ imply three equations for the four quantities $|V_{ud}|$, $|V_{us}|$, f_K/f_π , $f_+(0)$. Thus it is sufficient to add one additional constraint, such as the lattice result for f_K/f_π or $f_+(0)$, to determine all four of these quantities. Averaging over the numbers obtained for f_K/f_π and $f_+(0)$ with $N_f = 2 + 1$ dynamical quark flavours, we find

$$\begin{aligned} |V_{ud}| &= 0.97427 \pm 0.00021, & |V_{us}| &= 0.2254 \pm 0.0009, \\ f_+(0) &= 0.9597 \pm 0.0038, & \frac{f_K}{f_\pi} &= 1.1925 \pm 0.0050. \end{aligned} \quad (7)$$

The results obtained from the data with $N_f = 2$ are the same within errors:

$$\begin{aligned} |V_{ud}| &= 0.97433 \pm 0.0042, & |V_{us}| &= 0.2251 \pm 0.0018, \\ f_+(0) &= 0.9604 \pm 0.0075, & \frac{f_K}{f_\pi} &= 1.194 \pm 0.010. \end{aligned} \quad (8)$$

Since the lattice results are consistent with CKM unitarity, it was to be expected that the above values for $f_+(0)$ and f_K/f_π are consistent with those derived from the direct determinations, listed in equation (6). The main effect of the unitarity constraint is a reduction of the uncertainties.

As far as the low-energy constants are concerned, there are many results coming from lattice calculations which are of interest. A coherent picture does not emerge yet for all cases, but for two quantities related to the SU(2) chiral expansion, the lattice provides results which are competitive with what has been obtained from phenomenology. These are

$$\bar{\ell}_3 = 3.2 \pm 0.8 \quad \text{and} \quad \frac{F_\pi}{F} = 1.073 \pm 0.015 \quad (9)$$

³The experimental information on $|V_{ub}|$ shows that the contribution from this term is negligibly small.

which are estimates based on $N_f = 2$, $N_f = 2+1$ and even $N_f = 2+1+1$ calculations. We refer the interested reader to Section 5 for further results and all details about the calculations.

For the B_K parameter of K - \bar{K} mixing we quote (B_K refers to the $\overline{\text{MS}}$ -scheme at scale 2 GeV, while \hat{B}_K denotes the corresponding renormalization group invariant parameter):

$$\begin{aligned} B_K &= 0.536 \pm 0.017, & \hat{B}_K &= 0.738 \pm 0.020 & (N_f = 2 + 1), \\ B_K &= 0.516 \pm 0.022, & \hat{B}_K &= 0.729 \pm 0.030 & (N_f = 2). \end{aligned} \quad (10)$$

1.3 Plan of the paper

The plan for the remainder of this paper is as follows. In the next section we suggest criteria by which the quality of lattice calculations can be judged and compared. We recognize of course that these are necessarily subjective and generally give an incomplete picture of the quality of a given simulation. Nevertheless we feel that some framework of quality standards is necessary. There then follow five sections with physics results: quark masses (section 3), V_{us} as determined from leptonic and semileptonic Kaon decays (section 4), the low energy constants of $\text{SU}(2)_L \times \text{SU}(2)_R$ and $\text{SU}(3)_L \times \text{SU}(3)_R$ chiral perturbation theory (sections 5.1 and 5.2 respectively) and the B_K parameter which contains the non-perturbative strong interaction effects in K^0 - \bar{K}^0 mixing (section 6).

The final point we wish to raise in this introduction is a particularly delicate one. As stated above, our aim is to make lattice QCD results easily accessible to non-lattice-experts and we are well aware that it is likely that some readers will only consult the present paper and not the original lattice literature. We consider it very important that this paper is not the only one which gets cited when the lattice results which are discussed and analyzed here are quoted. Readers who find the review and compilations offered in this paper to be useful are therefore kindly requested also to cite the original sources – the bibliography at the end of this paper should make this task easier. Indeed we hope that the bibliography will be one of the most widely used elements of the whole paper.

2 Quality criteria

In this article we present a collection of results and references concerning lattice results of physical quantities in low energy particle physics. In addition however, we aim to help the reader in assessing the reliability of particular lattice results without necessarily studying the original article in depth. We understand that this is a delicate issue and are well aware of the risk of making things “simpler than they are”. On the other hand, it is rather common nowadays that theorists and experimentalists use the results of lattice calculations in order to draw the physics conclusions coming from a new measurement or a new analysis of a set of measurements, without a critical assessment of the quality of the various calculations. This may lead to a substantial underestimate of systematic errors or in the worst case to a distorted physics conclusion. We believe that despite the risks mentioned, it is important to provide some compact information about the quality of a calculation.

2.1 Colour code

In the past, at lattice conferences, some speakers have used a “colour code” to provide such information, for example when showing plots [51]. We find that this way of summarizing the

quality of a lattice calculation serves well its purpose and adopt it in what follows. We identify a number of sources of systematic errors for which a systematic improvement is possible and assign to each calculation a colour with respect to each of these:

- ★ when the systematic error has been estimated in a satisfactory manner and convincingly shown to be under control;
- when a reasonable attempt at estimating the systematic error has been made, although this could be improved;
- when no or a clearly unsatisfactory attempt at estimating the systematic error has been made.

The precise criteria used in determining the colour coding is unavoidably time-dependent because as lattice calculations become more accurate the standards against which they are measured become tighter. Today, our definition of the colour code related to the systematic error coming from *i*) the chiral extrapolation, *ii*) the continuum extrapolation, *iii*) the finite-volume effects, and (where applicable) *iv*) the renormalization and *v*) the running of operators and their matrix elements are as follows:

- Chiral extrapolation:

- ★ $M_{\pi,\min} < 250$ MeV
- $250 \text{ MeV} \leq M_{\pi,\min} \leq 400$ MeV
- $M_{\pi,\min} > 400$ MeV

It is assumed that the chiral extrapolation is done with at least a three-point analysis – otherwise this will be explicitly mentioned in a footnote. In case of nondegeneracies among the different pion states $M_{\pi,\min}$ stands for a root-mean-squared (RMS) pion mass.

- Continuum extrapolation:

- ★ 3 or more lattice spacings, at least 2 points below 0.1 fm
- 2 or more lattice spacings, at least 1 point below 0.1 fm
- otherwise

It is assumed that the action is $O(a)$ -improved, i.e. the discretization errors vanish quadratically with the lattice spacing – otherwise this will be explicitly mentioned in a footnote. Moreover the colour coding criteria for non-improved actions change as follows: one lattice spacing more needed.

- Finite-volume effects:

- ★ $M_{\pi,\min}L > 4$ or at least 3 volumes
- $M_{\pi,\min}L > 3$ and at least 2 volumes
- otherwise

These criteria apply to calculations in the p -regime, and it is assumed that $L_{\min} \geq 2$ fm, otherwise this will be explicitly mentioned in a footnote and a red square will be assigned. In case of nondegeneracies among the different pion states $M_{\pi,\min}$ stands for a root-mean-squared (RMS) pion mass.

- Renormalization (where applicable):

- ★ non-perturbative
- 2-loop perturbation theory
- otherwise

- Running (where applicable):

For scale-dependent quantities, such as quark masses or B_K , it is essential that contact with continuum perturbation theory can be established. Various different methods are used for this purpose (cf. Appendix A.3): Regularization-independent Momentum Subtraction (RI/MOM), Schrödinger functional, direct comparison with (resummed) perturbation theory. In the case of the quark masses, a further approach has been proposed recently: determination of m_s via the ratio m_c/m_s . Quite irrespective of the particular method used, the uncertainty associated with the choice of intermediate renormalization scales in the construction of physical observables must be brought under control. This is best achieved by performing comparisons between non-perturbative and perturbative running over a reasonably large range of scales. These comparisons were initially only made in the Schrödinger functional (SF) approach, but are now also being performed in RI/MOM schemes.

In the framework of the Schrödinger functional, the comparison of the lattice results for the relevant renormalization factors with perturbation theory has thoroughly been explored. Among the calculations relying on the RI/MOM framework, the most recent ones are aiming for a level of control over running and matching which is of comparable quality. However, since these approaches are new, we postpone the formulation of quantitative criteria until the systematics associated with their use is better understood. We mark those data for which information about non-perturbative running checks is available and give some details, but do not attempt to translate this into a colour-code.

The mass of the pion plays an important role in our colour coding, but there are fermion action discretizations in which pion states are non-degenerate. This is the case in particular for the twisted-mass formulation of lattice QCD. In that discretization, isospin symmetry and parity are traded for a chiral symmetry which simplifies the renormalization of the theory [52] and, at “maximal twist”, eliminates leading $O(a)$ discretization errors from all observables [53]. As a consequence of the loss of isospin symmetry, the charged and neutral pions have different masses, even when the u and d quarks are mass degenerate. This mass difference is an $O(a^2)$ discretization effect, whose actual size depends on the specific choice of the lattice regularization (in both the gauge and fermionic part of the action). In the $N_f = 2$ simulation of [54] it is found $1 - M_{\pi^0}/M_{\pi^+} \sim 0.2$ for $a \sim 0.09$ fm. Since the charged pion mass turns out also to be larger than the mass of the neutral pion, when applying the criterion adopted for assessing the quality of the chiral extrapolation to twisted mass fermion simulations we will conservatively choose as $M_{\pi,\min}$ the mass of the charged pion.

In staggered fermion calculations,⁴ the Nambu-Goldstone pion has “taste” partners whose masses are those of the Nambu-Goldstone boson plus a discretization error of order a^2 , which can be significant at larger lattice spacings. For instance, in MILC’s simulations, at $a = 0.15$ fm and for a Nambu-Goldstone mass of 241 MeV, the largest taste partner (i.e. the taste singlet) mass is 673 MeV and the RMS taste-partner mass is 542 MeV [59]. The situation improves significantly as the lattice spacing is reduced: the singlet and RMS masses become 341 MeV and 334 MeV at $a = 0.045$ fm for a Nambu-Goldstone of mass 324 MeV. While it is possible to pick out the Nambu-Goldstone pion in the valence sector, the contributions of the sea correspond to some complicated admixture of the 16 taste partners. MILC reduces to one the contribution of the four quark tastes associated with a single quark flavor by taking

⁴We refer the interested reader to a number of good reviews written about the subject [6, 55–58].

the fourth root of the quark determinant, and hence the name rooted staggered fermions. In any event, the effective pion mass in the sea can be significantly larger than that of the valence Nambu-Goldstone and, in comparing staggered fermion calculations with those performed using other discretizations, it makes sense to quote as an $M_{\pi,\min}$ a value which is characteristic of the sea pion mass contributions. For most quantities, the RMS taste-partner pion mass is a reasonable choice.

Of course any colour coding has to be treated with caution. First of all we repeat that the criteria are subjective and evolving. Sometimes a single source of systematic error dominates the systematic uncertainty and it is more important to reduce this uncertainty than to aim for green stars for other sources of error. In spite of these caveats we hope that our attempt to introduce quality measures for lattice results will prove to be a useful guide. In addition we would like to underline that the agreement of lattice results obtained using different actions and procedures evident in many of the tables presented below provides further reassurance.

Finally it is important to stress that the colour coding does not imply any credit for the development of theoretical or technical ideas used in the simulations. Frequently new ideas and techniques are first tested on smaller lattices, perhaps on quenched configurations or at heavier quark masses, to demonstrate their feasibility. They may then be applied on more modern lattices by other collaborations to obtain physical results, but since our primary aim is to review the latest results concerning quantities of physical interest, we do not try to attribute credit to the underlying ideas or techniques.

For a coherent assessment of the present situation, the quality of the data plays a key role, but the colour code cannot be made visible in the figures. Simply showing all data on equal footing would give the misleading impression that the overall consistency of the information available on the lattice is questionable. As a way out, the figures do indicate the quality in a rudimentary way: data for which the colour code is free of red tags are shown as green symbols, otherwise they are depicted in red. Note that the pictures do not distinguish updates from earlier data obtained by the same collaboration – the reader needs to compare the legends to identify closely correlated data.

2.2 Averages and estimates

For some observables there may be enough independent lattice calculations of good quality that it makes sense to average them and propose such an *average* as the best current lattice number. In order to decide if this situation is realized for a certain observable we rely on the colour coding. Unless special reasons are given for making an exception, we restrict the averages to data for which the colour code does not contain any red tags. In some cases, the averaging procedure nevertheless leads to a result which in our opinion does not cover all uncertainties – this happens, in particular, if some of the data have comparatively small systematic errors. In such cases, we may provide our *estimate* as the best current lattice number. This estimate is not obtained with a prescribed mathematical procedure, but is based on our own assessment of the information collected on the lattice.

There are two other important criteria which also play a role in this respect, but which cannot be represented with the colour coding, because a systematic improvement is not possible. These are: *i)* the publication status, and *ii)* the number of flavours. As far as the former is concerned we adopt the following policy: we consider in our averages only calculations which have been published, *i.e.* which have been endorsed by a referee. The only exception to this rule is an obvious update of numbers appearing in a previous publication. Other cases

will be listed and identified as such also by a (coloured) symbol, but not used in averages:

- Publication status:
 - A published or plain update of published results
 - P preprint
 - C conference contribution

Several active lattice collaborations do their calculations with only two dynamical flavours ($N_f = 2$). We are not aware of visible differences between results obtained in this framework and QCD with $N_f = 3$. At the present level of accuracy, it is thus perfectly meaningful to compare results obtained for $N_f = 2$ with experiment. On the other hand, the two theories are intrinsically different; the manner in which quantities like the coupling constant or the quark masses depend on the running scale depends on N_f .

Since we are not aware of an *a priori* way to quantitatively estimate the difference between $N_f = 3$ and $N_f = 2$ calculations we will present separate averages (where applicable) for the two sets of calculations. Averages of $N_f = 3$ and $N_f = 2$ calculations will not be provided. A first lattice calculation with $N_f = 4$ dynamical flavours has recently appeared [60]. While in principle it would be cleaner to keep $N_f = 4$ separate from the rest, we believe that, for the quantities under discussion in this review, the effects of the c -quark are below the precision of current lattice calculations: if appropriate, we will average $N_f = 4$ and $N_f = 3$ results.

We stress that $N_f = 2$ calculations have in several cases a better control over systematic effects than $N_f = 3$ calculations, as will be clear in colour coding tables below, and therefore play a very important role today in the comparison with experiment. Several calculations discussed below provide examples of the relevance of $N_f = 2$ calculations today, and in particular they enter in some of our estimates. In the future, as the accuracy and the control over systematic effects in lattice calculations will increase, it will hopefully be possible to see a difference between $N_f = 2$ and $N_f = 3$ calculations and so determine the size of the Zweig-rule violations related to strange quark loops. This is a very interesting issue *per se*, and one which can be quantitatively addressed only with lattice calculations.

One of the problems that arises when forming averages is that not all of the data sets are independent – in fact, some rely on the same ensembles. For this reason, we do not average updates with earlier results. Note that, in this respect, the figures give a somewhat distorted picture: they include all of the data listed in the tables and, moreover, indicate their quality only in a very rudimentary way. Specific problems encountered in connection with correlations between different data sets are mentioned in the text. In our opinion, the variety of algorithms and configurations used and the fact that we attach conservative errors to our estimates ensure that these correlations do not distort our results in a significant manner.

We take the mean values from the standard procedure, where χ^2 is evaluated by adding the statistical and systematic errors in quadrature (data sets for which the error estimate only accounts for the statistical uncertainties are not taken into consideration). The standard procedure also offers an estimate for the net uncertainty δ to be attached to the mean: if the fit is of good quality ($\chi_{min}^2/\text{dof} \leq 1$), calculate δ from $\chi^2 = \chi_{min}^2 + 1$; otherwise, stretch the result obtained in this way by the factor $S = \sqrt{\chi_{min}^2/\text{dof}}$. The problem with this recipe is that the systematic errors are not stochastic. In particular, applying it to the lattice data on m_{ud} , m_s , m_s/m_{ud} and f_K/f_π , one arrives at a total error that is smaller than the smallest systematic error of the individual data sets. In our opinion, the latter represents a lower limit for the total error to be attached to the average. It is not a trivial matter, however, to split the total error of the average into a statistical and a systematic part. We are not

aware of a generally accepted prescription for doing this and refrain from proposing one in this review. In application to the lattice data to be discussed below, where the statistical errors are small compared to the systematic ones and thus barely affect the result, replacing the quantity δ by the smallest systematic error of the individual data sets does not lead to a significant underestimate of the total error. In the following, we adopt this prescription, which has the advantage of being simple and transparent. For a more sophisticated discussion of the problem, we refer to [61]. At the precision used in the present review, the numerical results obtained for the total errors with the method proposed there are the same.

3 Quark masses

Quark masses are fundamental parameters of the Standard Model. An accurate determination of these parameters is important for both phenomenological and theoretical applications. The charm and bottom masses, for instance, enter the theoretical expressions of several cross sections and decay rates, in heavy quark expansions. The up, down and strange quark masses govern the amount of explicit chiral symmetry breaking in QCD. From a theoretical point of view, the values of quark masses provide information about the flavour structure of physics beyond the Standard Model. The Review of Particle Physics of the Particle Data Group contains a review of quark masses [48], which covers light as well as heavy flavours. The present summary only deals with the light quark masses (those of the up, down and strange quarks), but discusses the lattice results for these in more detail.

Quark masses cannot be measured directly with experiment, because quarks cannot be isolated, as they are confined inside hadrons. On the other hand, quark masses are free parameters of the theory and, as such, cannot be obtained on the basis of purely theoretical considerations. Their values can only be determined by comparing the theoretical prediction for an observable, which depends on the quark mass of interest, with the corresponding experimental value. What makes light quark masses particularly difficult to determine is the fact that they are very small (for the up and down) or small (for the strange) compared to typical hadronic scales. Thus, their impact on typical hadronic observables is minute and it is difficult to isolate their contribution accurately.

Fortunately, the spontaneous breaking of $SU(3)_L \otimes SU(3)_R$ chiral symmetry provides observables which are particularly sensitive to the light quark masses: the masses of the resulting Nambu-Goldstone bosons (NGB), i.e. pions, kaons and etas. Indeed, the Gell-Mann-Oakes-Renner relation [62] predicts that the squared mass of a NGB is directly proportional to the sum of the masses of the quark and antiquark which compose it, up to higher order mass corrections. Moreover, because these NGBs are light and are composed of only two valence particles, their masses have a particularly clean statistical signal in lattice QCD calculations. In addition to which, the experimental uncertainties on these meson masses are negligible.

Three flavour QCD has four free parameters: the strong coupling, α_s (alternatively Λ_{QCD}) and the up, down and strange quark masses, m_u , m_d and m_s . However, present day lattice calculations are performed in the isospin limit, and the up and down quark masses get replaced by a single parameter: the isospin averaged up and down quark mass, $m_{ud} = \frac{1}{2}(m_u + m_d)$. A lattice determination of these parameters requires two steps:

1. Calculations of three experimentally measurable quantities are used to fix the three bare parameters. As already discussed, NGB masses are particularly appropriate for fixing

the light quark masses. Another observable, such as the mass of a member of the baryon octet, can be used to fix the overall scale. It is important to note that most of present day calculations are performed at values of m_{ud} which are still substantially larger than its physical value, typically four times as large. Thus, reaching the physical up and down quark mass point still requires a significant extrapolation. The only exceptions are the PACS-CS 08, 09, 10 [42, 63, 64] and BMW 08, 10A [17, 65] calculations discussed below, where masses very close to the physical value are reached. The situation is radically different for the strange quark. Indeed, modern simulations can include strange quarks whose masses bracket its physical value, and only interpolations are needed.

2. Renormalizations of these bare parameters must be performed to relate them to the corresponding cutoff-independent, renormalized parameters.⁵ These are short distance calculations, which may be performed perturbatively. Experience shows that one-loop calculations are particularly unreliable for the renormalization of quark masses, in all discretizations. Thus, at least two loops are required to have trustworthy results. Nevertheless, it is best to perform the renormalizations non-perturbatively, to avoid potentially large perturbative uncertainties due to neglected higher order terms.

Of course, in quark mass ratios the renormalization factor cancels, so that this second step is no longer relevant.

3.1 Contributions from the electromagnetic interaction

As mentioned in section 2, the present review relies on the hypothesis that, at low energies, the Lagrangian $\mathcal{L}_{\text{QCD}} + \mathcal{L}_{\text{QED}}$ describes nature to a high degree of precision. Moreover, we assume that, at the accuracy reached by now and for the quantities discussed here, the difference between the results obtained from simulations with three dynamical flavours and full QCD is small in comparison with the quoted systematic uncertainties. The electromagnetic interaction, on the other hand, cannot be ignored. Quite generally, when comparing QCD calculations with experiment, radiative corrections need to be applied. In lattice simulations, where the QCD parameters are fixed in terms of the masses of some of the hadrons, the electromagnetic contributions to these masses must be accounted for.⁶

The electromagnetic interaction plays a crucial role in determinations of the ratio m_u/m_d , because the isospin breaking effects generated by this interaction are comparable to those from $m_u \neq m_d$ (see subsection 3.4). In determinations of the ratio m_s/m_{ud} , the electromagnetic interaction is less important, but at the accuracy reached, it cannot be neglected. The reason is that, in the determination of this ratio, the pion mass enters as an input parameter. Because

⁵Throughout this review, the quark masses m_u , m_d and m_s refer to the $\overline{\text{MS}}$ scheme at running scale $\mu = 2 \text{ GeV}$ and the numerical values are given in MeV units.

⁶Since the decomposition of the sum $\mathcal{L}_{\text{QCD}} + \mathcal{L}_{\text{QED}}$ into two parts is not unique, specifying the QCD part requires a convention. In order to give results for the quark masses in the Standard Model at scale $\mu = 2 \text{ GeV}$, on the basis of a calculation done within QCD, it is convenient to match the two theories at that scale. We use this convention throughout the present review. Note that a different convention is used in the analysis of the precision measurements carried out in low energy pion physics. The result $a_0 M_{\pi^+} = 0.220(5)(2)(6)$ of the NA48/2 collaboration [66] for the $I = 0$ S-wave $\pi\pi$ scattering length, for instance, also concerns QCD in the isospin limit, but refers to the convention where \hat{M}_π is identified with M_{π^+} . When comparing lattice results with experiment, it is important to fix the QCD parameters in accordance with the convention used in the analysis of the experimental data (for a more detailed discussion, see [67–70]).

M_π represents a small symmetry breaking effect, it is rather sensitive to the perturbations generated by QED.

We distinguish the physical mass M_P , $P \in \{\pi^+, \pi^0, K^+, K^0\}$, from the mass \hat{M}_P within QCD alone. The e.m. self-energy is the difference between the two, $M_P^\gamma \equiv M_P - \hat{M}_P$. Since the self-energy of the Nambu-Goldstone bosons diverges in the chiral limit, it is convenient to replace it by the contribution of the e.m. interaction to the *square* of the mass,

$$\Delta_P^\gamma \equiv M_P^2 - \hat{M}_P^2 = 2 M_P M_P^\gamma + O(e^4). \quad (11)$$

The main effect of the e.m. interaction is an increase in the mass of the charged particles, generated by the photon cloud that surrounds them. The self-energies of the neutral ones are comparatively small, particularly for the Nambu-Goldstone bosons, which do not have a magnetic moment. Dashen's theorem [71] confirms this picture, as it states that, to leading order (LO) of the chiral expansion, the self-energies of the neutral NGBs vanish, while the charged ones obey $\Delta_{K^+}^\gamma = \Delta_{\pi^+}^\gamma$. It is convenient to express the self-energies of the neutral particles as well as the mass difference between the charged and neutral pions within QCD in units of the observed mass difference, $\Delta_\pi \equiv M_{\pi^+}^2 - M_{\pi^0}^2$:

$$\Delta_{\pi^0}^\gamma \equiv \epsilon_{\pi^0} \Delta_\pi, \quad \Delta_{K^0}^\gamma \equiv \epsilon_{K^0} \Delta_\pi, \quad \hat{M}_{\pi^+}^2 - \hat{M}_{\pi^0}^2 \equiv \epsilon_m \Delta_\pi. \quad (12)$$

In this notation, the self-energies of the charged particles are given by

$$\Delta_{\pi^+}^\gamma = (1 + \epsilon_{\pi^0} - \epsilon_m) \Delta_\pi, \quad \Delta_{K^+}^\gamma = (1 + \epsilon + \epsilon_{K^0} - \epsilon_m) \Delta_\pi, \quad (13)$$

where the dimensionless coefficient ϵ parametrizes the violation of Dashen's theorem,

$$\Delta_{K^+}^\gamma - \Delta_{K^0}^\gamma - \Delta_{\pi^+}^\gamma + \Delta_{\pi^0}^\gamma \equiv \epsilon \Delta_\pi. \quad (14)$$

Any determination of the light quark masses based on a calculation of the masses of π^+ , K^+ and K^0 within QCD requires an estimate for the coefficients ϵ , ϵ_{π^0} , ϵ_{K^0} and ϵ_m .

The first determination of the self-energies on the lattice was carried out by Duncan, Eichten and Thacker [72]. Using the quenched approximation, they arrived at $M_{K^+}^\gamma - M_{K^0}^\gamma = 1.9 \text{ MeV}$. Actually, the parametrization of the masses given in that paper yields an estimate for all but one of the coefficients introduced above (since the mass splitting between the charged and neutral pions in QCD is neglected, the parametrization amounts to setting $\epsilon_m = 0$ ab initio). Evaluating the differences between the masses obtained at the physical value of the electromagnetic coupling constant and at $e = 0$, we obtain $\epsilon = 0.50(8)$, $\epsilon_{\pi^0} = 0.034(5)$ and $\epsilon_{K^0} = 0.23(3)$. The errors quoted are statistical only: an estimate of lattice systematic errors is not possible from the limited results of [72]. The result for ϵ indicates that the violations of Dashen's theorem are sizable: according to this calculation, the non-leading contributions to the self-energy difference of the kaons amount to 50% of the leading term. The result for the self-energy of the neutral pion cannot be taken at face value, because it is small, comparable with the neglected mass difference $\hat{M}_{\pi^+} - \hat{M}_{\pi^0}$. To illustrate this, we note that the numbers quoted above are obtained by matching the parametrization with the physical masses for π^0 , K^+ and K^0 . This gives a mass for the charged pion that is too high by 0.32 MeV. Tuning the parameters instead such that M_{π^+} comes out correctly, the result for the self-energy of the neutral pion becomes larger: $\epsilon_{\pi^0} = 0.10(7)$. Also, the uncertainties due to the systematic errors of the lattice calculation need to be taken into account.

In an update of this calculation by the RBC collaboration [73] (RBC 07), the electromagnetic interaction is still treated in the quenched approximation, but the strong interaction is simulated with $N_f = 2$ dynamical quark flavours. The quark masses are fixed with the physical masses of π^0 , K^+ and K^0 . The outcome for the difference in the electromagnetic self-energy of the kaons reads $M_{K^+}^\gamma - M_{K^0}^\gamma = 1.443(55)$ MeV. This corresponds to a remarkably small violation of Dashen's theorem. Indeed, a recent extension of this work to $N_f = 2 + 1$ dynamical flavours [74] leads to a significantly larger self-energy difference: $M_{K^+}^\gamma - M_{K^0}^\gamma = 1.87(10)$ MeV, in good agreement with the estimate of Eichten et al. Expressed in terms of the coefficient ϵ that measures the size of the violation of Dashen's theorem, it corresponds to $\epsilon = 0.5(1)$.

More recently, the BMW collaboration has reported preliminary results for the electromagnetic self-energies, based on simulations in which a $U(1)$ degree of freedom is superimposed on their $N_f = 2 + 1$ QCD configurations [75]. The result for the kaon self-energy difference reads $M_{K^+}^\gamma - M_{K^0}^\gamma = 2.2(2)$ MeV, that is $\epsilon = 0.66(14)$, where the error indicates the statistical uncertainties.

The input for the electromagnetic corrections used by the MILC collaboration is specified in [76]. In their analysis of the lattice data, ϵ_{π^0} , ϵ_{K^0} and ϵ_m are set equal to zero. For the remaining coefficient, which plays a crucial role in determinations of the ratio m_u/m_d , the very conservative range $\epsilon = 1 \pm 1$ was used in MILC 04 [77], while in more recent work, in particular in MILC 09 [6] and MILC 09A [59], this input is replaced by $\epsilon = 1.2 \pm 0.5$, as suggested by phenomenological estimates for the corrections to Dashen's theorem [78, 79]. First results of an evaluation of the electromagnetic self-energies based on $N_f = 2 + 1$ dynamical quarks in the QCD sector and on the quenched approximation in the QED sector are also reported by the MILC collaboration [80]. Further calculations using staggered quarks and quenched photons are underway [81].

The effective Lagrangian that governs the self-energies to next-to-leading order (NLO) of the chiral expansion was set up in [82]. The estimates in [78, 79] are obtained by replacing QCD with a model, matching this model with the effective theory and assuming that the effective coupling constants obtained in this way represent a decent approximation to those of QCD. For alternative model estimates and a detailed discussion of the problems encountered in models based on saturation by resonances, see [83–85]. In the present review of the information obtained on the lattice, we avoid the use of models altogether.

There is an indirect phenomenological determination of ϵ , which is based on the decay $\eta \rightarrow 3\pi$ and does not rely on models. The result for the quark mass ratio Q obtained from a dispersive analysis of this decay implies $\epsilon = 0.70(28)$ (see section 3.4). While the values found on the lattice [72–75] are lower, the phenomenological estimate used by MILC 09A [59] is on the high side. In the following, we take the central value from η -decay, but stretch the error, so that the numbers given in [59, 72–75] are all within one standard deviation: $\epsilon = 0.7(5)$.

We add a few comments concerning the physics of the self-energies and then specify the estimates used as an input in our analysis of the data. The Cottingham formula [86] represents the self-energy of a particle as an integral over electron scattering cross sections; elastic as well as inelastic reactions contribute. For the charged pion, the term due to elastic scattering, which involves the square of the e.m. form factor, makes a substantial contribution. In the case of the π^0 , this term is absent, because the form factor vanishes on account of charge conjugation invariance. Indeed, the contribution from the form factor to the self-energy of the π^+ roughly reproduces the observed mass difference between the two particles. Furthermore, the numbers given in [87–89] indicate that the inelastic contributions are significantly smaller than the elastic contributions to the self-energy of the π^+ . The low energy theorem of Das,

Guralnik, Mathur, Low and Young [90] ensures that, in the limit $m_u, m_d \rightarrow 0$, the e.m. self-energy of the π^0 vanishes, while the one of the π^+ is given by an integral over the difference between the vector and axial spectral functions. The estimates for ϵ_{π^0} obtained in [72] are consistent with the suppression of the self-energy of the π^0 implied by chiral $SU(2) \times SU(2)$. In our opinion, $\epsilon_{\pi^0} = 0.07(7)$ is a conservative estimate for this coefficient. The self-energy of the K^0 is suppressed less strongly, because it remains different from zero if m_u and m_d are taken massless and only disappears if m_s is turned off as well. Note also that, since the e.m. form factor of the K^0 is different from zero, the self-energy of the K^0 does pick up an elastic contribution. The lattice result for ϵ_{K^0} indicates that the violation of Dashen's theorem is smaller than in the case of ϵ . In the following, we use $\epsilon_{K^0} = 0.3(3)$.

Finally, we consider the mass splitting between the charged and neutral pions in QCD. This effect is known to be very small, because it is of second order in $m_u - m_d$. There is a parameter-free prediction, which expresses the difference $\hat{M}_{\pi^+}^2 - \hat{M}_{\pi^0}^2$ in terms of the physical masses of the pseudoscalar octet and is valid to NLO of the chiral perturbation series. Numerically, the relation yields $\epsilon_m = 0.04$ [91], indicating that this contribution does not play a significant role at the present level of accuracy. We attach a conservative error also to this coefficient: $\epsilon_m = 0.04(2)$. The lattice result for the self-energy difference of the pions, reported in [74], $M_{\pi^+}^\gamma - M_{\pi^0}^\gamma = 4.50(23)$ MeV, agrees with this estimate: expressed in terms of the coefficient ϵ_m that measures the pion mass splitting in QCD, the result corresponds to $\epsilon_m = 0.04(5)$. The corrections of next-to-next-to-leading order (NNLO) have been worked out [92], but the numerical evaluation of the formulae again meets with the problem that the relevant effective coupling constants are not reliably known.

In summary, we use the following estimates for the e.m. corrections:

$$\epsilon = 0.7(5), \quad \epsilon_{\pi^0} = 0.07(7), \quad \epsilon_{K^0} = 0.3(3), \quad \epsilon_m = 0.04(2). \quad (15)$$

While the range used for the coefficient ϵ affects our analysis in a significant way, the numerical values of the other coefficients only serve to set the scale of these contributions. The range given for ϵ_{π^0} and ϵ_{K^0} may be overly generous, but because of the exploratory nature of the lattice determinations, we consider it advisable to use a conservative estimate.

Treating the uncertainties in the four coefficients as statistically independent and adding errors in quadrature, the numbers in equation (15) yield the following estimates for the e.m. self-energies,

$$\begin{aligned} M_{\pi^+}^\gamma &= 4.7(3) \text{ MeV}, & M_{\pi^0}^\gamma &= 0.3(3) \text{ MeV}, & M_{\pi^+}^\gamma - M_{\pi^0}^\gamma &= 4.4(1) \text{ MeV}, \\ M_{K^+}^\gamma &= 2.5(7) \text{ MeV}, & M_{K^0}^\gamma &= 0.4(4) \text{ MeV}, & M_{K^+}^\gamma - M_{K^0}^\gamma &= 2.1(6) \text{ MeV}, \end{aligned} \quad (16)$$

and for the pion and kaon masses occurring in the QCD sector of the Standard Model,

$$\begin{aligned} \hat{M}_{\pi^+} &= 134.8(3) \text{ MeV}, & \hat{M}_{\pi^0} &= 134.6(3) \text{ MeV}, & \hat{M}_{\pi^+} - \hat{M}_{\pi^0} &= 0.2(1) \text{ MeV}, \\ \hat{M}_{K^+} &= 491.2(7) \text{ MeV}, & \hat{M}_{K^0} &= 497.2(4) \text{ MeV}, & \hat{M}_{K^+} - \hat{M}_{K^0} &= -6.1(6) \text{ MeV}. \end{aligned} \quad (17)$$

The self-energy difference between the charged and neutral pion involves the same coefficient ϵ_m that describes the mass difference in QCD – this is why the estimate for $M_{\pi^+}^\gamma - M_{\pi^0}^\gamma$ is so sharp.

3.2 Pion and kaon masses in the isospin limit

As mentioned above, most of the lattice calculations concerning the properties of the light mesons are performed in the isospin limit of QCD ($m_u - m_d \rightarrow 0$ at fixed $m_u + m_d$). We

denote the pion and kaon masses in that limit by \overline{M}_π and \overline{M}_K , respectively. Their numerical values can be estimated as follows. Since the operation $u \leftrightarrow d$ interchanges π^+ with π^- and K^+ with K^0 , the expansion of the quantities $\hat{M}_{\pi^+}^2$ and $\frac{1}{2}(\hat{M}_{K^+}^2 + \hat{M}_{K^0}^2)$ in powers of $m_u - m_d$ only contains even powers. As shown in [93], the effects generated by $m_u - m_d$ in the mass of the charged pion are strongly suppressed: the difference $\hat{M}_{\pi^+}^2 - \overline{M}_\pi^2$ represents a quantity of $O[(m_u - m_d)^2(m_u + m_d)]$ and is therefore small compared to the difference $\hat{M}_{\pi^+}^2 - \hat{M}_{\pi^0}^2$, for which an estimate was given above. In the case of $\frac{1}{2}(\hat{M}_{K^+}^2 + \hat{M}_{K^0}^2) - \overline{M}_K^2$, the expansion does contain a contribution at NLO, determined by the combination $2L_8 - L_5$ of low energy constants, but the lattice results for that combination show that this contribution is very small, too. Numerically, the effects generated by $m_u - m_d$ in $\hat{M}_{\pi^+}^2$ and in $\frac{1}{2}(\hat{M}_{K^+}^2 + \hat{M}_{K^0}^2)$ are negligible compared to the uncertainties in the electromagnetic self-energies. The estimates for these given in equation (15) thus imply

$$\overline{M}_\pi = 134.8(3) \text{ MeV} , \quad \overline{M}_K = 494.2(5) \text{ MeV} . \quad (18)$$

This shows that, for the convention used above to specify the QCD sector of the Standard Model, and within the accuracy to which this convention can currently be implemented, the mass of the pion in the isospin limit agrees with the physical mass of the neutral pion: $\overline{M}_\pi - M_{\pi^0} = -0.2(3) \text{ MeV}$.

3.3 Lattice determination of m_s and m_{ud}

We now turn to a review of the lattice calculations of the light quark masses and begin with m_s , the isospin averaged up and down quark mass, m_{ud} , and their ratio. Most groups quote only m_{ud} , not the individual up and down quark masses. We then discuss the ratio m_u/m_d and the individual determination of m_u and m_d .

Quark masses have been calculated on the lattice since the mid-nineties. However early calculations were performed in the quenched approximation, leading to unquantifiable systematics. Thus in the following, we only review modern, unquenched calculations, which include the effects of light sea quarks.

Tables 1 and 2 list the results of $N_f = 2$ and $N_f = 2 + 1$ lattice calculations of m_s and m_{ud} . These results are given in the $\overline{\text{MS}}$ scheme at 2 GeV, which is standard nowadays. The tables also show the colour coding of the calculations leading to these results. The corresponding results for m_s/m_{ud} are given in Table 3. As indicated in the Introduction, we treat $N_f = 2$ and $N_f = 2 + 1$ calculations separately. The latter include the effects of a strange sea quark, but the former do not.

3.3.1 $N_f = 2$ lattice calculations

We begin with $N_f = 2$ calculations. A quick inspection of Table 1 indicates that only the most recent calculation, ETM 10B [94], controls all systematic effects. Only ETM 10B [94] and ETM 07 [49] really enter the chiral regime, with pion masses down to about 300 MeV. All the others have significantly more massive pions, the lightest being about 430 MeV, in the calculation by CP-PACS 01 [101]. Moreover, the latter calculation is performed on very coarse lattices, with lattice spacings $a \geq 0.11 \text{ fm}$ and only one loop perturbation theory is used to renormalize the results.

One calculation of m_s which performs quite well in terms of colour coding is that of ALPHA 05 [98]. This is due to the fact that both non-perturbative running and non-perturbative

Collaboration	Ref.	publication status	chiral extrapolation	continuum extrapolation	finite volume	renormalization	running	m_{ud}	m_s
ETM 10B	[94]	A	●	★	●	★	<i>a</i>	3.6(1)(2)	95(2)(6)
JLQCD/TWQCD 08A	[95]	A	●	■	■	★	–	4.452(81)(38) _{(-227)⁺⁰}	–
RBC 07 [†]	[73]	A	■	■	★	★	–	4.25(23)(26)	119.5(5.6)(7.4)
ETM 07	[49]	A	●	■	●	★	–	3.85(12)(40)	105(3)(9)
QCDSF/ UKQCD 06	[96]	A	■	★	■	★	–	4.08(23)(19)(23)	111(6)(4)(6)
SPQcdR 05	[97]	A	■	●	●	★	–	4.3(4) _{(-0.0)^{+1.1}}	101(8) _{(-0)⁺²⁵}
ALPHA 05	[98]	A	■	●	★	★	<i>b</i>	–	97(4)(18) [§]
QCDSF/ UKQCD 04	[99]	A	■	★	■	★	–	4.7(2)(3)	119(5)(8)
JLQCD 02	[100]	A	■	■	●	■	–	3.223 _{(-69)⁺⁴⁶}	84.5 _{(-1.7)^{+12.0}}
CP-PACS 01	[101]	A	■	■	★	■	–	3.45(10) _{(-18)⁺¹¹}	89(2) _{(-6)⁺²}

[†] The calculation includes quenched e.m. effects.

[§] The data used to obtain the bare value of m_s are from RBC/UKQCD 04 [99]

* This value of m_s was obtained using the kaon mass as input. If the ϕ meson mass is used instead, the authors find $m_s = 90_{-11}^{+5}$.

a The masses are renormalized non-perturbatively at scales $1/a \sim 2 \div 3$ GeV in the $N_f = 2$ RI/MOM scheme. In this scheme, non-perturbative and N³LO running for the quark masses are shown to agree from 4 GeV down to 2 GeV to better than 3% [102].

b The masses are renormalized and run non-perturbatively up to a scale of 100 GeV in the $N_f = 2$ SF scheme. In this scheme, non-perturbative and NLO running for the quark masses are shown to agree well from 100 GeV all the way down to 2 GeV [98].

Table 1: $N_f = 2$ lattice results for the masses m_{ud} and m_s , together with the colour coding of the calculation used to obtain these. If information about non-perturbative running is available, this is indicated in the column "running", with details given at the bottom of the table.

renormalization are performed in a controlled fashion, using Schrödinger functional methods. However, the lightest sea pion in the calculation is 600 MeV, significantly above our thresholds for a controlled chiral extrapolation. In that sense, this calculation should be viewed more as a means of giving a first estimate of possible sea quark corrections to the equally precise quenched calculation ALPHA 99 [112], than a full fledged dynamical fermion calculation.

The conclusion of our analysis of $N_f = 2$ calculations is that the results of ETM 10B [94] (which updates and extends ETM 07 [49]), is the only one to date which satisfies our selection criteria. Thus we do not offer an average of $N_f = 2$ results for the strange and isospin averaged quark masses and their ratios, but simply quote the results of ETM 10B [94]:

$$N_f = 2 : \quad m_s = 95(2)(6) \text{ MeV}, \quad m_{ud} = 3.6(1)(2) \text{ MeV}, \quad \frac{m_s}{m_{ud}} = 27.3(5)(7). \quad (19)$$

The combined statistical and systematic errors on these results are 7%, 6% and 3% respectively. The errors are smaller in the ratio because many systematics cancel, most notably those associated with renormalization and the setting of the scale. Moreover, because of statistical correlations between m_s and m_{ud} , those errors are also reduced in the ratio.

Collaboration	Ref.	publication status	chiral extrapolation	continuum extrapolation	finite volume	renormalization	running	m_{ud}	m_s
PACS-CS 10	[64]	P	★	■	■	★	<i>a</i>	2.78(27)	86.7(2.3)
MILC 10A	[103]	C	●	★	★	●	–	3.19(4)(5)(16)	–
HPQCD 10	[104]	A	●	★	★	★	–	3.39(6)*	92.2(1.3)
BMW 10A, 10B ⁺	[65, 105]	P	★	★	★	★	<i>b</i>	3.469(47)(48)	95.5(1.1)(1.5)
RBC/UKQCD 10A	[106]	P	●	●	★	★	<i>c</i>	3.59(13)(14)(8)	96.2(1.6)(0.2)(2.1)
Blum 10 [†]	[74]	P	●	■	●	★	–	3.44(12)(22)	97.6(2.9)(5.5)
PACS-CS 09	[42]	A	★	■	■	★	<i>a</i>	2.97(28)(3)	92.75(58)(95)
HPQCD 09	[107]	A	●	★	★	★	–	3.40(7)	92.4(1.5)
MILC 09A	[59]	C	●	★	★	●	–	3.25 (1)(7)(16)(0)	89.0(0.2)(1.6)(4.5)(0.1)
MILC 09	[6]	A	●	★	★	●	–	3.2(0)(1)(2)(0)	88(0)(3)(4)(0)
PACS-CS 08	[63]	A	★	■	■	■	–	2.527(47)	72.72(78)
RBC/UKQCD 08	[108]	A	●	■	★	★	–	3.72(16)(33)(18)	107.3(4.4)(9.7)(4.9)
CP-PACS/ JLQCD 07	[109]	A	■	★	★	■	–	3.55(19)(⁺⁵⁶ ₋₂₀)	90.1(4.3)(^{+16.7} _{-4.3})
HPQCD 05	[110]	A	●	●	●	●	–	3.2(0)(2)(2)(0) [‡]	87(0)(4)(4)(0) [‡]
MILC 04, HPQCD/ MILC/UKQCD 04	[77, 111]	A	●	●	●	■	–	2.8(0)(1)(3)(0)	76(0)(3)(7)(0)

* Value obtained by combining the HPQCD 10 result for m_s with the MILC 09 result for m_s/m_{ud} .

[†] The fermion action used is tree-level improved.

[‡] The calculation includes quenched e.m. effects.

[‡] The bare numbers are those of MILC 04. The masses are simply rescaled, using the ratio of the 2-loop to 1-loop renormalization factors.

a The masses are renormalized and run non-perturbatively up to a scale of 40 GeV in the $N_f = 3$ SF scheme. In this scheme, non-perturbative and NLO running for the quark masses are shown to agree well from 40 GeV all the way down to 3 GeV [64].

b The masses are renormalized and run non-perturbatively up to a scale of 4 GeV in the $N_f = 3$ RI/MOM scheme. In this scheme, non-perturbative and N³LO running for the quark masses are shown to agree from 6 GeV down to 3 GeV to better than 1% [105].

c The masses are renormalized non-perturbatively at a scale of 2 GeV in a couple of $N_f = 3$ RI/SMOM schemes. A careful study of perturbative matching uncertainties has been performed by comparing results in the two schemes in the region of 2 GeV to 3 GeV [106].

Table 2: $N_f = 2 + 1$ lattice results for the masses m_{ud} and m_s , together with the colour coding of the calculation used to obtain these. If information about non-perturbative running is available, this is indicated in the column "running", with details given at the bottom of the table.

3.3.2 $N_f = 2 + 1$ lattice calculations

We turn now to $N_f = 2 + 1$ calculations. These and the corresponding results are summarized in Table 2 and 3. Somewhat paradoxically, these calculations are more mature than those with $N_f = 2$. This is thanks, in large part, to the head start and sustained effort of MILC, which has been performing $N_f = 2 + 1$ rooted staggered fermion calculations for the past ten or so years. They have covered an impressive range of parameter space, with lattice spacings which, today, go down to 0.045 fm and valence pion masses down to approximately 180 MeV [59]. The most recent updates, MILC 10A [103] and MILC 09A [59], include significantly more data and use two loop renormalization. Since these data sets subsume those of their previous calculations, these latest results are the only ones that must be kept in any world average.

We recall that valence and sea quarks are treated differently in the rooted staggered approach, as discussed in section 2, and that the lightest effective sea-pion mass of all of their ensembles is about 260 MeV rather than 180 MeV. Regarding the specific subject of light quark masses, a weak point of present day staggered fermion calculations is the use

Collaboration	Ref.	publication status	chiral extrapolation	continuum extrapolation	finite volume	m_s/m_{ud}
BMW 10A, 10B ⁺	[65, 105]	P	★	★	★	27.53(20)(8)
RBC/UKQCD 10A	[106]	P	●	●	★	26.8(0.8)(1.1)
Blum 10 [†]	[74]	P	●	■	●	28.31(0.29)(1.77)
PACS-CS 09	[42]	A	★	■	■	31.2(2.7)
MILC 09A	[59]	C	●	★	★	27.41(5)(22)(0)(4)
MILC 09	[6]	A	●	★	★	27.2(1)(3)(0)(0)
PACS-CS 08	[63]	A	★	■	■	28.8(4)
RBC/UKQCD 08	[108]	A	●	■	★	28.8(0.4)(1.6)
MILC 04, HPQCD/ MILC/UKQCD 04	[77, 111]	A	●	●	●	27.4(1)(4)(0)(1)
ETM 10B	[94]	A	●	★	●	27.3(5)(7)
RBC 07 [†]	[73]	A	■	■	★	28.10(38)
ETM 07	[49]	A	●	■	●	27.3(0.3)(1.2)
QCDSF/UKQCD 06	[96]	A	■	★	■	27.2(3.2)

⁺ The fermion action used is tree-level improved.

[†] The calculation includes quenched e.m. effects.

Table 3: Lattice results for m_s/m_{ud} , together with the colour coding of the calculation used to obtain them. The upper half of the table corresponds to $N_f = 2 + 1$ calculations, the lower half to $N_f = 2$ results.

of perturbative renormalization. As already noted, it is preferable, a priori, to renormalize non-perturbatively, to avoid introducing uncontrolled systematic errors from neglected, higher order contributions. That this is a problem, in practice, for the staggered calculations can be seen from the following observation. In MILC 04 [77] and HPQCD/MILC/UKQCD 04 [111], only one loop perturbation theory was used. $O(\alpha_s^2)$ corrections were included in the HPQCD 05 [110] update. The only difference between this update and the earlier calculation is the inclusion of these corrections: the bare lattice results are the same in both. Yet, the $O(\alpha_s^2)$ correction increased the renormalized value of m_s by 11 MeV, i.e. 14%. In light of this, one may question whether the perturbative expansion is under control. Moreover, preliminary results including non-perturbative renormalization suggest that the omitted terms may contribute an additional increase of $\sim 20\%$ in m_s [113].

Of all the entries in Tables 2 and 3, Blum 10 [74] is the only one which provides an improved determination of the electromagnetic self-energies on the lattice and points the way for future promising developments: still, at present, these data do not pass the selection criteria formulated in section 2.2 as the authors did not investigate all sources of systematic error. There are four other calculations with $N_f = 2 + 1$, however, that do and that we discuss now.

The most recent one is BMW 10A, 10B [65, 105] which, as shown by the color coding in Tables 2 and 3 has addressed all sources of systematic effects. One of the most impressive aspects of this calculation is that they have reached the physical up and down quark mass by *interpolation* and did not need any chiral extrapolation. Moreover, their calculation was

performed at five lattice spacings ranging from 0.054 to 0.116 fm, with full non-perturbative renormalization and running and in volumes of up to $(6 \text{ fm})^3$ guaranteeing that all sources of systematic error are controlled. However, according to the rules set forth in section 2.2, these results will have to be published before they can be included in our averages.

The second calculation that we discuss is PACS-CS 10 [64], which updates 09 [42]: these calculations have been performed with $O(a)$ -improved Wilson fermions on lattices with $a \simeq 0.09 \text{ fm}$. The important aspect of this calculation is that it also probes pion masses down to $M_\pi \simeq 135 \text{ MeV}$, i.e. down to the physical mass point. This is achieved by reweighting the simulations performed in PACS-CS 08 [63] at $M_\pi \simeq 160 \text{ MeV}$. If adequately controlled, this procedure eliminates the need to extrapolate to the physical mass point and, hence, the corresponding systematic error. Moreover, renormalization of quark masses is implemented non-perturbatively, through the Schrödinger functional method [114]. As it stands, the main drawback of the calculation, which makes the inclusion of its results in a world average of lattice results inappropriate at this stage, is that for the lightest quark mass the volume is very small, corresponding to $LM_\pi \simeq 2.0$, a value for which finite volume effects will be difficult to control. Another problem is that the calculation was performed at a single lattice spacing, forbidding a continuum extrapolation. Furthermore, it is unclear at this point what might be the systematic errors associated with the reweighting procedure. The PACS-CS collaboration plans to perform physical point simulations with larger and finer lattices.

The third calculation of particular interest is RBC/UKQCD 10A [106] (which updates RBC/UKQCD 08 [108]). This calculation uses the theoretically appealing domain wall fermions. It reaches down to 330 MeV pion masses in the sea and to 242 MeV valence pions. Moreover, it makes use of non-perturbative renormalization à la Rome-Southampton [115]. The latest update removes the main drawback of the previous calculation by adding a second, finer lattice spacing of about 0.09 fm to the first rather coarse lattice spacing of 0.11 fm, and allows a first estimate of the systematic error from the continuum extrapolation.

Finally we come to the fourth calculation which satisfies our selection criteria, HPQCD 10 [104] (which updates HPQCD 09 [107]). The strange quark mass is computed using a precise determination of the charm quark mass, $m_c(m_c) = 1.273(6) \text{ GeV}$ [104, 116], whose accuracy is better than 0.5%, and a calculation of the quark mass ratio $m_c/m_s = 11.85(16)$ [107], which achieves a precision slightly above 1%. The determination of m_s via the ratio m_c/m_s circumvents the problem of running by calculating a scale-invariant ratio non-perturbatively. The MILC 09 determination of the quark mass ratio m_s/m_{ud} [6] is also used in HPQCD 10 [104] to calculate m_{ud} .

The high precision quoted by HPQCD 10 on the strange quark mass relies in large part on the precision reached in the determination of the charm quark mass [104, 116]. This calculation uses a novel approach based on the lattice determination of moments of charm-quark pseudoscalar, vector and axial-vector correlators. These moments are then combined with four-loop results from continuum perturbation theory to obtain a determination of the charm quark mass in the $\overline{\text{MS}}$ scheme. In the preferred case, in which pseudoscalar correlators are used for the analysis, there are no renormalization factors required, since the corresponding axial-vector current is partially conserved in the staggered lattice formalism. Overall, the 0.5% accuracy claimed in the calculation of m_c is certainly impressive, since it implies that all sources of uncertainty, coming from the scale determination, discretization effects (the bare charm mass in lattice units is as large as $am_c \simeq 0.85$), perturbation theory as well as non-perturbative effects in the estimate of moments, are all controlled at the per mille level.

This discussion leaves us with three results to average for m_s , those of MILC 09A [59],

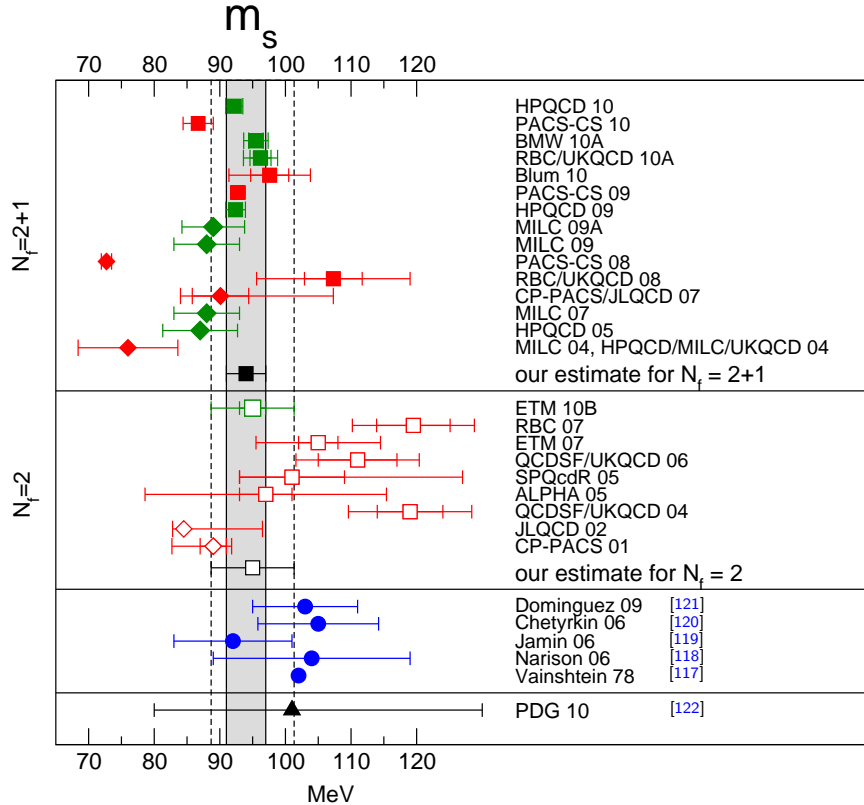


Figure 1: Mass of the strange quark ($\overline{\text{MS}}$ scheme, running scale 2 GeV). The upper part shows the lattice results listed in Tables 1 and 2. Full and empty symbols correspond to simulations with $N_f = 2 + 1$ and $N_f = 2$, respectively. Diamonds represent results based on perturbative renormalization, while squares indicate that, in the relation between the lattice-regularized and renormalized $\overline{\text{MS}}$ masses, non-perturbative effects are accounted for. The vertical bands indicate our estimates (19) and (20). The lower part shows recent determinations obtained from the evaluation of sum rules, together with the earliest result based on this method, as well as the most recent estimate of the Particle Data Group.

RBC/UKQCD 10A [106] and HPQCD 10 [104]. Treating them as independent measurements and simply adding the statistical and systematic errors in quadrature, we obtain a good fit, with $\chi^2 = 2.5$ for 3 data points and 1 free parameter. With the prescription specified in section 2.2, the average becomes $m_s = 92.8(1.3)$ MeV. When repeating the exercise for m_{ud} , we replace MILC 09A by the more recent analysis reported in MILC 10A [103] and again obtain a good fit: $\chi^2 = 2.3$ for 2 degrees of freedom and $m_{ud} = 3.38(6)$ MeV for the average. The outcome of the averaging procedure thus amounts to a determination of m_s and m_{ud} of 1.4% and 1.8%, respectively.

The results in BMW 10A, 10B [65, 105], which are not included in the averaging procedure on account of our criteria concerning the publication status, offer an independent, remarkably sharp determination of m_{ud} and m_s . These data are perfectly consistent with the averages quoted above.

The heavy sea quarks affect the determination of the light quark masses only through

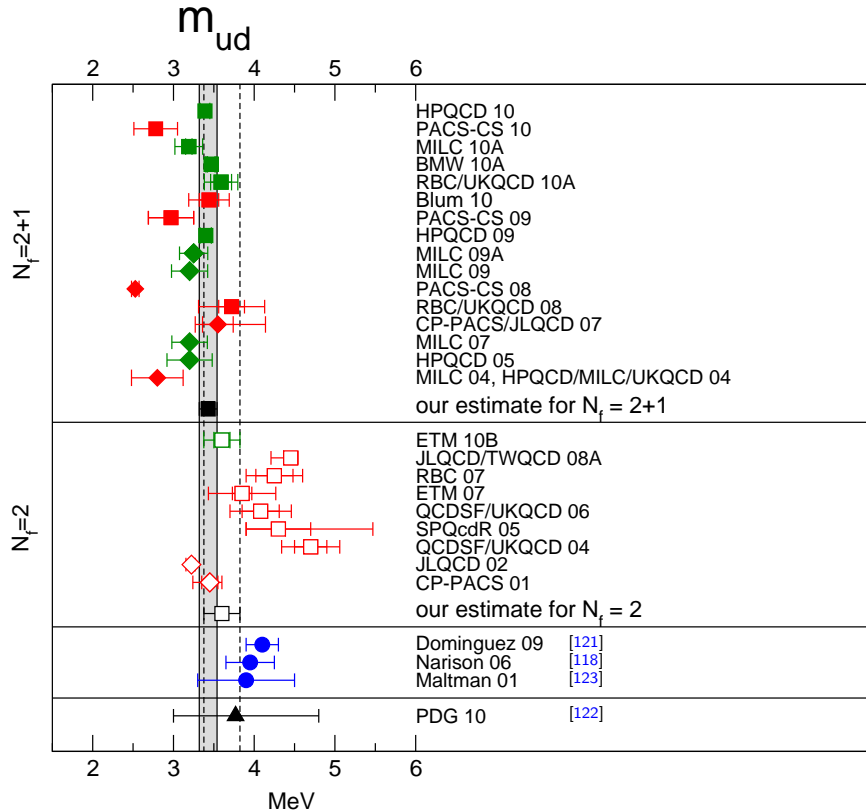


Figure 2: Mean mass of the two lightest quarks, $m_{ud} = \frac{1}{2}(m_u + m_d)$. The meaning of the various symbols is explained in the caption of Fig. 1.

contributions of order $1/m_c^2$, which moreover are suppressed by the Zweig-rule. We expect these contributions to be small, but do not know of a reliable quantitative evaluation. The problem originates in the fact that the relation between the parameters of QCD_3 and those of full QCD can currently be analyzed only in the framework of perturbation theory. The β - and γ -functions, which control the renormalization of the coupling constants and quark masses, respectively, are known to four loops [124–127]. The precision achieved in this framework for the decoupling of the t - and b -quarks is excellent, but the c -quark is not heavy enough: at the percent level, the corrections of order $1/m_c^2$ cannot be neglected and the decoupling formulae of perturbation theory do not provide a reliable evaluation, because the scale $m_c(m_c) \simeq 1.27 \text{ GeV}$ is too low for these formulae to be taken at face value. Consequently, the accuracy to which it is possible to identify the running masses of the light quarks of full QCD in terms of those occurring in QCD_3 is limited. For this reason, it is preferable to characterize the masses m_u , m_d , m_s in terms of QCD_4 , where the connection with full QCD is under good control. The role of the c -quarks in the determination of the light quark masses will soon be studied in detail – some simulations with 2+1+1 dynamical quarks have already been carried out [60].

A crude upper bound on the size of the effects due to the neglected heavy quarks can be established within the $N_f = 2 + 1$ simulations themselves, without invoking perturbation theory. In [17] it is found that when the scale is set by M_Ξ , the result for M_Λ agrees well with experiment within the 2.3% accuracy of the calculation. Because of the very strong

correlations between the statistical and systematic errors of these two masses, we expect the uncertainty in the difference $M_{\Xi} - M_{\Lambda}$ to also be of order 2%. To leading order in the chiral expansion, this mass difference is proportional to $m_s - m_{ud}$. We conclude that the agreement of $N_f = 2 + 1$ calculations with experiment yields an upper bound on the sensitivity of m_s to heavy sea quarks of order 2%.

In order to stay on the conservative side in this rapidly developing field, our final estimates for m_{ud} and m_s come with sizable uncertainties:

$$N_f = 2 + 1 : \quad m_{ud} = 3.43(11) \text{ MeV}, \quad m_s = 94(3) \text{ MeV}. \quad (20)$$

As discussed in section 2.2, these numbers are not obtained from a mathematical prescription, but are chosen so as to cover all of the high quality data discussed in the present section (note also that the central values are slightly higher than those of the averages discussed above).

The estimates (20) represent the conclusions we draw from the information gathered on the lattice until now. They are shown as vertical bands in Figures 1 and 2, together with the $N_f = 2$ results (19) and a few estimates from other sources. The values quoted in the 2010 edition of the Review of Particle Properties [122] are $m_{ud} = 3.9(9)$, $m_s = 101(^{+29}_{-21})$ MeV. The errors attached to our estimates are smaller by an order of magnitude. In our opinion, the remarkable recent progress achieved with the simulation of light dynamical quarks and the fact that all of the data that pass our quality criteria are consistent with one another fully justify this reduction of the uncertainties.

The lower half of Figure 1 shows that the sum rule results for m_s agree with the $N_f = 2 + 1$ data, but Figure 2 indicates that in the case of m_{ud} , the sum rule estimates are on the high side. For the most recent sum rule evaluation [121], the origin of this apparent discrepancy is readily identified. In that work, the sum rules are used to estimate the value of $m_s + m_{ud}$. In order to disentangle the two terms, the authors take the ratio m_s/m_{ud} from the early literature on χ PT. If the numerical value of this ratio is updated to the range given in (24), the value of m_s practically stays put, but the outcome for m_{ud} is lowered substantially, so that the difference shrinks to about 1σ . In other words, there is no discrepancy to speak of between the lattice and sum rule results for the masses of the light quarks – the size of m_s and m_{ud} is well understood.

In the ratio m_s/m_{ud} , one of the sources of systematic error – the uncertainties in the renormalization factors – drops out. Also, we can compare the lattice results with the leading order formula of χ PT,

$$\frac{m_s}{m_{ud}} \stackrel{\text{LO}}{=} \frac{\hat{M}_{K^+}^2 + \hat{M}_{K^0}^2 - \hat{M}_{\pi^+}^2}{\hat{M}_{\pi^+}^2}, \quad (21)$$

which relates the quantity m_s/m_{ud} to a ratio of meson masses in QCD. Expressing these in terms of the physical masses and the four coefficients introduced in (12)-(14), linearizing the result with respect to the corrections and inserting the observed mass values, we obtain

$$\frac{m_s}{m_{ud}} \stackrel{\text{LO}}{=} 25.9 - 0.1 \epsilon + 1.9 \epsilon_{\pi^0} - 0.1 \epsilon_{K^0} - 1.8 \epsilon_m. \quad (22)$$

If the coefficients ϵ , ϵ_{π^0} , ϵ_{K^0} and ϵ_m are set equal to zero, the right hand side reduces to the value $m_s/m_{ud} = 25.9$ that follows from Weinberg's leading order formulae for m_u/m_d and m_s/m_d [128], in accordance with the fact that these do account for the e.m. interaction at leading order, but neglect the mass difference between the charged and neutral pions in QCD.

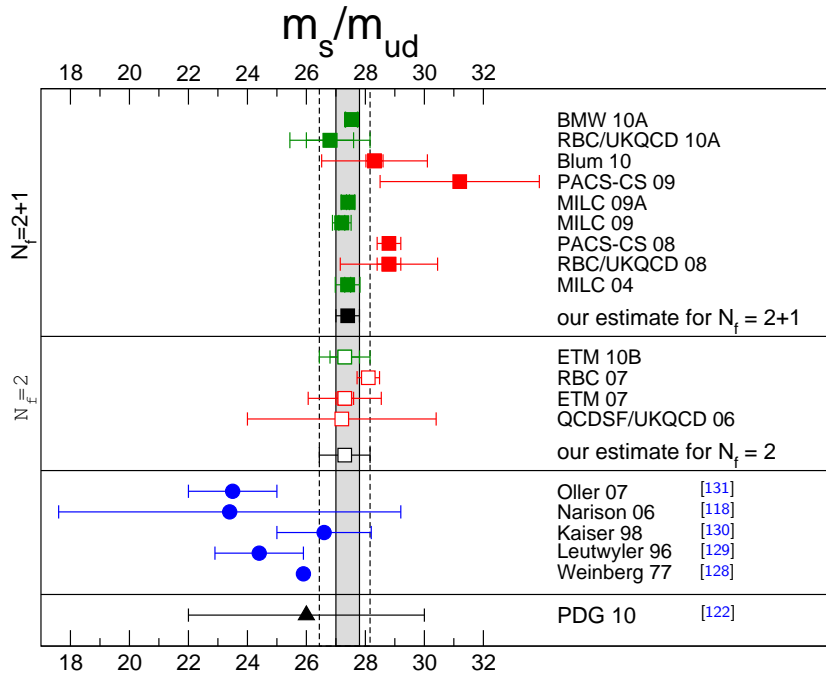


Figure 3: Results for the ratio m_s/m_{ud} , in which the renormalization factors cancel. The upper part of the figure shows the lattice results listed in Table 3 (full and empty symbols correspond to $N_f = 2 + 1$ and $N_f = 2$). The vertical bands indicate our estimates (19) and (24). The lower part shows results obtained on the basis of χ PT or from QCD sum rules, as well as the most recent estimate of the Particle Data Group.

Inserting the estimates (15), the LO prediction becomes

$$\frac{m_s}{m_{ud}} \stackrel{\text{LO}}{=} 25.9(1). \quad (23)$$

The quoted uncertainty does not include an estimate for the higher order contributions, but only accounts for the error bars in the coefficients, which is dominated by the one in the estimate given for ϵ_{π^0} . The result shows that, at the accuracy reached in lattice determinations of the ratio m_s/m_{ud} , the uncertainties due to the electromagnetic corrections is smaller than the systematic errors from other sources.

The lattice results in Table 3 indicate that the corrections generated by the non-leading terms of the chiral perturbation series are remarkably small, in the range 5–11%. Despite the fact that the SU(3) flavour symmetry breaking effects in the Nambu-Goldstone boson masses are very large ($M_K^2 \simeq 13 M_\pi^2$), the mass spectrum of the pseudoscalar octet obeys the SU(3)×SU(3) formula (21) very well.

Our average for m_s/m_{ud} is based on the results of MILC 09A and RBC/UKQCD 10A – the value quoted by HPQCD 10 does not represent independent information as it relies on the result for m_s/m_{ud} obtained by the MILC collaboration. Adding the statistical and systematic errors in quadrature, we obtain a good fit with $m_s/m_{ud} = 27.39(23)$ and $\chi^2 = 0.2$ for 2 data points and one free parameter. The fit is dominated by MILC 09A. Since the errors associated with renormalization drop out in the ratio, the uncertainties are even smaller than in the case

of the quark masses themselves: the above number for m_s/m_{ud} amounts to an accuracy of 0.8%. Again, the results of the BMW collaboration are not included in the fit because they are not yet published. The result reported in BMW 10A, 10B, $m_s/m_{ud} = 27.53(22)$, is perfectly consistent with the above average and reaches comparable accuracy.

At this level of precision, the uncertainties in the electromagnetic and strong isospin breaking corrections are not completely negligible. The error estimate in the LO result (23) indicates the expected order of magnitude. The uncertainties in m_s and m_{ud} associated with the heavy sea quarks cancel at least partly. In view of this, we are convinced that our final estimate,

$$N_f = 2 + 1 : \quad \frac{m_s}{m_{ud}} = 27.4(4), \quad (24)$$

is on the conservative side – it corresponds to an accuracy of 1.5%.

The lattice results show that the LO prediction of χ PT in (23) receives only small corrections from higher orders of the chiral expansion: according to (24), these generate a shift of $5.8 \pm 1.5\%$. Our estimate does therefore not represent a very sharp determination of the higher order contributions. Note however, that in comparison with the value $m_s/m_{ud} = 26(4)$ quoted by the Particle Data Group [122], the uncertainty is reduced by a factor of 10.

The ratio m_s/m_{ud} can also be extracted from the masses of the neutral Nambu-Goldstone bosons: neglecting effects of order $(m_u - m_d)^2$ also here, the leading order formula reads $m_s/m_{ud} \stackrel{\text{LO}}{=} \frac{3}{2} \hat{M}_\eta^2 / \hat{M}_\pi^2 - \frac{1}{2}$. Numerically, this gives $m_s/m_{ud} \stackrel{\text{LO}}{=} 24.2$. The relation has the advantage that the e.m. corrections are expected to be much smaller here, but it is more difficult to calculate the η -mass on the lattice. The comparison with (24) shows that, in this case, the contributions of NLO are somewhat larger: $13 \pm 2\%$.

3.4 Lattice determination of m_u and m_d

The determination of m_u and m_d separately requires additional input. MILC 09A [59] uses the mass difference between K^0 and K^+ , from which they subtract electromagnetic effects, using Dashen's theorem with corrections, as discussed in section 3.1. The up and down sea quarks remain degenerate in their calculation, fixed to the value of m_{ud} obtained from M_{π^0} . Instead of subtracting electromagnetic effects using phenomenology, RBC 07 [73] and Blum 10 [74] actually include a quenched electromagnetic field in their calculation. This means that their results include corrections to Dashen's theorem, albeit only in the presence of quenched electromagnetism. Since the up and down quarks in the sea are treated as degenerate, very small isospin corrections are neglected, as in MILC's calculation. The results are summarized in Table 4.

In order to discuss these results, we consider the LO formula

$$\frac{m_u}{m_d} \stackrel{\text{LO}}{=} \frac{\hat{M}_{K^+}^2 - \hat{M}_{K^0}^2 + \hat{M}_{\pi^+}^2}{\hat{M}_{K^0}^2 - \hat{M}_{K^+}^2 + \hat{M}_{\pi^+}^2}. \quad (25)$$

Using equations (12)–(14) to express the meson masses in QCD in terms of the physical ones and linearizing in the corrections, this relation takes the form

$$\frac{m_u}{m_d} \stackrel{\text{LO}}{=} 0.558 - 0.084 \epsilon - 0.02 \epsilon_{\pi^0} + 0.11 \epsilon_m. \quad (26)$$

Inserting the estimates (15) and adding errors in quadrature, the LO prediction becomes

$$\frac{m_u}{m_d} \stackrel{\text{LO}}{=} 0.50(4). \quad (27)$$

Collaboration	Ref.	publication status	chiral extrapolation	continuum extrapolation	finite volume	renormalization	running	m_u	m_d	m_u/m_d
HPQCD 10 [‡]	[104]	P	●	★	★	★	–	2.01(14)	4.77(15)	
BMW 10A, 10B ⁺	[65, 105]	P	★	★	★	★	<i>a</i>	2.15(03)(10)	4.79(07)(12)	0.448(06)(29)
Blum 10 [†]	[74]	P	●	■	●	★	–	2.24(10)(34)	4.65(15)(32)	0.4818(96)(860)
MILC 09A	[59]	C	●	★	★	●	–	1.96(0)(6)(10)(12)	4.53(1)(8)(23)(12)	0.432(1)(9)(0)(39)
MILC 09	[6]	A	●	★	★	●	–	1.9(0)(1)(1)(1)	4.6(0)(2)(2)(1)	0.42(0)(1)(0)(4)
MILC 04, HPQCD/ MILC/UKQCD 04	[77, 111]	A	●	●	●	■	–	1.7(0)(1)(2)(2)	3.9(0)(1)(4)(2)	0.43(0)(1)(0)(8)
RBC 07 [†]	[73]	A	■	■	★	★	–	3.02(27)(19)	5.49(20)(34)	0.550(31)

[‡] Values obtained by combining the HPQCD 10 result for m_s with the MILC 09 results for m_s/m_{ud} and m_u/m_d .

⁺ The fermion action used is tree-level improved.

[†] The calculation includes quenched e.m. effects.

a The masses are renormalized and run non-perturbatively up to a scale of 4 GeV in the $N_f = 3$ RI/MOM scheme. In this scheme, non-perturbative and N³LO running for the quark masses are shown to agree from 6 GeV down to 3 GeV to better than 1% [105].

Table 4: Lattice results for m_u , m_d and m_u/m_d , together with the colour coding of the calculation used to obtain them. The upper part of the table lists results obtained with $N_f = 2 + 1$, while the lowest row represents a calculation with $N_f = 2$.

Again, the quoted error exclusively accounts for the errors attached to the estimates (12) - contributions of non-leading order are ignored. The uncertainty in the leading order prediction is dominated by the one in the coefficient ϵ , which specifies the difference between the mass splittings generated by the e.m. interaction in the kaon and pion multiplets. Since the input $\epsilon = 1.2(5)$ used in MILC 09A [59] differs from the results $\epsilon = 0.13(4)$ and $\epsilon = 0.5(1)$ obtained by RBC 07 [73] and Blum 10 [74], respectively, it does not come as a surprise that the values for m_u/m_d are different. Evaluating the relation (26) for these values of ϵ and neglecting the self-energies of the neutral particles, we obtain $m_u/m_d = 0.46(4)$, $0.547(3)$ and $0.52(1)$ for MILC 09A, RBC 07 and Blum 10, respectively. Within errors, these numbers agree with the values for m_u/m_d quoted in the last column of Table 4. This indicates that, as in the case of m_s/m_{ud} , the corrections to the leading order prediction are small.

The uncertainties in the lattice results discussed so far for the ratio m_u/m_d are dominated by those in the e.m. contributions to the meson masses. Given the exploratory nature of the RBC 07 calculation, we do not draw a conclusion concerning the values of m_u and m_d obtained with $N_f = 2$. As discussed in section 3.3.2, the results of Blum 10 do not pass our selection criteria either. We therefore resort to the phenomenological estimates of the electromagnetic self-energies discussed in section 3.1 and use the MILC data for $N_f = 2 + 1$ to assess the size of the corrections from higher orders of the chiral expansion. With this input, we can calculate the mass ratio of the two lightest quarks, with the result $m_u/m_d = 0.47(4)$. The two individual masses can then be worked out from the estimate (20) for their mean. The result reads

$$N_f = 2 + 1 : m_u = 2.19(15) \text{ MeV}, m_d = 4.67(20) \text{ MeV}, \frac{m_u}{m_d} = 0.47(4). \quad (28)$$

These estimates have uncertainties of order 7%, 4% and 9%, respectively.

In contrast to the situation with the ratio m_s/m_{ud} , the error in the result for m_u/m_d is totally dominated by the uncertainties in the input used for the electromagnetic corrections. In fact, the comparison of equations (27) and (28) indicates that more than half of the difference between the prediction $m_u/m_d = 0.558$ obtained from Weinberg's mass formulae [128] and the result for m_u/m_d obtained on the lattice stems from electromagnetism – the higher orders in the chiral perturbation series only generate a small correction.

To determine m_u/m_d , BMW 10A, 10B [65, 105] follow a slightly different strategy. They obtain this ratio from their result for m_s/m_{ud} combined with a phenomenological determination of the isospin breaking quark mass ratio $Q = 22.3(8)$ from $\eta \rightarrow 3\pi$ decays [70]. In fact, as discussed in section 3.5, the central value of the e.m. parameter ϵ in (15) is taken from the same source. Their results for m_u/m_d , m_u and m_d are thus correlated with our estimates in (28) and are compatible with them, but are more precise.

In view of the fact that a *massless up quark* would solve the strong CP-problem, many authors have considered this an attractive possibility, but the results presented above exclude this possibility: the value of m_u in (28) differs from zero by 15 standard deviations. We conclude that nature solves the strong CP-problem differently. This conclusion relies on lattice calculations of kaon masses and on the phenomenological estimates of the e.m. self-energies discussed in section 3.1. The uncertainties therein currently represent the limiting factor in determinations of m_u and m_d . As demonstrated in [72–74], lattice methods can be used to calculate the e.m. self-energies. Further progress on the determination of the light quark masses hinges on an improved understanding of the e.m. effects.

3.5 Estimates for R and Q

The quark mass ratios

$$R \equiv \frac{m_s - m_{ud}}{m_d - m_u} \quad \text{and} \quad Q^2 \equiv \frac{m_s^2 - m_{ud}^2}{m_d^2 - m_u^2} \quad (29)$$

compare SU(3) breaking with isospin breaking. The quantity Q is of particular interest because of a low energy theorem [132], which relates it to a ratio of meson masses,

$$Q_M^2 \equiv \frac{\hat{M}_K^2}{\hat{M}_\pi^2} \cdot \frac{\hat{M}_K^2 - \hat{M}_\pi^2}{\hat{M}_{K^0}^2 - \hat{M}_{K^+}^2}, \quad \hat{M}_\pi^2 \equiv \frac{1}{2}(\hat{M}_{\pi^+}^2 + \hat{M}_{\pi^0}^2), \quad \hat{M}_K^2 \equiv \frac{1}{2}(\hat{M}_{K^+}^2 + \hat{M}_{K^0}^2). \quad (30)$$

Chiral symmetry implies that the expansion of Q_M^2 in powers of the quark masses (i) starts with Q^2 and (ii) does not receive any contributions at NLO:

$$Q_M \stackrel{\text{NLO}}{=} Q. \quad (31)$$

Inserting the estimates for the mass ratios m_s/m_{ud} , and m_u/m_d given in equations (24) and (28), respectively, we obtain

$$R = 36.6(3.8), \quad Q = 22.8(1.2). \quad (32)$$

As is the case with the ratio m_u/m_d , the errors are dominated by the uncertainties in the electromagnetic corrections. To investigate the sensitivity to the latter, we use χ PT to express the quark mass ratios in terms of the pion and kaon masses in QCD and then again

use equations (12)–(14) to relate the QCD masses to the physical ones. Linearizing in the corrections, this leads to

$$\begin{aligned} R &\stackrel{\text{LO}}{=} 43.9 - 10.8 \epsilon + 0.2 \epsilon_{\pi^0} - 0.2 \epsilon_{K^0} - 10.6 \epsilon_m, \\ Q &\stackrel{\text{NLO}}{=} 24.3 - 3.0 \epsilon + 0.9 \epsilon_{\pi^0} - 0.1 \epsilon_{K^0} + 2.1 \epsilon_m. \end{aligned} \tag{33}$$

While the first relation only holds to LO of the chiral perturbation series, the second remains valid at NLO, on account of the low energy theorem mentioned above. The first terms on the right hand side represent the values of R and Q obtained with the Weinberg leading order formulae for the quark mass ratios [128]. Inserting the estimates (15), we find that the e.m. corrections lower the Weinberg values to $R \stackrel{\text{LO}}{=} 36.7(7.6)$ and $Q \stackrel{\text{NLO}}{=} 22.3(2.1)$, respectively. The comparison with the full results quoted above shows that there is little room for the higher order terms in the chiral expansion.

As mentioned in section 3.1, there is a phenomenological determination of Q based on the decay $\eta \rightarrow 3\pi$ [133, 134]. The key point is that the transition $\eta \rightarrow 3\pi$ violates isospin conservation. The dominating contribution to the transition amplitude stems from the mass difference $m_u - m_d$. At NLO of χ PT, the QCD part of the amplitude can be expressed in a parameter free manner in terms of Q . It is well-known that the electromagnetic contributions to the transition amplitude are suppressed (a thorough recent analysis is given in [135]). This implies that the result for Q is less sensitive to the electromagnetic uncertainties than the value obtained from the masses of the Nambu-Goldstone bosons. For a recent update of this determination and for further references to the literature, we refer to [136]. Using dispersion theory to pin down the momentum dependence of the amplitude, the observed decay rate implies $Q = 22.3(8)$ (since the uncertainty quoted in [136] does not include an estimate for all sources of error, we have retained the error estimate given in [129], which is twice as large). The formulae for the corrections of NNLO are available also in this case [137] – the poor knowledge of the effective coupling constants, particularly of those that are relevant for the dependence on the quark masses, is currently the limiting factor encountered in the application of these formulae.

As was to be expected, the central value of Q obtained from η -decay agrees exactly with the central value obtained from the low energy theorem: we have used that theorem to estimate the coefficient ϵ , which dominates the e.m. corrections. Using the numbers for ϵ_m , ϵ_{π^0} and ϵ_{K^0} in (15) and adding the corresponding uncertainties in quadrature to those in the phenomenological result for Q , we obtain

$$\epsilon \stackrel{\text{NLO}}{=} 0.70(28). \tag{34}$$

The estimate (15) for the size of the coefficient ϵ is taken from here, except that the error bar is stretched, to account for the fact that the above relation is valid only up to NNLO contributions.

The MILC data offer a welcome check on the size of the neglected higher orders: with the input $\epsilon = 1.2(5)$ and $\epsilon_{\pi^0} = \epsilon_{K^0} = \epsilon_m = 0$ used in the MILC analysis, equation (34) implies $Q_M = 21.3(1.0)$. On the other hand, inserting the MILC results for the quark mass ratios m_s/m_{ud} and m_u/m_d (see Tables 3 and 4) in the definition of Q , equation (29), and ignoring a possible correlation between the results for the two ratios, we get $Q = 21.7(1.1)$. For MILC 09A, the central values of Q_M and Q thus agree to an accuracy of 2%, indicating that the corrections of NNLO or higher are smaller than the uncertainty of the result.

In contrast to this, the picture which follows from the numbers obtained with the $N_f = 2$ simulation of RBC 07 [73] is difficult to understand. Repeating the above calculation with the estimate $\epsilon = 0.13(4)$ that corresponds to the kaon self-energy difference obtained in this reference and again neglecting the other terms in equation (34), we get $Q_M = 23.9(1)$, while the value of Q that follows from the quark mass ratios m_s/m_{ud} and m_u/m_d given in the same reference, implies $Q = 26.1(1.2)$. A difference of this size calls for large contributions of NNLO, in conflict with the data analysis, which assumes that it is meaningful to truncate the chiral series at NLO.

The recent extension of this calculation to $N_f = 2 + 1$ dynamical flavours described in [74] appears to solve the puzzle. The values obtained for the kaon and pion self-energies obtained in this reference imply $\epsilon = 0.5(1)$, $\epsilon_m = 0.04(5)$. Inserting this in equation (34) and neglecting the self-energies of the neutral particles, we obtain $Q_M = 22.8(3)$, to be compared with the value $Q = 23.9(3.4)$ that follows from the quark mass ratios given in the same reference. This implies that the NNLO corrections to the low energy theorem (31) are too small to be seen at the accuracy of this calculation: $Q_M/Q = 0.96(12)$.

The determination of R and Q in BMW 10A, 10B [65, 105] relies on the phenomenological value of Q discussed above [70] – their results do not bring new information on Q . The value of R which follows from their result for the ratio m_s/m_{ud} and the input used for Q is $R = 34.9(2.5)$, slightly different from our estimate in (32), but perfectly compatible with it.⁷

Our final results for the masses m_u , m_d , m_s and the mass ratios m_u/m_d , m_s/m_{ud} , R , Q are collected in the table below.

N_f	m_u	m_d	m_s	m_{ud}	m_u/m_d	m_s/m_{ud}	R	Q
2+1	2.19(15)	4.67(20)	94(3)	3.43(11)	0.47(4)	27.4(4)	36.6(3.8)	22.8(1.2)
2	–	–	95(6)	3.6(2)	–	27.3(9)	–	–

Table 5: Our estimates for the masses of the three lightest quarks, and related ratios (the masses refer to the $\overline{\text{MS}}$ scheme at running scale $\mu = 2 \text{ GeV}$ for $N_f = 3$, the numerical values are given in MeV units).

⁷Repeating the calculation with the same input for Q , but replacing the BMW result for m_s/m_{ud} by our estimate in equation (24), we obtain $R = 35.0(2.6)$.

4 $|V_{ud}|$ and $|V_{us}|$

4.1 Experimental information concerning $|V_{ud}|$, $|V_{us}|$, $f_+(0)$ and f_K/f_π

The following review relies on the fact that precision data on kaon decays very accurately determine the product $|V_{us}|f_+(0)$ and the ratio $|V_{us}f_K|/|V_{ud}f_\pi|$ [138]:

$$|V_{us}|f_+(0) = 0.2163(5), \quad \left| \frac{V_{us}f_K}{V_{ud}f_\pi} \right| = 0.2758(5). \quad (35)$$

V_{ud} and V_{us} are elements of the Cabibbo-Kobayashi-Maskawa matrix and $f_+(t)$ represents one of the form factors relevant for the semileptonic decay $K^0 \rightarrow \pi^- \ell \nu$, which depends on the momentum transfer t between the two mesons. What matters here is the value at $t = 0$: $f_+(0) \equiv f_+^{K^0\pi^-}(t)|_{t \rightarrow 0}$. The pion and kaon decay constants are defined by⁸

$$\langle 0 | \bar{d}\gamma_\mu\gamma_5 u | \pi^+(p) \rangle = i p_\mu f_\pi, \quad \langle 0 | \bar{s}\gamma_\mu\gamma_5 u | K^+(p) \rangle = i p_\mu f_K.$$

In this normalization, $f_\pi \simeq 130$ MeV, $f_K \simeq 155$ MeV.

The measurement of $|V_{ud}|$ based on superallowed nuclear β transitions has now become remarkably precise. The result of the recent update of Hardy and Towner [50], which is based on 20 different superallowed transitions, reads⁹

$$|V_{ud}| = 0.97425(22). \quad (36)$$

The matrix element $|V_{us}|$ can be measured in τ decays [148–151]. Separating the inclusive decay $\tau \rightarrow \text{hadrons} + \nu$ into non-strange and strange final states, Gamiz et al. [152] obtain

$$|V_{us}| = 0.2165(26)_{exp}(5)_{th}. \quad (37)$$

Maltman et al. [153] arrive at very similar values.

As recently pointed out by Maltman [150], the theoretical uncertainties of the analysis which underlies the result (37) can be reduced by invoking the experimental information about the spectral function of the electromagnetic current, but the experimental uncertainties then play a more important role. Applying this method, the outcome for $|V_{us}|$ reads [154]

$$|V_{us}| = 0.2208(39). \quad (38)$$

In principle, τ decay offers a clean measurement of $|V_{us}|$, but a number of open issues yet remain to be clarified. In particular, the measured exclusive decay rates for $\tau \rightarrow \pi\nu$ and $\tau \rightarrow K\nu$ are below the Standard Model predictions, which determine these rates in terms

⁸The pion decay constant represents a QCD-matrix-element – in the full Standard Model, the one-pion state is not a meaningful notion: the correlation function of the charged axial current does not have a pole at $p^2 = M_{\pi^+}^2$, but a branch cut extending from $M_{\pi^+}^2$ to ∞ . The analytic properties of the correlation function and the problems encountered in the determination of f_π are thoroughly discussed in [139]. The "experimental" value of f_π depends on the convention used when splitting the sum $\mathcal{L}_{\text{QCD}} + \mathcal{L}_{\text{QED}}$ into two parts (compare section 3.1). The lattice determinations of f_π do not yet reach the accuracy where this is of significance, but at the precision claimed by the Particle Data Group [140], the numerical value does depend on the convention used [67–69, 139]. A recent analysis of the electromagnetic and strong isospin breaking effects in the leptonic decays of the pseudoscalar mesons is given in [141].

⁹It is not a trivial matter to perform the data analysis at this precision. In particular, isospin-breaking effects need to be properly accounted for [142–146]. For a review of recent work on this issue, we refer to [147].

Collaboration	Ref.	N_f	publication status	chiral extrapolation	continuum extrapolation	finite volume errors	$f_+(0)$
RBC/UKQCD 10	[158]	2+1	A	●	■	★	0.9599(34) ⁽⁺³¹⁾ ₍₋₄₇₎ (14)
RBC/UKQCD 07	[159]	2+1	A	●	■	★	0.9644(33)(34)(14)
ETM 10D	[160]	2	C	●	★	●	0.9544(68) _{stat}
ETM 09A	[161]	2	A	●	●	●	0.9560(57)(62)
QCDSF 07	[162]	2	C	■	■	★	0.9647(15) _{stat}
RBC 06	[163]	2	A	■	■	★	0.968(9)(6)
JLQCD 05	[164]	2	C	■	■	★	0.967(6), 0.952(6)

Table 6: Colour code for the data on $f_+(0)$.

of the same matrix elements $|V_{ud}f_\pi|$ and $|V_{us}f_K|$ that govern the leptonic decays $\pi \rightarrow \mu\nu$ and $K \rightarrow \mu\nu$ (violation of τ/μ universality). On the other hand, the value obtained for $|V_{us}f_K|/|V_{ud}f_\pi|$ from the ratio of the tau decay rates is perfectly consistent with the one from the leptonic π and K -decays quoted in (35), but this does not shed any light on the value of $|V_{us}|$. It is important to pursue the measurement of modes that have previously been studied only with low statistics (especially the large mode $K^0\pi^0\pi^-$), as well as those of higher multiplicity (final states with more than two pions, for instance). The recent developments on the theoretical side [155–157] also need to be pursued. The most interesting possibility is that τ decay involves new physics, but more work is required before τ decay becomes a competitive source of information about the CKM matrix elements.

4.2 Lattice results for $f_+(0)$ and f_K/f_π

The traditional way of determining $|V_{us}|$ relies on using theory for the value of $f_+(0)$, invoking the Ademollo-Gatto theorem [165]. Since this theorem only holds to leading order of the expansion in powers of m_u , m_d and m_s , theoretical models are used to estimate the corrections. Lattice methods have now reached the stage where quantities like $f_+(0)$ or f_K/f_π can be determined to good accuracy. As a consequence, the uncertainties inherent in the theoretical estimates for the higher order effects in the value of $f_+(0)$ do not represent a limiting factor any more and we shall therefore not invoke those estimates. Also, we will use the experimental results based on nuclear β decay and τ decay exclusively for comparison – the main aim of the present review is to assess the information gathered with lattice methods and to use it for testing the consistency of the SM and its potential to provide constraints for its extensions.

The database underlying the present review of $f_+(0)$ and f_K/f_π is listed in Tables 6 and 7. The properties of the lattice data play a crucial role for the conclusions to be drawn from these results: range of M_π , size of LM_π , continuum extrapolation, extrapolation in the quark masses, finite size effects, etc. The key features of the various data sets are characterized by means of the colour code specified in section 2.

The quantity $f_+(0)$ represents a matrix element of a strangeness changing null plane charge, $f_+(0) = (K|Q^{us}|\pi)$. The vector charges obey the commutation relations of the Lie algebra of SU(3), in particular $[Q^{us}, Q^{su}] = Q^{uu-ss}$. This relation implies the sum rule $\sum_n |(K|Q^{us}|n)|^2 - \sum_n |(K|Q^{su}|n)|^2 = 1$. Since the contribution from the one-pion intermediate state to the first sum is given by $f_+(0)^2$, the relation amounts to an exact representation for this quantity [166]:

$$f_+(0)^2 = 1 - \sum_{n \neq \pi} |(K|Q^{us}|n)|^2 + \sum_n |(K|Q^{su}|n)|^2. \quad (39)$$

While the first sum on the right extends over non-strange intermediate states, the second runs over exotic states with strangeness ± 2 and is expected to be small compared to the first.

The expansion of $f_+(0)$ in powers of m_u , m_d and m_s starts with $f_+(0) = 1 + f_2 + f_4 + \dots$ [91]. Since all of the low energy constants occurring in f_2 can be expressed in terms of M_π , M_K , M_η and f_π [167], the correction of NLO is known. In the language of the sum rule (39), f_2 stems from non-strange intermediate states with three mesons. Like all other non-exotic intermediate states, it lowers the value of $f_+(0)$: $f_2 = -0.023$. The corresponding expressions have also been derived in quenched or partially quenched chiral perturbation theory [168]. At the same order in the SU(2) expansion [169], $f_+(0)$ is parametrized in terms of M_π and two *a priori* unknown parameters. The latter can be determined from the dependence of the lattice results on the masses of the quarks. Note that any calculation that relies on the χ PT formula for f_2 is subject to the uncertainties inherent in NLO results: instead of using the physical value of the pion decay constant f_π , one may, for instance, work with the constant f_0 that occurs in the effective Lagrangian and represents the value of f_π in the chiral limit. Although trading f_π for f_0 in the expression for the NLO term affects the result only at NNLO, it may make a significant numerical difference in calculations where the latter are not explicitly accounted for (the lattice results concerning the value of the ratio f_π/f_0 are reviewed in section 5.2).

The lattice results shown in the left panel of Figure 4 indicate that the higher order contributions $\Delta f \equiv f_+(0) - 1 - f_2$ are negative and thus amplify the effect generated by f_2 . This confirms the expectation that the exotic contributions are small. The entries in the lower part of the left panel represent various model estimates for f_4 . In [179] the symmetry breaking effects are estimated in the framework of the quark model. The more recent calculations are more sophisticated, as they make use of the known explicit expression for the $K_{\ell 3}$ form factors to NNLO of χ PT [180, 181]. The corresponding formula for f_4 accounts for the chiral logarithms occurring at NNLO and is not subject to the ambiguity mentioned above. The numerical result, however, depends on the model used to estimate the low energy constants occurring in f_4 [181–184]. The figure indicates that the most recent numbers obtained in this way correspond to a positive rather than a negative value for Δf .

A lattice determination of the low energy constants that occur in f_4 would be very useful to identify the origin of the problem. Lattice results concerning the dependence of the scalar form factor on the momentum transfer would also very useful, in particular they might help sorting out the discrepancies in the experimental results for the slope of this form factor [185–188]. Note that when analyzing lattice data on the basis of the χ PT formulae, the loop integrals occurring therein need to be evaluated for the masses at which the Nambu-Goldstone bosons propagate in a given lattice simulation.¹⁰

¹⁰Fortran programs for the numerical evaluation of the form factor representation in [181] are available on

Collaboration	Ref.	N_f	publication status	chiral extrapolation	continuum extrapolation	finite volume errors	f_K/f_π
ETM 10E	[170]	2+1+1	C	●	●	●	1.224(13) _{stat}
MILC 10	[171]	2+1	C	●	★	★	1.197(2)(⁺³ ₋₇)
RBC/UKQCD 10A	[106]	2+1	P	●	●	★	1.204(7)(25)
BMW 10	[41]	2+1	A	★	★	★	1.192(7)(6)
JLQCD/TWQCD 09A	[172]	2+1	C	●	■	■	1.210(12) _{stat}
MILC 09A	[59]	2+1	C	●	★	★	1.198(2)(⁺⁶ ₋₈)
MILC 09	[6]	2+1	A	●	★	★	1.197(3)(⁺⁶ ₋₁₃)
Aubin 08	[173]	2+1	C	●	●	●	1.191(16)(17)
PACS-CS 08, 08A	[63, 174]	2+1	A	★	■	■	1.189(20)
RBC/UKQCD 08	[108]	2+1	A	●	■	★	1.205(18)(62)
HPQCD/UKQCD 07	[175]	2+1	A	●	★	●	1.189(2)(7)
NPLQCD 06	[176]	2+1	A	●	■	■	1.218(2)(⁺¹¹ ₋₂₄)
MILC 04	[77]	2+1	A	★	●	●	1.210(4)(13)
ETM 10D	[160]	2	C	●	★	●	1.190(8) _{stat}
ETM 09	[177]	2	A	●	★	●	1.210(6)(15)(9)
QCDSF/UKQCD 07	[178]	2	C	●	●	★	1.21(3)

Table 7: Colour code for the data on f_K/f_π .

4.3 Direct determination of $f_+(0)$ and f_K/f_π

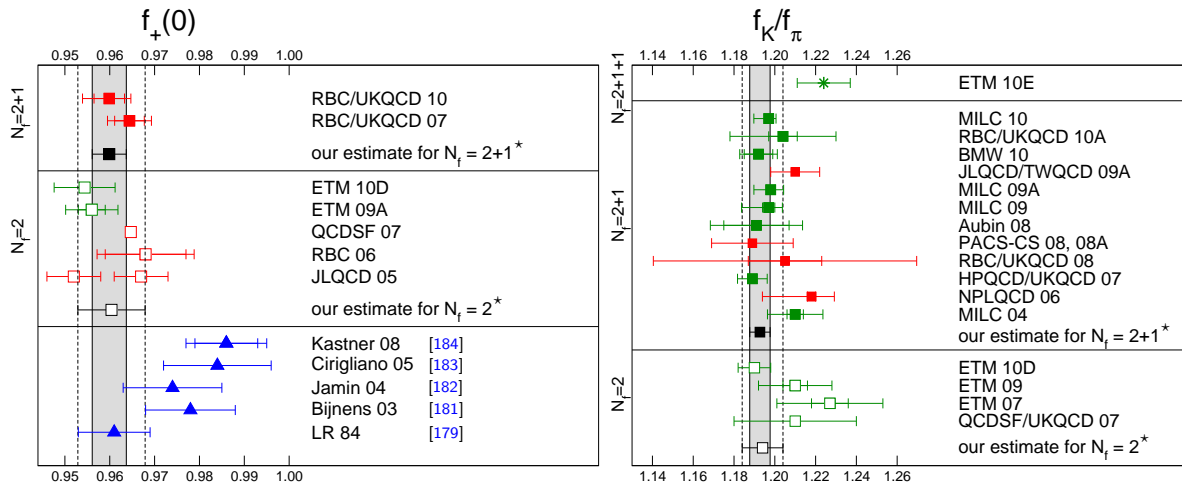
Figure 4 shows that the lattice results for $f_+(0)$ and f_K/f_π obtained by the various collaborations which do a comprehensive error analysis are consistent with each other. We now proceed to form the corresponding averages, separately for the data with $N_f = 2 + 1$ and $N_f = 2$ dynamical flavours. As will be discussed in detail in section 4.5, CKM unitarity and experiment correlate $f_+(0)$ with f_K/f_π . Indeed, the lattice data are consistent also with this correlation. First, however, we analyze the lattice information available separately for $f_+(0)$ and for f_K/f_π . We refer to results obtained in this way as "direct" determinations.

The colour code in Table 5 shows that for $f_+(0)$, presently only the results of the ETM collaboration with $N_f = 2$ dynamical flavours of fermions are without a red tag. In the following, we rely on the published work ETM 09A [161]. The table contains two data sets with $N_f = 2 + 1$, but since one represents an update of the other, we only discuss RBC/UKQCD 10. These data carry a red tag, because a systematic study of cut-off effects is missing. These two computations of $f_+(0)$ are the most advanced ones and we quote their results:

$$\begin{aligned}
f_+(0) &= 0.9599(34)(⁺³¹₋₄₇)(14), & (\text{direct, } N_f = 2 + 1), \\
f_+(0) &= 0.9560(57)(62), & (\text{direct, } N_f = 2).
\end{aligned}
\tag{40}$$

The first error in the result quoted for $N_f = 2 + 1$ is statistical, the second is due to the uncertainties in the chiral extrapolation of the lattice data and the third is an estimate of

request from Johan Bijnens.



* Estimates obtained from an analysis of the lattice data within the Standard Model, see section 4.5.

Figure 4: Comparison of lattice results (red squares) for $f_+(0)$ and f_K/f_π with various model estimates based on χ PT (blue triangles). Full and empty squares represent simulations with $N_f = 2 + 1$ and $N_f = 2$, respectively. The vertical bands indicate our estimates.*

potential discretization effects. Flavour symmetry implies that if m_{ud} is set equal to m_s , the lattice data yield $f_+(0) = 1$, irrespective of the lattice spacing or the size of the box and for any value of m_s . Cut-off effects can therefore only affect the difference $1 - f_+(0)$, which turns out to be about 0.04. Indeed, the estimate provided by RBC/UKQCD 10 for the uncertainties due to discretization effects shows that these are sub-dominant: inflating the corresponding error by a factor of up to 2 barely affects the net systematic uncertainty.

In the result quoted for $N_f = 2$, the brackets indicate the statistical and systematic errors, respectively. The ETM collaboration provides a more comprehensive study of the systematics by presenting results for three lattice spacings [189] and simulating at lighter pion masses (down to $M_\pi = 260$ MeV). This allows to better constrain the chiral extrapolation, using both SU(3) [167] and SU(2) [169] chiral perturbation theory. Moreover, a rough estimate for the size of the effects due to quenching the strange quark is given, based on the comparison of the result for $N_f = 2$ dynamical quark flavours [177] with the one in the quenched approximation, obtained earlier by the SPQcdR collaboration [190].

The quality criteria laid out in section 2 require a systematic study of lattice artifacts. As indicated by the colour code in Table 6, the errors due to the continuum extrapolation yet need to be investigated in more detail for the data with $N_f = 2 + 1$, while for $N_f = 2$, where the quoted uncertainties are larger, these errors are under somewhat better control. The value

$$f_+(0) = 0.956(8) \quad (\text{our estimate, direct}) \quad (41)$$

covers both results in equation (40). In our opinion, it represents a conservative estimate for the range permitted by the presently available direct determinations of $f_+(0)$ in lattice QCD, not only for $N_f = 2$, but also for $N_f = 2 + 1$.

For f_K/f_π , Table 7 contains several simulations with $N_f = 2+1$ dynamical quark flavours. The latest update of the MILC program is reported in MILC 10 [171]. We use the results quoted there when forming averages. Three further data sets meet the criteria formulated in

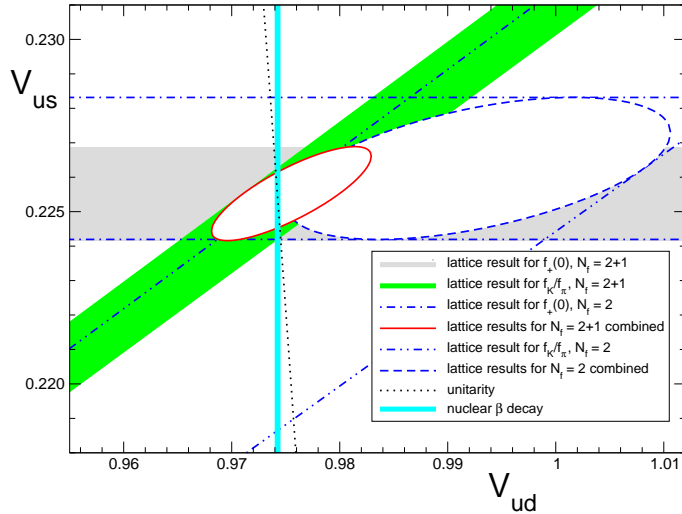


Figure 5: The plot compares the information for $|V_{ud}|$, $|V_{us}|$ obtained on the lattice with the experimental result extracted from nuclear β transitions. The dotted arc indicates the correlation between $|V_{ud}|$ and $|V_{us}|$ that follows if the three-flavour CKM-matrix is unitary.

the introduction: BMW 10 [41] and HPQCD/UKQCD 07 [175] with $N_f = 2 + 1$ and ETM 09 [177] with $N_f = 2$ dynamical flavours. We ignore possible correlations due to the fact that MILC 10 and HPQCD/UKQCD 07 have partly used the same set of gauge configurations and apply the procedure outlined in section 2.2 to the three sets with $N_f = 2 + 1$. The resulting fit is of good quality, with $f_K/f_\pi = 1.193(4)$ and $\chi^2 = 0.4$ for 3 data points and 1 free parameter. The systematic errors of the individual data sets are larger: 0.005, 0.007 and 0.006 for MILC 10, HPQCD/UKQCD 07 and BMW 10, respectively. Following the prescription of section 2.2, we replace the error by the smallest one of these numbers. Together with the ETM 09 result for $N_f = 2$, our estimates thus read

$$\begin{aligned} f_K/f_\pi &= 1.193(5), & (\text{direct}, N_f = 2 + 1), \\ f_K/f_\pi &= 1.210(6)(17), & (\text{direct}, N_f = 2). \end{aligned} \quad (42)$$

It is instructive to convert the above results for $f_+(0)$ and f_K/f_π into a corresponding range for the CKM matrix elements V_{ud} and V_{us} , using the relations (35). Consider first the results for $N_f = 2 + 1$. The range for $f_+(0)$ in (40) is mapped into the interval $V_{us} = 0.2255(14)$, depicted as a horizontal gray band in Figure 5, while the one for f_K/f_π in (42) is converted into $V_{us}/V_{ud} = 0.2312(11)$, shown as a green band. The red curve is the intersection of these two bands. More precisely, it represents the 68% likelihood contour, obtained by treating the above two results as independent measurements. A Gaussian in $f_+(0)$ corresponds to a Gaussian in the variable $1/V_{us}$. Since the width is small, the distribution in the variable V_{us} is also approximately Gaussian. The corresponding likelihood function is given by $\chi_a^2 = (V_{us} - 0.2255)^2/0.0014^2$. Likewise, a Gaussian in f_K/f_π is mapped into an approximately Gaussian distribution of the variable V_{us}/V_{ud} , with $\chi_b^2 = (V_{us}/V_{ud} - 0.2312)^2/0.0011^2$. Expressed in terms of the CKM matrix elements, the $N_f = 2 + 1$ results for $f_+(0)$ and f_K/f_π are thus characterized by the likelihood function $\chi^2 = \chi_a^2 + \chi_b^2$. The minimum occurs at the intersection of the centers of the two bands, where χ^2 vanishes. The contour shown is the line

Collaboration	Ref.	N_f	from	$ V_{us} $
MILC 10	[171]	2 + 1	f_K/f_π	0.2245(5)($^{+12}_{-5}$)
RBC/UKQCD 10A	[106]	2 + 1	f_K/f_π	0.2233(13)(44)
RBC/UKQCD 10	[158]	2 + 1	$f_+(0)$	0.2253(10)($^{+12}_{-8}$)
BMW 10	[41]	2 + 1	f_K/f_π	0.2254(13)(11)
HPQCD/UKQCD 07	[175]	2 + 1	f_K/f_π	0.2260(5)(13)
ETM 09	[177]	2	f_K/f_π	0.2222(11)(31)
ETM 09A	[161]	2	$f_+(0)$	0.2263(14)(15)

Table 8: Values of $|V_{us}|$ obtained from lattice determinations of $f_+(0)$ or f_K/f_π with CKM unitarity. The first (second) number in brackets represents the statistical (systematic) error.

where χ^2 differs from the minimum by unity. Values of V_{us} , V_{ud} in the region enclosed by this contour are consistent with the lattice data for $N_f = 2 + 1$, within one standard deviation. In particular, the plot shows that the nuclear β decay result for V_{ud} is perfectly consistent with these data.

Repeating the exercise with the $N_f = 2$ results leads to the dashed ellipse. The figure thus indicates that the data are consistent within errors. We conclude that, at the accuracy reached up to now for the quantities $f_+(0)$, f_K/f_π , V_{us} and V_{ud} , the distortions generated by the quenching of the strange quark are too small to be visible.

4.4 Testing the Standard Model

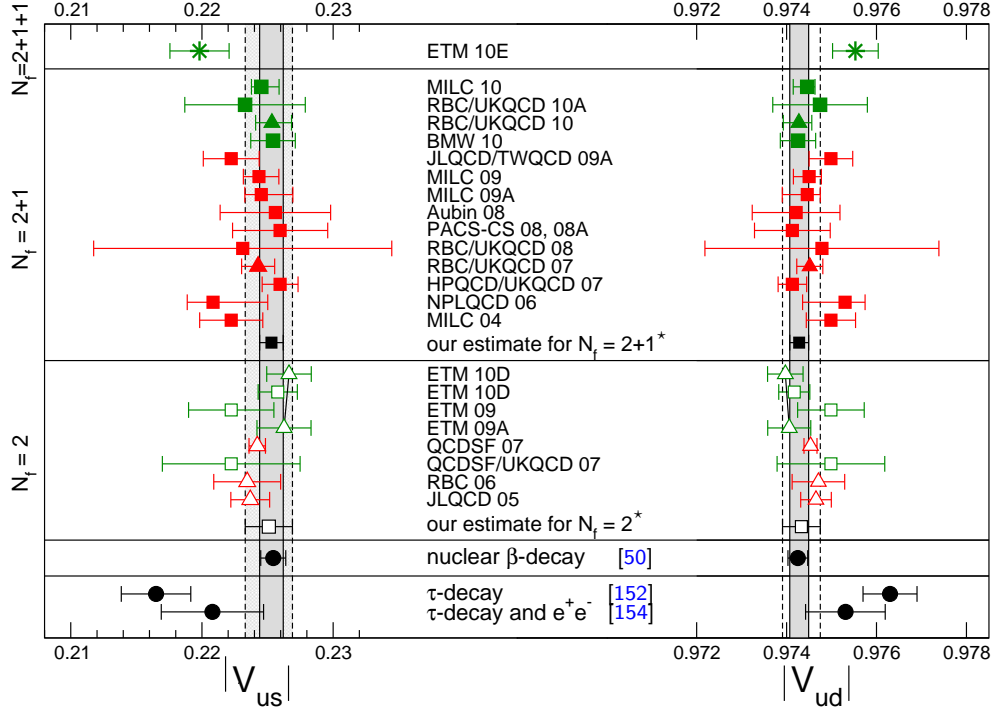
In the Standard Model, the CKM matrix is unitary. In particular, the elements of the first row obey

$$|V_u|^2 \equiv |V_{ud}|^2 + |V_{us}|^2 + |V_{ub}|^2 = 1. \quad (43)$$

The tiny contribution from $|V_{ub}|$ is known much better than needed in the present context: $|V_{ub}| = 3.89(44) \cdot 10^{-3}$ [191]. In the following, we first discuss the evidence for the validity of the relation (43) and only then use it to analyze the lattice data within the Standard Model.

In Figure 5, the correlation between V_{ud} and V_{us} imposed by the unitarity of the CKM matrix is indicated by a dotted arc (more precisely, in view of the uncertainty in V_{ub} , the correlation corresponds to a band of finite width, but the effect is too small to be seen here). The plot shows that the data for $N_f = 2 + 1$ are perfectly consistent with this constraint. Numerically, the outcome for the sum of the squares of the first row of the CKM matrix reads $|V_u|^2 = 1.002(15)$. The Standard Model thus passes a nontrivial test that exclusively involves lattice data and well-established kaon decay branching ratios. Combining the lattice results for $f_+(0)$ and f_K/f_π in (40) and (42) with the β -decay value of $|V_{ud}|$ quoted in (36), the test sharpens considerably: the lattice result for $f_+(0)$ leads to $|V_u|^2 = 1.0000(7)$, while the one for f_K/f_π implies $|V_u|^2 = 0.9999(6)$, thus confirming CKM unitarity at the permille level.

Repeating the analysis for $N_f = 2$, we find $|V_u|^2 = 1.037(36)$ with the lattice data alone. The number is somewhat larger than 1, in accordance with the fact that the dotted curve passes just outside the blue contour, but the difference barely exceeds one standard deviation. Moreover, it only concerns the comparison of the $N_f = 2$ results for $f_+(0)$



* Estimates obtained from an analysis of the lattice data within the Standard Model, see section 4.5.

Figure 6: Results for $|V_{us}|$ and $|V_{ud}|$ that follow from the lattice data for $f_+(0)$ (red triangles) and f_K/f_π (red squares), on the basis of the assumption that the CKM matrix is unitary. The black squares and the bands represent our estimates, obtained by combining these two different ways of measuring $|V_{us}|$ and $|V_{ud}|$ on a lattice. For comparison, the figure also indicates the results obtained if the data on nuclear β decay and τ decay are analyzed within the Standard Model.

with those for f_K/f_π . Taken by themselves, these results are perfectly consistent with the value of $|V_{ud}|$ found in nuclear β decay: combining this value with the data on $f_+(0)$ yields $|V_u|^2 = 1.0004(10)$, combining it with the data on f_K/f_π gives $|V_u|^2 = 0.9985(16)$.

Note that the above tests also offer a check of the basic hypothesis that underlies our analysis: we are assuming that the weak interaction between the quarks and the leptons is governed by the same Fermi constant as the one that determines the strength of the weak interaction among the leptons and determines the lifetime of the muon. In certain modifications of the Standard Model, this is not the case. In those models it need not be true that the rates of the decays $\pi \rightarrow \ell\nu$, $K \rightarrow \ell\nu$ and $K \rightarrow \pi\ell\nu$ can be used to determine the matrix elements $|V_{ud}f_\pi|$, $|V_{us}f_K|$ and $|V_{us}f_+(0)|$, respectively and that $|V_{ud}|$ can be measured in nuclear β decay. The fact that the lattice data are consistent with unitarity and with the value of $|V_{ud}|$ found in nuclear β decay indirectly also checks the equality of the Fermi constants.

4.5 Analysis within the Standard Model

The Standard Model implies that the CKM matrix is unitary. The precise experimental constraints quoted in (35) and the unitarity condition (43) then reduce the four quantities $|V_{ud}|, |V_{us}|, f_+(0), f_K/f_\pi$ to a single unknown: any one of these determines the other three within narrow uncertainties.

Figure 6 shows that the results obtained for $|V_{us}|$ and $|V_{ud}|$ from the data on f_K/f_π (red squares) are quite consistent with the determinations via $f_+(0)$ (red triangles). In order to calculate the corresponding average values, we restrict ourselves to those determinations that we have considered best in section 4.3. The corresponding results for $|V_{us}|$ are listed in Table 8 (the noise in the experimental numbers used to convert the values of $f_+(0)$ and f_K/f_π into values for $|V_{us}|$ is included in the statistical error).

We consider the fact that the results from the four $N_f = 2 + 1$ data sets RBC/UKQCD 10 [158], BMW 10 [41], MILC 10 [171] and HPQCD/UKQCD 07 [175] are consistent with each other to be an important reliability test of the lattice work. Treating the four sets as independent measurements, and applying the standard averaging procedure, we obtain a fit of good quality, with $|V_{us}| = 0.2253(6)$ and $\chi^2 = 0.6$ for 4 data points and 1 free parameter. The results listed in the upper half of Table 8 show, however, that the standard procedure underestimates the systematic uncertainties also in this case. Applying the prescription of section 2.2, we arrive at a somewhat larger error: $|V_{us}| = 0.2253(9)$. This result is indicated on the left hand side of Fig. 6 by the narrow vertical band. The broader band shows the corresponding value for $N_f = 2$ (standard error analysis, $|V_{us}| = 0.2253(17)$, with $\chi^2 = 1.2$ for 2 data points and 1 free parameter, $S = 1.09$). The figure shows that the result obtained for the data with $N_f = 2$ is perfectly consistent with the one found for $N_f = 2 + 1$.

Alternatively, we can solve the relations for $|V_{ud}|$ instead of $|V_{us}|$. Again, the result $|V_{ud}| = 0.97428(21)$ which follows from the lattice data with $N_f = 2 + 1$ is perfectly consistent with the value $|V_{ud}| = 0.97433(42)$ obtained from those with $N_f = 2$. The reduction of the uncertainties in the result for $|V_{ud}|$ due to CKM unitarity is to be expected from Figure 5: the unitarity condition reduces the region allowed by the lattice results to a nearly vertical interval.

Next, we determine the value of $f_+(0)$ that follows from the lattice data within the Standard Model. Using CKM unitarity to convert the lattice determinations of f_K/f_π into corresponding values for $f_+(0)$ and then combining these with the direct determinations of $f_+(0)$, we find $f_+(0) = 0.9599(38)$ from the data with $N_f = 2 + 1$ and $f_+(0) = 0.9604(75)$ for $N_f = 2$. The results are shown in the left panel of Fig. 4.

Finally, we work out the analogous Standard Model fits for f_K/f_π , converting the direct determinations of $f_+(0)$ into corresponding values for f_K/f_π and combining the outcome with the direct determinations of that quantity. The results read $f_K/f_\pi = 1.1927(50)$ for $N_f = 2 + 1$ and $f_K/f_\pi = 1.194(10)$ for $N_f = 2$, respectively; they are shown in the right panel of Fig. 4.

The results obtained by analyzing the lattice data in the framework of the Standard Model are collected in the upper half of Table 9. In the lower half of this table, we list the analogous results, found by working out the consequences of CKM-unitarity for the experimental values of $|V_{ud}|$ and $|V_{us}|$ obtained from nuclear β -decay and τ -decay, respectively. The comparison shows that the lattice result for $|V_{ud}|$ not only agrees very well with the totally independent determination based on nuclear β transitions, but is also remarkably precise. On the other hand, the values of $|V_{ud}|, f_+(0)$ and f_K/f_π which follow from the τ -decay data if the Standard

	Ref.	$ V_{us} $	$ V_{ud} $	$f_+(0)$	f_K/f_π
$N_f = 2 + 1$		0.2253(9)	0.97428(21)	0.9599(38)	1.1927(50)
$N_f = 2$		0.2251(18)	0.97433(42)	0.9604(75)	1.194(10)
β -decay	[50]	0.22544(95)	0.97425(22)	0.9595(46)	1.1919(57)
τ -decay	[152]	0.2165(26)	0.9763(6)	0.999(12)	1.244(16)
τ -decay	[154]	0.2208(39)	0.9753(9)	0.980(18)	1.218(23)

Table 9: The upper half of the table shows our final results for $|V_{us}|$, $|V_{ud}|$, $f_+(0)$ and f_K/f_π , which are obtained by analyzing the lattice data within the Standard Model. For comparison, the lower half lists the values that follow if the lattice results are replaced by the experimental results on nuclear β decay and τ decay, respectively.

Model is assumed to be valid, are not in good agreement with the lattice results for these quantities. The disagreement is reduced considerably if the analysis of the τ data is supplemented with experimental results on electroproduction [154]: the discrepancy then amounts to little more than one standard deviation.

5 Low-energy constants

In studying the quark mass dependence of QCD observables calculated on the lattice it is good practice to invoke χ PT. For a given quantity this framework predicts the nonanalytic quark mass dependence and it provides symmetry relations among different observables. These symmetry relations are best expressed with the help of a set of universal and independent low-energy constants (LECs), which appear as coefficients of the polynomial terms in different observables. If one expands around the SU(2) chiral limit, in the Chiral Effective Lagrangian there are 2 LECs at order p^2

$$F \equiv F_\pi \Big|_{m_u, m_d \rightarrow 0}, \quad B \equiv -\frac{\langle 0 | \bar{u}u | 0 \rangle}{F_\pi^2} \Big|_{m_u, m_d \rightarrow 0}, \quad (44)$$

and seven at order p^4 , indicated by $\bar{\ell}_i$, $i = 1, \dots, 7$. In the analysis of the SU(3) chiral limit, at order p^2 there are also only two LECs

$$F_0 \equiv F_\pi \Big|_{m_u, m_d, m_s \rightarrow 0}, \quad B_0 \equiv -\frac{\langle 0 | \bar{u}u | 0 \rangle}{F_\pi^2} \Big|_{m_u, m_d, m_s \rightarrow 0}, \quad (45)$$

but ten at order p^4 indicated by the capital letter $L_i(\mu)$, $i = 1, \dots, 10$. These constants are independent of the quark masses,¹¹ but they become scale dependent after renormalization (sometimes a superscript r is added). The SU(2) constants are scale independent, since they are defined at $\mu = M_\pi$ (as indicated by the bar). For the precise definition of these constants, their scale dependence etc, we refer the reader to [91, 93].

¹¹More precisely, they are independent of the 2 or 3 light quark masses which are explicitly considered in the respective framework. However, all low-energy constants depend on the masses of the remaining quarks s, c, b, t or c, b, t in the SU(2) and SU(3) framework, respectively.

First of all, lattice calculations can be used to test if chiral symmetry is indeed broken as $SU(N_f)_L \times SU(N_f)_R \rightarrow SU(N_f)_{L+R}$ by measuring non-zero chiral condensates and by verifying, for instance, the validity of the GMOR relation $M_\pi^2 \propto m$ close to the chiral limit. If the chiral extrapolation of quantities calculated on the lattice is made with the help of χ PT, not only does one get the observable at the physical value of the quark masses, but one also determines the relevant LECs. This is a very important by-product for two reasons:

1. All the LECs up to order p^4 (with the exception of B and B_0 , since only the product of these times the quark masses can be estimated from phenomenology) have been either determined by comparison to experiments or estimated theoretically. A lattice determination of the better known ones provides therefore a stringent test of the χ PT approach.
2. The less well known LECs are those which describe the quark mass dependence of observables – these cannot be determined from experiments, and therefore the lattice provides for these unique quantitative information. This information is essential for improving those χ PT predictions in which these LECs play a role.

We stress that this program is based on the non-obvious assumption that χ PT is valid in the region of masses used in the lattice simulation under consideration.

The fact that, at large volume, the finite-size effects, which occur if a system undergoes spontaneous symmetry breakdown, are controlled by the Nambu-Goldstone modes, was first noted in solid state physics, in connection with magnetic systems [192, 193]. As pointed out in [194], in the context of QCD, the thermal properties of such systems can be studied in a systematic and model independent manner by means of the corresponding effective field theory, provided only the temperature is low enough. While finite volumes are not of physical interest in particle physics, lattice simulations are necessarily carried out in a box. As shown in [195–197], the ensuing finite size effects can also be studied on the basis of the effective theory – χ PT in the case of QCD – provided the simulation is close enough to the continuum limit, the volume is sufficiently large and the explicit breaking of chiral symmetry generated by the quark masses is sufficiently small. Indeed, χ PT represents a useful tool also for the analysis of the finite size effects in lattice simulations.

In the following two sections we will summarize the lattice results for the $SU(2)$ and $SU(3)$ LECs at order p^2 and p^4 . The $O(p^2)$ constants are determined from the chiral extrapolation of masses and decay constants or, alternatively, from a finite-size study of correlators in the ϵ -regime or from spectral observables. At order p^4 some LECs influence two-point functions while others appear only in three- or four-point functions; the latter need to be determined via a chiral extrapolation of form factors or scattering amplitudes. The χ PT analysis of the phenomenology is nowadays based on $O(p^6)$ formulae.¹² At this level the number of LECs explodes and we will not discuss any of these here. We will, however, discuss how comparing different orders and different expansions (x versus ξ , see below) can help to reliably assess the theoretical uncertainties of the LECs determined on the lattice.

¹²Some of the $O(p^6)$ formulae presented below have been derived in an unpublished note by three of us (GC, SD and HL) and Jürg Gasser. We thank him for allowing us to publish them here.

5.1 SU(2) Low-Energy Constants

5.1.1 Quark-mass dependence of pseudoscalar masses and decay constants

The expansions of M_π^2 and F_π in powers of the quark mass are known to next-to-next-to-leading order in the SU(2) chiral effective theory.¹³ In the isospin limit, $m_u = m_d = m$, the explicit expressions may be written in the form [198]

$$\begin{aligned} M_\pi^2 &= M^2 \left\{ 1 - \frac{1}{2}x \ln \frac{\Lambda_3^2}{M^2} + \frac{17}{8}x^2 \left(\ln \frac{\Lambda_M^2}{M^2} \right)^2 + x^2 k_M + O(x^3) \right\}, \\ F_\pi &= F \left\{ 1 + x \ln \frac{\Lambda_4^2}{M^2} - \frac{5}{4}x^2 \left(\ln \frac{\Lambda_F^2}{M^2} \right)^2 + x^2 k_F + O(x^3) \right\}. \end{aligned} \quad (46)$$

The expansion parameter is given by

$$x = \frac{M^2}{(4\pi F)^2}, \quad M^2 = 2Bm = \frac{2m\Sigma}{F^2}. \quad (47)$$

The logarithmic scales Λ_3, Λ_4 are related to the effective coupling constants $\bar{\ell}_3, \bar{\ell}_4$ of the chiral Lagrangian at running scale M_π :

$$\bar{\ell}_n = \ln \frac{\Lambda_n^2}{M_\pi^2}, \quad n = 1, \dots, 7. \quad (48)$$

Note that in Eq. (46), the logarithms are evaluated at M^2 , and not at M_π^2 . The coupling constants k_i in Eq. (46) are mass-independent. The scales of the quadratic logarithms can be expressed in terms of the coupling constants:

$$\begin{aligned} \ln \frac{\Lambda_M^2}{M^2} &= \frac{1}{51} \left(28 \ln \frac{\Lambda_1^2}{M^2} + 32 \ln \frac{\Lambda_2^2}{M^2} - 9 \ln \frac{\Lambda_3^2}{M^2} + 49 \right), \\ \ln \frac{\Lambda_F^2}{M^2} &= \frac{1}{30} \left(14 \ln \frac{\Lambda_1^2}{M^2} + 16 \ln \frac{\Lambda_2^2}{M^2} + 6 \ln \frac{\Lambda_3^2}{M^2} - 6 \ln \frac{\Lambda_4^2}{M^2} + 23 \right). \end{aligned} \quad (49)$$

By analyzing the quark mass dependence of M_π and F_π with Eq. (46), possibly truncated at NLO, one can therefore determine¹⁴ the $O(p^2)$ LECs B and F , as well as the $O(p^4)$ LECs $\bar{\ell}_3$ and $\bar{\ell}_4$. The quark condensate in the chiral limit is determined by $\Sigma = F^2 B$. With precise enough data at several low pion masses, one could in principle also determine Λ_M, Λ_F and k_M, k_F . This is not yet the case. The results for the LO and NLO constants will be presented in Sec. 5.1.6.

Alternatively, one can invert Eq. (46) and express M and F as an expansion in

$$\xi \equiv \frac{M_\pi^2}{16\pi^2 F_\pi^2}. \quad (50)$$

¹³Here and in the following, we stick to the notation used in the papers where the χ PT formulae were established, i.e. we work with $F_\pi \equiv f_\pi/\sqrt{2} = 92.2(1)$ MeV and $F_K \equiv f_K/\sqrt{2}$. The occurrence of different normalization conventions is not convenient, but avoiding it by reformulating the formulae in terms of f_π, f_K is not a good way out. Since we are using different symbols, confusion cannot arise.

¹⁴Notice that one could analyze the quark mass dependence entirely in terms of the parameter M defined in Eq. (47) and determine equally well all other LECs. Using the determination of the quark masses described in Sec. 3 one can then extract B or Σ .

The corresponding expressions read

$$\begin{aligned} M^2 &= M_\pi^2 \left\{ 1 + \frac{1}{2} \xi \ln \frac{\Lambda_3^2}{M_\pi^2} - \frac{5}{8} \xi^2 \left(\ln \frac{\Omega_M^2}{M_\pi^2} \right)^2 + \xi^2 c_M + O(\xi^3) \right\}, \\ F &= F_\pi \left\{ 1 - \xi \ln \frac{\Lambda_4^2}{M_\pi^2} - \frac{1}{4} \xi^2 \left(\ln \frac{\Omega_F^2}{M_\pi^2} \right)^2 + \xi^2 c_F + O(\xi^3) \right\}. \end{aligned} \quad (51)$$

The scales of the quadratic logarithms are determined by $\Lambda_1, \dots, \Lambda_4$:

$$\begin{aligned} \ln \frac{\Omega_M^2}{M_\pi^2} &= \frac{1}{15} \left(28 \ln \frac{\Lambda_1^2}{M_\pi^2} + 32 \ln \frac{\Lambda_2^2}{M_\pi^2} - 33 \ln \frac{\Lambda_3^2}{M_\pi^2} - 12 \ln \frac{\Lambda_4^2}{M_\pi^2} + 52 \right), \\ \ln \frac{\Omega_F^2}{M_\pi^2} &= \frac{1}{3} \left(-7 \ln \frac{\Lambda_1^2}{M_\pi^2} - 8 \ln \frac{\Lambda_2^2}{M_\pi^2} + 18 \ln \frac{\Lambda_4^2}{M_\pi^2} - \frac{29}{2} \right). \end{aligned} \quad (52)$$

5.1.2 Two-point correlation functions in the ϵ -regime

The finite-size effects encountered in lattice calculations can be used to determine some of the Low-Energy Constants of QCD. In order to illustrate the method, we focus on the two lightest quarks, take the isospin limit $m_u = m_d = m$ and consider a box of size L_s in the three space directions and size L_t in the time direction. If m is sent to zero at fixed box size, chiral symmetry is restored. The behaviour of the various observables in the symmetry restoration region is controlled by the parameter $\mu = m \Sigma V$, where $V = L_s^3 L_t$ is the volume of the box. Up to a sign and a factor of two, the parameter μ represents the minimum of the classical action that belongs to the leading order effective Lagrangian of QCD.

For $\mu \gg 1$, the system behaves qualitatively as if the box was infinitely large. In that region, the p -expansion, which counts $1/L_s, 1/L_t$ and M as quantities of the same order, is adequate. In view of $\mu = \frac{1}{2} F^2 M^2 V$, this region includes configurations with $ML \gtrsim 1$, where the finite-size effects due to pion loop diagrams are suppressed by the factor e^{-ML} .

If μ is comparable to or smaller than 1, however, the chiral perturbation series must be reordered. The ϵ -expansion achieves this by counting $1/L_s, 1/L_t$ as quantities of $O(\epsilon)$, while the quark mass m is booked as a term of $O(\epsilon^4)$. This ensures that the symmetry restoration parameter μ represents a term of order $O(\epsilon^0)$, so that the manner in which chiral symmetry is restored can be worked out.

As an example, we consider the correlator of the axial charge carried by the two lightest quarks, $q(x) = \{u(x), d(x)\}$. The axial current and the pseudoscalar density are given by

$$A_\mu^i(x) = \bar{q}(x) \frac{1}{2} \tau^i \gamma_\mu \gamma_5 q(x), \quad P^i(x) = \bar{q}(x) \frac{1}{2} \tau^i i \gamma_5 q(x), \quad (53)$$

where τ^1, τ^2, τ^3 , are the Pauli matrices. In euclidean space, the correlators of the axial charge and of the space integral over the pseudoscalar density are given by

$$\begin{aligned} \delta^{ik} C_{AA}(t) &= L_s^3 \int d^3 \vec{x} \langle A_4^i(\vec{x}, t) A_4^k(0) \rangle, \\ \delta^{ik} C_{PP}(t) &= L_s^3 \int d^3 \vec{x} \langle P^i(\vec{x}, t) P^k(0) \rangle. \end{aligned} \quad (54)$$

χ PT yields explicit finite-size scaling formulae for these quantities [197, 199, 200]. In the

ϵ -regime, the expansion starts with

$$\begin{aligned} C_{AA}(t) &= \frac{F^2 L_s^3}{L_t} \left[a_A + \frac{L_t}{F^2 L_s^3} b_A h_1\left(\frac{t}{L_t}\right) + O(\epsilon^4) \right], \\ C_{PP}(t) &= \Sigma^2 L_s^6 \left[a_P + \frac{L_t}{F^2 L_s^3} b_P h_1\left(\frac{t}{L_t}\right) + O(\epsilon^4) \right], \end{aligned} \quad (55)$$

where the coefficients a_A , b_A , a_P , b_P stand for quantities of $O(\epsilon^0)$. They can be expressed in terms of the variables L_s , L_t and m and exclusively involve the two leading low-energy constants F and Σ . In fact, at leading order, only the combination $\mu = m \Sigma L_s^3 L_t$ matters, the correlators are independent of t and the dependence on μ is fully determined by the structure of the groups involved in the spontaneous symmetry breakdown. In the case of $SU(2) \times SU(2) \rightarrow SU(2)$, relevant for QCD in the symmetry restoration region of the two lightest quarks, the coefficients can be expressed in terms of Bessel functions. The t -dependence of the correlators starts showing up at $O(\epsilon^2)$, in the form of a parabola: $h_1(\tau) = \frac{1}{2} \left[\left(\tau - \frac{1}{2}\right)^2 - \frac{1}{12} \right]$. Explicit expressions for a_A , b_A , a_P , b_P can be found in [197, 199, 200], where some of the correlation functions are worked out to NNLO. By matching the finite-size scaling of correlators computed on the lattice with these predictions one can extract F and Σ .

The fact that the representation of the correlators to NLO is not “contaminated” by higher order unknown LECs, makes the ϵ -regime potentially convenient for a clean extraction of the LO couplings. The determination of the LECs is then affected by different systematic uncertainties with respect to the standard case; simulations in this regime yield complementary information which can serve as a valuable cross-check to get a comprehensive picture of the low-energy properties of QCD.

The effective theory can also be used to study the distribution of the topological charge in QCD [201] and the various quantities of interest may be defined for a fixed value of this charge. The expectation values and correlation functions then not only depend on the symmetry restoration parameter μ , but also on the topological charge ν . The dependence on these two variables can explicitly be calculated. It turns out that the two-point correlation functions considered above retain the form (55), but the coefficients a_A , b_A , a_P , b_P now depend on the topological charge as well as on the symmetry restoration parameter (see [202–204] for explicit expressions).

A specific issue with ϵ -regime calculations is the scale setting. Ideally one would perform a p -regime study with the same bare parameters to measure a hadronic scale (e.g. the proton mass). In the literature, sometimes a gluonic scale (e.g. r_0) is used instead; this introduces an extra uncertainty of the order of 5%.

It is important to stress that in the ϵ -expansion higher order finite-volume corrections might be significant, and the physical box size (in fm) should still be large in order to keep them under control. The criteria for the chiral extrapolation and finite volume effects are obviously different with respect to the p -regime. For these reasons we have to adjust the colour coding defined in Sect. 2 (see 5.1.6 for more details).

Recently, the chiral effective theory has been extended also to the so-called mixed regime, where some quarks are in the p -regime and others in the ϵ -regime [205]. In [206] a technique is proposed to smoothly connect p - and ϵ -regimes. These theoretical advances can be adopted for future extraction of the Low Energy Couplings from lattice simulations.

5.1.3 Energy levels of the QCD Hamiltonian in a box, δ -regime

At low temperature, the properties of the partition function are governed by the lowest eigenvalues of the Hamiltonian. In the case of QCD, the lowest levels are due to the Nambu-Goldstone bosons and can be worked out with χ PT [207]. In the chiral limit, the level pattern follows the one of a quantum-mechanical rotator: $E_\ell = \ell(\ell + 2)/(2\Theta)$, $\ell = 0, 1, 2, \dots$. For a cubic spatial box and to leading order in the expansion in inverse powers of the box size L_s , the moment of inertia is fixed by the value of the pion decay constant in the chiral limit: $\Theta = F^2 L_s^3$. In order to analyze the dependence of the levels on the quark masses and on the parameters that specify the size of the box, a reordering of the chiral series is required, the so-called δ -expansion; the region where the properties of the system are controlled by this expansion is referred to as the δ -regime. Evaluating the chiral perturbation series in this regime, one finds that the expansion of the partition function goes in even inverse powers of FL_s , that the rotator formula for the energy levels holds up to NNLO and the expression for the moment of inertia is now also known up to and including order $(FL_s)^{-4}$ [208–210]. Since the level spectrum is governed by the value of the pion decay constant in the chiral limit, an evaluation of this spectrum on the lattice can be used to measure F . More generally, the evaluation of various observables in the δ -regime offers an alternative method for a determination of some of the low energy constants occurring in the effective Lagrangian. At present, however, the numerical results obtained in this way [211, 212] are not yet competitive with those found in the p - or ϵ -regimes.

5.1.4 Other methods for the extraction of the Low-Energy Constants

An observable that can be used to extract the LECs is the topological susceptibility, which is defined as

$$\chi_t = \int d^4x \langle \omega(x) \omega(0) \rangle, \quad (56)$$

where $\omega(x)$ is the topological charge density,

$$\omega(x) = \frac{1}{32\pi^2} \epsilon^{\mu\nu\rho\sigma} \text{Tr} [F_{\mu\nu}(x) F_{\rho\sigma}(x)]. \quad (57)$$

At infinite volume, the expansion of the topological susceptibility in powers of the quark masses starts with [213]

$$\chi_t = \bar{m} \Sigma \{1 + O(m)\}, \quad \bar{m} \equiv \left(\frac{1}{m_u} + \frac{1}{m_d} + \frac{1}{m_s} + \dots \right)^{-1}. \quad (58)$$

The quark condensate Σ can thus be extracted from the properties of the topological susceptibility close to the chiral limit. The behaviour at finite volume, in particular also in the region where the symmetry is restored, are discussed in [200]. The dependence on the vacuum angle θ and the projection on sectors of given topological charge have also been investigated [201]. For a discussion of the finite-size effects to NLO, including the dependence on θ , we refer to [204, 214].

Another method to compute directly the quark condensate has been proposed in [215], where it is shown that starting from the Banks-Casher relation [216], it is possible to extract the condensate from suitable (renormalizable) spectral observables, for instance the number of Dirac operator modes contained in a given interval. For those spectral observables higher

order corrections can be systematically computed in terms of the chiral effective theory.

An alternative strategy is based on the fact that at LO in the ϵ -expansion, the partition function in a given topological sector ν is equivalent to the one of a chiral Random Matrix Theory (RMT) [217–220]. In RMT it is possible to extract the probability distributions of individual eigenvalues [221–223] in terms of two dimensionless variables $\zeta = \lambda\Sigma V$ and $\mu = m\Sigma V$, where λ represents the eigenvalue of the massless Dirac operator and m is the sea quark mass. Hence it is possible to match the QCD low-lying spectrum of the Dirac operator with the RMT predictions in order to extract¹⁵ the chiral condensate Σ . The main issue concerning this method is that for the distributions of individual eigenvalues higher order corrections are still not known by means of the chiral effective theory, and this may introduce systematic effects which are not under control.¹⁶ Another open question is that, while it is clear how the spectral density is renormalized [227], this is not the case for the individual eigenvalues, and one has to rely on assumptions. There have been many lattice studies [228–232] where the matching of the low-lying Dirac spectrum with RMT has been investigated. In this review we don't include the results of the LECs obtained in this way.¹⁷

5.1.5 Pion form factors

The scalar and vector form factors of the pion are defined by the matrix elements

$$\begin{aligned}\langle \pi^i(p_2) | \bar{q} q | \pi^j(p_1) \rangle &= \delta^{ij} F_S^\pi(t), \\ \langle \pi^i(p_2) | \bar{q} \frac{1}{2} \tau^k \gamma^\mu q | \pi^j(p_1) \rangle &= i \epsilon^{ijk} (p_1^\mu + p_2^\mu) F_V^\pi(t),\end{aligned}\tag{59}$$

where the operators only contain the lightest two quark flavours, τ^1, τ^2, τ^3 are the Pauli matrices and $t \equiv (p_1 - p_2)^2$ denotes the momentum transfer.

The vector form factor has been measured by several experiments for timelike as well as for spacelike values of t . The scalar form factor is not measurable but can be evaluated theoretically from data on the $\pi\pi$ and πK phase shifts [233] on the basis of analyticity and unitarity, *i.e.* in a model-independent way. Lattice calculations can be compared with data or model-independent theoretical evaluations at different values of t . At present, however, most lattice calculations concentrate on the region close to $t = 0$ and on the evaluation of the slope and curvature, defined as:

$$\begin{aligned}F_V^\pi(t) &= 1 + \frac{1}{6} \langle r^2 \rangle_V^\pi t + c_V t^2 + \dots, \\ F_S^\pi(t) &= F_S^\pi(0) \left[1 + \frac{1}{6} \langle r^2 \rangle_S^\pi t + c_S t^2 + \dots \right].\end{aligned}\tag{60}$$

The slopes are related to the mean quadratic vector and scalar radii which are the quantities on which most experiments and lattice calculations concentrate.

In chiral perturbation theory, the form factors are known at NNLO [234]. The corresponding formulae are available in fully analytical form and are compact enough that they can be used for the chiral extrapolation of the data (as done, for example in [235, 236]). The

¹⁵By introducing an imaginary isospin chemical potential, this framework can be extended such that the low spectrum of the Dirac operator is sensitive also to the pseudoscalar decay constant F at LO [224].

¹⁶Higher order systematic effects in the matching with RMT have been recently investigated in [225, 226].

¹⁷The results obtained for Σ and F lie in the same range as the determinations reported in Tables 10 and 11.

expressions for the scalar and vector radii and for the $c_{S,V}$ coefficients at two-loop level reads

$$\begin{aligned}
\langle r^2 \rangle_S^\pi &= \xi \left\{ 6 \ln \frac{\Lambda_4^2}{M_\pi^2} - \frac{13}{2} - \frac{29}{3} \xi \left(\ln \frac{\Omega_{r_S}^2}{M_\pi^2} \right)^2 + 6\xi k_{r_S} + O(\xi^2) \right\}, \\
\langle r^2 \rangle_V^\pi &= \xi \left\{ \ln \frac{\Lambda_6^2}{M_\pi^2} - 1 + 2\xi \left(\ln \frac{\Omega_{r_V}^2}{M_\pi^2} \right)^2 + 6\xi k_{r_V} + O(\xi^2) \right\}, \\
c_S &= \xi \left\{ \frac{19}{120} + \xi \left[\frac{43}{36} \left(\ln \frac{\Omega_{c_S}^2}{M_\pi^2} \right)^2 + k_{c_S} \right] \right\}, \\
c_V &= \xi \left\{ \frac{1}{60} + \xi \left[\frac{1}{72} \left(\ln \frac{\Omega_{c_V}^2}{M_\pi^2} \right)^2 + k_{c_V} \right] \right\},
\end{aligned} \tag{61}$$

where

$$\begin{aligned}
\ln \frac{\Omega_{r_S}^2}{M_\pi^2} &= \frac{1}{29} \left(31 \ln \frac{\Lambda_1^2}{M_\pi^2} + 34 \ln \frac{\Lambda_2^2}{M_\pi^2} - 36 \ln \frac{\Lambda_4^2}{M_\pi^2} + \frac{145}{24} \right), \\
\ln \frac{\Omega_{r_V}^2}{M_\pi^2} &= \frac{1}{2} \left(\ln \frac{\Lambda_1^2}{M_\pi^2} - \ln \frac{\Lambda_2^2}{M_\pi^2} + \ln \frac{\Lambda_4^2}{M_\pi^2} + \ln \frac{\Lambda_6^2}{M_\pi^2} - \frac{31}{12} \right), \\
\ln \frac{\Omega_{c_S}^2}{M_\pi^2} &= \frac{43}{63} \left(11 \ln \frac{\Lambda_1^2}{M_\pi^2} + 14 \ln \frac{\Lambda_2^2}{M_\pi^2} + 18 \ln \frac{\Lambda_4^2}{M_\pi^2} - \frac{6041}{120} \right), \\
\ln \frac{\Omega_{c_V}^2}{M_\pi^2} &= \frac{1}{72} \left(2 \ln \frac{\Lambda_1^2}{M_\pi^2} - 2 \ln \frac{\Lambda_2^2}{M_\pi^2} - \ln \frac{\Lambda_6^2}{M_\pi^2} - \frac{26}{30} \right),
\end{aligned} \tag{62}$$

and $k_{r_{S,V}}$ and $k_{c_{S,V}}$ are four constants independent of the quark masses. Their expression in terms of the ℓ_i and of the $O(p^6)$ constants c_i is known but will not be reproduced here.

5.1.6 Results

In this section we summarize the lattice results for the SU(2) couplings in a set of tables (10–13) and figures (7–9). The tables present our usual colour coding which summarizes the main aspects related to the treatment of the systematic errors of the various calculations.

A delicate issue in the lattice determination of chiral LECs (in particular at NLO) which cannot be reflected by our colour coding is a reliable assessment of the theoretical error. We add a few remarks on this point:

1. Using *both* the x and the ξ expansion is a good way to test how the ambiguity of the chiral expansion (at a given order) affects the numerical values of the LECs that are determined from a particular set of data. For instance, to determine $\bar{\ell}_4$ (or Λ_4) from lattice data for F_π as a function of the quark mass, one may compare the fits based on the parametrization $F_\pi = F\{1 + x \ln(\Lambda_4^2/M^2)\}$ [see Eq. (46)] with those obtained from $F_\pi = F/\{1 - \xi \ln(\Lambda_4^2/M^2)\}$ [see Eq. (51)]. The difference between the two results provides an estimate of the uncertainty due to the truncation of the chiral series.¹⁸

¹⁸Notice however that this difference could be accidentally small and then lead to an underestimate of the true systematic error.

Which central value one chooses is in principle arbitrary, but we find it advisable to use the one obtained with the ξ expansion,¹⁹ in particular because it makes the comparison with phenomenological determinations (where it is an established practice to use the ξ expansion) more meaningful. The fact that there is an apparent discrepancy in Tab. 13 between the lattice and the phenomenological determination of $\bar{\ell}_1 - \bar{\ell}_2$, but not for $\langle r^2 \rangle_S^\pi$ (on which it is based), calls for a re-assessment of the theoretical error which includes an x versus ξ expansion analysis.

2. As an alternative one could try to estimate the influence of higher chiral orders by reshuffling irrelevant higher-order terms. For instance, in the example mentioned above one might use $F_\pi = F/\{1 - x \ln(\Lambda_4^2/M^2)\}$ as a different functional form at NLO. Another way to make this estimate is through introducing by hand “analytic” higher-order terms (e.g. “analytic NNLO”), as done, in the past, by MILC [6]. In principle it would be preferable to include all NNLO terms or none, such that the structure of the chiral expansion is preserved at any order; this is what ETM [237] and JLQCD/TWQCD [95] are doing now for SU(2) χ PT and MILC for SU(3) χ PT [59]. In any case it is not advisable to include terms to which the data are not sensitive. The use of priors in fits has not yet found general consensus in the lattice community.
3. Another issue concerns the s -quark mass dependence of the LECs $\bar{\ell}_i$ or Λ_i in the SU(2) framework. This has been studied analytically in a series of papers [91, 238, 239]. An analysis of the difference of the LECs determinations done in $N_f = 2$ or $N_f = 2 + 1$ lattice simulations provides a unique means to analyze quantitatively this dependence.
4. Finally, the determination of the LECs is in general affected by discretization effects, and it is important that these are corrected for with the help of the appropriate effective chiral Lagrangian (as done, *e.g.* by MILC). For actions which respect chiral symmetry at finite lattice spacing (like the overlap formulation adopted by JLQCD/TWQCD or domain wall fermions used by RBC/UKQCD in the limit of large lattice size in the fifth dimension), this step is unnecessary.

In the tables and figures we summarize the results of various lattice collaborations for the SU(2) LECs at leading order (F or F/F_π , B or Σ) and at NLO ($\bar{\ell}_1 - \bar{\ell}_2$, $\bar{\ell}_3$, $\bar{\ell}_4$, $\bar{\ell}_5$, $\bar{\ell}_6$). The tables group the results into those which stem from $N_f = 2 + 1$ calculations and those which stem from $N_f = 2$ calculations. Furthermore, we make a distinction whether the results are obtained from simulations in the p -regime or whether alternative methods (ϵ -regime, spectral quantities, topological susceptibility, etc.) have been used. For comparison we add, in each case, a few phenomenological determinations with high standing.

There is only one set of $N_f = 2$ lattice results for the SU(2) LECs which does not have any red tag, the one by the ETM collaboration [235, 237]. These results are at present the lattice determinations of these quantities with the best control of systematic effects (for $N_f = 2$ and in some cases even overall) and the only ones which qualify for making an average according to our criteria. We therefore offer no $N_f = 2$ averages, and the dashed bands in the plots coincide with the lattice points of the ETM collaboration.

¹⁹There are theoretical arguments suggesting that the ξ expansion is preferable to the x expansion, based on the observation that the coefficients in front of the squared logs in (46) are somewhat larger than in (51). This can be traced to the fact that a part of every formula in the x expansion is concerned with locating the position of the pion pole (at the previous order) while in the ξ expansion the knowledge of this position is built in exactly. Numerical evidence supporting this view is presented in [95].

Collaboration	Ref.	N_f	publication status	chiral extrapolation	continuum extrapolation	finite volume	renormalization	$\Sigma^{1/3}$ [MeV]
MILC 10A	[103]	2+1	C	●	★	★	●	281.5(3.4) $^{(+2.0)}_{(-5.9)}$ (4.0)
JLQCD/TWQCD 10	[240]	2+1	A	★	■	●	★	234(4)(17)
RBC/UKQCD 10A	[106]	2+1	P	●	●	★	★	256(5)(2)(2)
JLQCD 09	[241]	2+1	A	★	■	●	★	242(4) $^{(+19)}_{(-18)}$
MILC 09A	[59]	2+1	C	●	★	★	●	279(1)(2)(4)
MILC 09A	[59]	2+1	C	●	★	★	●	280(2) $^{(+4)}_{(-8)}$ (4)
MILC 09	[6]	2+1	A	●	★	★	●	278(1) $^{(+2)}_{(-3)}$ (5)
TWQCD 08	[242]	2+1	A	●	■	■	★	259(6)(9)
JLQCD/TWQCD 08B	[243]	2+1	C	●	■	■	★	253(4)(6)
PACS-CS 08	[63]	2+1	A	★	■	■	■	312(10)
PACS-CS 08	[63]	2+1	A	★	■	■	■	309(7)
RBC/UKQCD 08	[108]	2+1	A	●	■	★	★	255(8)(8)(13)
Bernardoni 10	[244]	2	A	●	■	■	★	262 $^{(+33)}_{(-34)}$ $^{(+4)}_{(-5)}$
JLQCD/TWQCD 10	[240]	2	A	★	■	■	★	242(5)(20)
ETM 09C	[237]	2	A	●	★	●	★	270(5) $^{(+3)}_{(-4)}$
ETM 08	[235]	2	A	●	●	●	★	264(3)(5)
CERN 08	[215]	2	A	●	■	●	★	276(3)(4)(5)
JLQCD/TWQCD 08A	[95]	2	A	●	■	■	★	235.7(5.0)(2.0) $^{(+12.7)}_{(-0.0)}$
JLQCD/TWQCD 07A	[245]	2	A	●	■	■	★	252(5)(10)
ETM 09B	[246]	2	C	★	●	■	★	239.6(4.8)
HHS 08	[247]	2	A	★	■	●	★	248(6)
JLQCD/TWQCD 07	[248]	2	A	★	■	■	★	239.8(4.0)

Table 10: Lattice results for the quark condensate Σ , in the $\overline{\text{MS}}$ scheme at scale $\mu = 2$ GeV. We separate $N_f = 2 + 1$ from $N_f = 2$ results and, in the latter case, results obtained in the p -regime (middle) from those obtained in the ϵ -regime (bottom). For MILC 09A and PACS-CS 08, converted values from SU(3) fits and values from direct SU(2) fits are included.

The determination of the SU(2) LECs in $N_f = 2 + 1$ lattice calculations requires more discussion: MILC has published values for Σ , F and F_π/F in their summary paper [6], but not for the $\bar{\ell}_i$, which were instead extracted from a SU(2) fit only in conference proceedings [59, 103]. As discussed in the previous sections, these results have no red tag and those presented in a regular article fully qualify for entering our averages. The RBC/UKQCD collaboration has calculated all the SU(2) LECs discussed here. After a first study with a single lattice spacing [108], a more recent publication with 2 lattice spacings appeared [106]. Those results have no red tag and are included in our averages. PACS-CS [63] has also performed a comprehensive analysis of SU(2) LECs, and at remarkably small quark masses – their calculation has two red tags related to the continuum extrapolation and finite-size effects

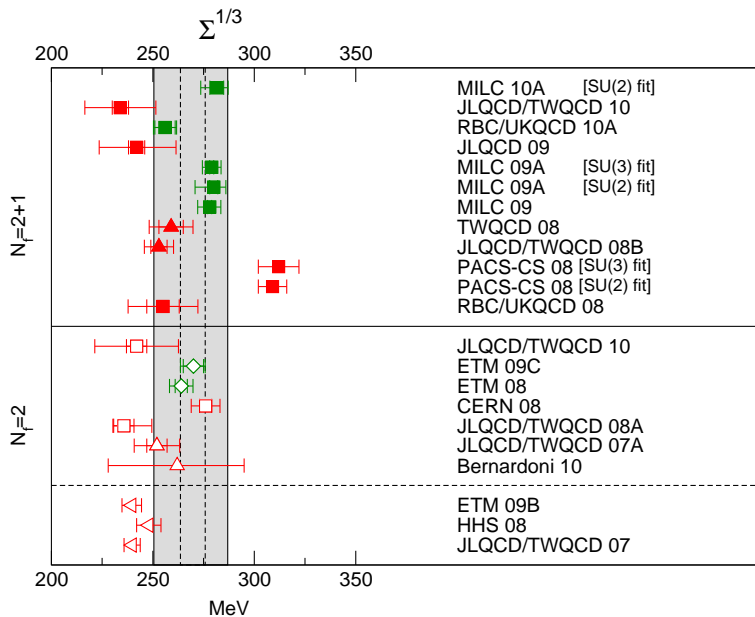


Figure 7: Summary of lattice results for the quark condensate Σ (in the $\overline{\text{MS}}$ scheme at scale $\mu = 2$ GeV). The filled symbols represent lattice simulations with $N_f = 2 + 1$ dynamical flavours, while the empty ones refer to $N_f = 2$ computations. Squares and left triangles indicate determinations from correlators in the p - and ϵ -regimes, respectively. Up triangles refer to extractions from the topological susceptibility, diamonds to determinations from the pion form factor. The gray (dashed) band indicates our estimate for $N_f = 2 + 1$ ($N_f = 2$).

and should also not be considered in averages. Finally JLQCD [240, 241] has performed a calculation of Σ (but no other SU(2) LECs) with $N_f = 2 + 1$ overlap dynamical quarks, but at a single lattice spacings and has also a red tag.

The ETM collaboration has recently started performing calculations with $N_f = 2 + 1 + 1$ dynamical quarks and a first paper [60] on the SU(2) LECs has appeared (a more recent paper [249] gives a progress report but not yet an update of the LECs). Assigning a color code to this calculation is not straightforward because of the even larger splitting between the neutral and charged pion than observed in $N_f = 2$ calculations, but as explained in the footnote in Table 11 we did not assign it any red tag. We also refer to the careful analysis by Bär [40] on the effect of this splitting on the LEC determination. All this considered, we compare and take into account their numbers when drawing our conclusions on $N_f = 2 + 1$ calculations of the SU(2) LECs.

A generic comment applies to the issue of the scale setting. Since none of the lattice studies involves simulations in the p -regime at the physical value of m_{ud} , the setting of the scale a^{-1} via an experimentally measurable quantity involves a chiral extrapolation. As a result, dimensionful quantities are particularly sensitive to this scale-setting ambiguity, while in dimensionless ratios such as F_π/F , F/F_0 , B/B_0 , Σ/Σ_0 , the problem is much reduced, and often finite lattice-to-continuum renormalization factors drop out. In those cases where the collaboration offers separate results for numerator and denominator but not for the ratio, we have calculated the quotient ourselves. Since the systematic errors are dominated by those due to the renormalization of the scale and these cancel in F_π/F , we have dropped the systematic errors altogether – a lattice determination of the ratio that properly accounts for the correlations would of course be preferable. In the tables, results obtained in this way are shown in slanted fonts. Since the difference between F_π and F manifests itself only at NNLO of the ϵ -expansion, the data taken in the ϵ -regime do not by themselves allow a determination

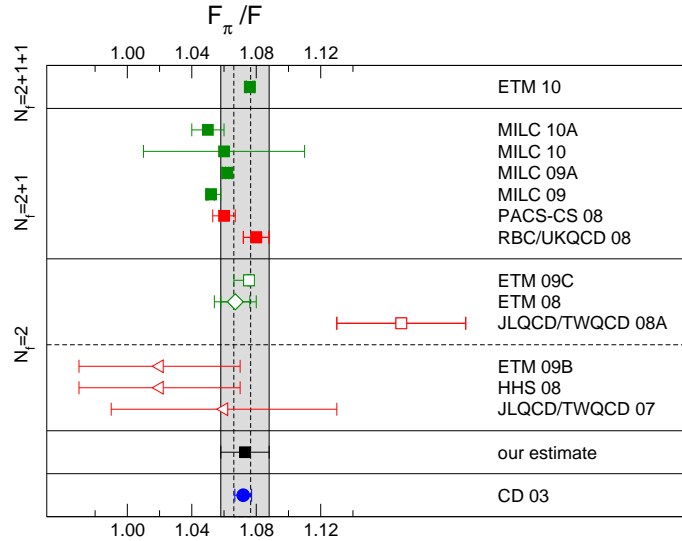


Figure 8: Summary of lattice results for the ratio F_π/F , which compares the physical value of the pion decay constant with the value in the limit $m_u, m_d \rightarrow 0$. The meaning of the symbols is the same as in Fig. 7. The gray band here represents our estimate, whereas the dashed one the current $N_f = 2$ value.

of the ratio F_π/F . The corresponding entries in Tab. 11 and Fig. 8 are obtained by dividing the physical value of F_π (cf. footnote 13) through the lattice result for F .

It is worth repeating here that the standard colour coding scheme of our tables is necessarily schematic and cannot do justice to every calculation. For instance, in the ϵ -regime we routinely assign²⁰ a green star in the “chiral extrapolation” column (since the pertinent expressions directly involve F and B , even if the calculation is done at finite quark mass), while the “infinite volume” assessment is exclusively based on the number of different volumes with $L > 1.5$ fm have been used (the $M_\pi L$ criterion does not make sense here). Similarly, in the calculation of form factors and charge radii the tables do not reflect whether an interpolation to the desired q^2 has been performed or whether the evaluation has taken place directly at the relevant q^2 , or very close to it, by means of “partially twisted boundary conditions” [250]. Nevertheless, we feel that these tables give an adequate overview of the qualities of the various calculations.

For most quantities our tables and figures show an overall reasonable consistency among the various lattice determinations. One notable exception is the case of Σ . The PACS-CS 08 determination [63] of this quantity is in flat disagreement with all other calculations. A glimpse at Tab. 10 reveals that this calculation is the only one which received three red boxes. In particular, as was pointed out by the authors, for this quantity perturbative renormalization may lead to theoretical errors which are hard to quantify. But even among the two $N_f = 2 + 1$ calculations without red tags, MILC 10A and RBC/UKQCD 10A there is some tension, at the level of 2.6 sigmas. As pointed out above, the origin of the problem may lie in the scale setting issue: the ratio Σ/Σ_0 would be a much more stringent test. In any case, since it is not meaningful to average these two calculations, the estimate shown in Figure 7, $\Sigma = 269(18)$ is constructed so as to cover both of them.

As far as F_π/F is concerned, there is some tension among the MILC and the RBC/UKQCD results, with the latest ETM $N_f = 2 + 1 + 1$ agreeing with the latter. The tension is at the

²⁰Also for [241] and for [240] (for $N_f = 2 + 1, 3$) the colour-coding criteria for the ϵ -regime have been applied.

Collaboration	Ref.	N_f		publication status	chiral extrapolation	continuum extrapolation	finite volume	renormalization	F [MeV]	F_π/F
ETM 10	[60]	2+1+1	A	●	●	● [†]	★		85.66(6)(13)	1.076(2)(2)
MILC 10A	[103]	2+1	C	●	★	★	●		87.5(1.0)(^{+0.7} _{-2.6})	1.05(1)
MILC 10	[171]	2+1	C	●	★	★	●		87.0(4)(5)	1.06(5)
MILC 09A	[59]	2+1	C	●	★	★	●		86.8(2)(4)	1.062(1)(3)
MILC 09	[6]	2+1	A	●	★	★	●			1.052(2)(⁺⁶ ₋₃)
PACS-CS 08	[63]	2+1	A	★	■	■	■		89.4(3.3)	1.060(7)
RBC/UKQCD 08	[108]	2+1	A	●	■	★	★		81.2(2.9)(5.7)	1.080(8)
ETM 09C	[237]	2	A	●	★	●	★			1.0755(6)(⁺⁸ ₋₉₄)
ETM 08	[235]	2	A	●	●	●	★		86.6(7)(7)	1.067(9)(9)
JLQCD/TWQCD 08A	[95]	2	A	●	■	■	★		79.0(2.5)(0.7)(^{+4.2} _{-0.0})	1.17(4)
ETM 09B	[246]	2	C	★	●	■	★		90.2(4.8) [§]	1.02(5)
HHS 08	[247]	2	A	★	■	●	★		90(4)	1.02(5)
JLQCD/TWQCD 07	[248]	2	A	★	■	■	★		87.3(5.6)	1.06(7)
CD 03	[251]								86.2(5)	1.0719(52)

[†] The values of $M_\pi + L$ correspond to a green tag, while those of $M_{\pi_0}L$ imply a red one – since both masses play a role in finite-volume effects, we opt for orange.

[§] Result for r_0F converted into a value for F with $r_0 = 0.49$ fm.

Table 11: Results for the leading order SU(2) low energy constant F and for the ratio F_π/F . Numbers in slanted fonts have been calculated by us (see text for details). Horizontal lines establish the same grouping as in Tab. 10. The table shows that the precision reached on the lattice is now comparable to the accuracy of the prediction, which is indicated in the last row.

level of about two sigmas, but it is worth stressing that the quoted lattice uncertainties are all below one percent. We believe it is fair and useful to quote an estimate which covers all three lattice determinations and has an uncertainty of about 1.5%,

$$\frac{F_\pi}{F} = 1.073(15) \quad \text{our estimate.} \quad (63)$$

The ETM result [237] shows that the value obtained with $N_f = 2$ dynamical flavours is the same within errors.²¹ The crucial point here is that the lattice results confirm the theoretical prediction [251]: the breaking of chiral symmetry generated by the small masses of the two lightest quarks is significantly larger than what dimensional reasoning would indicate, because it is amplified by a chiral logarithm with a large coefficient. The amplification is generated by the propagation of Nambu-Goldstone boson pairs that necessarily accompany the spontaneous breakdown of the symmetry.

At NLO, the ratio F_π/F is determined by the effective coupling $\bar{\ell}_4$. As we are dealing with an expansion in powers of the two lightest quark masses here, the corrections of higher order

²¹On the other hand, the result of JLQCD/TWQCD [95] shows a 2-sigma deviation from the other results obtained with $N_f = 2$. Since the quoted value for F_π/F has been obtained by dividing the physical value of F_π by the lattice result, we can't exclude that systematic errors are properly taken into account in this estimate.

are expected to be very small (not necessarily at the quark masses used in the simulations, but at their physical values). Unfortunately, however, some of the collaborations appear to underestimate the uncertainties in the determination of this coupling: in view of the small errors quoted, the results are not coherent (see the middle panel in Fig. 9). The dust needs to settle before a meaningful estimate can be given for $\bar{\ell}_4$.

The leading term in the chiral expansion of the scalar radius $\langle r^2 \rangle_S^\pi$ is also determined by the coupling $\bar{\ell}_4$. The bottom panel of Table 13 shows that the result for the scalar radius obtained from a lattice calculation of the scalar form factor by JLQCD/TWQCD 09 [252] is in good agreement with the result of CGL 01 [198], which is based on dispersion theory, but the red tags indicate that some of the systematic uncertainties in that calculation yet need to be studied.

The current situation with $\bar{\ell}_3$ is better than the one with $\bar{\ell}_4$: the $N_f = 2+1$ determinations agree well with one another and the two ETM calculations for $N_f = 2$ and $N_f = 2 + 1 + 1$ corroborate the result further. There is some discrepancy between two among the most recent determinations which have rather small error bars, namely ETM 10 [60] and RBC/UKQCD 10A [106]. We stress, however, that the value:

$$\bar{\ell}_3 = 3.2(8) \quad \text{our estimate ,} \quad (64)$$

comfortably covers all available calculations and represents a substantial progress with respect to earlier estimates. The uncertainty is three times smaller than the one attached to the old estimate in [93], which was based on analysis of the mass formulae for the pseudoscalar octet.

Table 13 collects the results obtained for the electromagnetic form factor of the pion: charge radius, curvature and the coupling constant $\bar{\ell}_6$, that determines the charge radius to leading order of the chiral expansion. The experimental information concerning the charge radius is excellent and the curvature is also known very precisely, on the basis of e^+e^- data and dispersion theory. The form factor calculations thus present an excellent testing ground for the lattice calculations. The table shows that most of the available lattice results pass the test. Concerning the value of $\bar{\ell}_6$, the situation is worse than for the charge radius also because the extraction of this constant is done differently by different groups (in particular some use the x rather than the ξ expansion and NLO rather than NNLO formulae): here the dust yet needs to settle.

Perhaps the most important physics result of this section is that the lattice simulations confirm the approximate validity of the Gell-Mann-Oakes-Renner formula and show that the square of the pion mass indeed grows in proportion to m_{ud} . The formula represents the leading term of the chiral perturbation series and necessarily receives corrections from higher orders. At first non-leading order, the correction is determined by the effective coupling constant $\bar{\ell}_3$. The results collected in Tab. 12 and in the top panel of Fig. 9 show that $\bar{\ell}_3$ is now known quite well. They corroborate the conclusion drawn in the pioneering work of reference [253]: the lattice confirms the early estimate of $\bar{\ell}_3$ derived in [93]. In the graph of M_π^2 versus m_{ud} , the values found on the lattice for $\bar{\ell}_3$ correspond to remarkably little curvature: the Gell-Mann-Oakes-Renner formula represents a crude first approximation out to values of m_{ud} that exceed the physical value by an order of magnitude.

As emphasized by Stern and collaborators [255–257], the analysis in the framework of χ PT is coherent only if (i) the leading term in the chiral expansion of M_π^2 dominates over the remainder and (ii) the ratio m_s/m_{ud} is close to the value 25.6 that follows from Weinberg's leading order formulae. In order to investigate the possibility that one or both of

Collaboration	Ref.	N_f	publication status	chiral extrapolation	continuum extrapolation	finite volume	$\bar{\ell}_3$	$\bar{\ell}_4$
ETM 10	[60]	2+1+1	A	●	●	●	3.70(7)(26)	4.67(3)(10)
MILC 10A	[103]	2+1	C	●	★	★	2.85(81)($^{+37}_{-92}$)	3.98(32)($^{+51}_{-28}$)
MILC 10	[171]	2+1	C	●	★	★	3.18(50)(89)	4.29(21)(82)
RBC/UKQCD 10A	[106]	2+1	P	●	●	★	2.57(18)	3.83(9)
MILC 09A	[59]	2+1	C	●	★	★	3.32(64)(45)	4.03(16)(17)
MILC 09A	[59]	2+1	C	●	★	★	3.0(6)($^{+9}_{-6}$)	3.9(2)(3)
PACS-CS 08	[63]	2+1	A	★	■	■	3.47(11)	4.21(11)
PACS-CS 08	[63]	2+1	A	★	■	■	3.14(23)	4.04(19)
RBC/UKQCD 08	[108]	2+1	A	●	■	★	3.13(33)(24)	4.43(14)(77)
ETM 09C	[237]	2	A	●	★	●	3.50(9)($^{+9}_{-30}$)	4.66(4)($^{+4}_{-33}$)
JLQCD/TWQCD 09	[252]	2	A	●	■	■		4.09(50)(52)
ETM 08	[235]	2	A	●	●	●	3.2(8)(2)	4.4(2)(1)
JLQCD/TWQCD 08A	[95]	2	A	●	■	■	3.38(40)(24)($^{+31}_{-0}$)	4.12(35)(30)($^{+31}_{-0}$)
CERN-TOV 06	[254]	2	A	●	●	■	3.0(5)(1)	
CGL 01	[198]							4.4(2)
GL 84	[93]						2.9(2.4)	4.3(9)

Table 12: Results for the coupling constants $\bar{\ell}_3$ and $\bar{\ell}_4$ of the effective SU(2) Lagrangian. For MILC 09A and PACS-CS 08, converted values from SU(3) fits and values from direct SU(2) fits are included. The MILC 10 results are obtained by converting the SU(3) LECs, while the MILC 10A results are obtained with a direct SU(2) fit. For comparison, the last two lines show the results obtained from a phenomenological analysis.

Collaboration	Ref.	N_f		publication status	chiral extrapolation	continuum extrapolation	finite volume	$\langle r^2 \rangle_V^\pi$ [fm ²]	c_V (GeV ⁻⁴)	$\bar{\ell}_6$
RBC/UKQCD 08A	[250]	2+1	A	●	■	★		0.418(31)	—	12.2(9)
LHP 04	[259]	2+1	A	●	■	●		0.310(46)	—	—
JLQCD/TWQCD 09	[252]	2	A	●	■	■		0.409(23)(37)	3.22(17)(36)	11.9(0.7)(1.0)
ETM 08	[235]	2	A	●	●	●		0.456(30)(24)	3.37(31)(27)	14.9(1.2)(0.7)
QCDSF/UKQCD 06A	[260]	2	A	★	●	●		0.441(19)(56)(29)	—	—
BCT 98	[234]							0.437(16)	3.85(60)	16.0(0.5)(0.7)
NA7 86	[261]							0.439(8)		
GL 84	[93]									16.5(1.1)

Collaboration	Ref.	N_f		publication status	chiral extrapolation	continuum extrapolation	finite volume	$\langle r^2 \rangle_S^\pi$ [fm ²]	$\bar{\ell}_1 - \bar{\ell}_2$
JLQCD/TWQCD 09	[252]	2	A	●	■	■		0.617(79)(66)	-2.9(0.9)(1.3)
CGL 01	[198]							0.61(4)	-4.7(6)

Table 13: *Top panel: vector form factor of the pion.* Lattice results for the charge radius $\langle r^2 \rangle_V^\pi$, the curvature c_V and the effective coupling constant $\bar{\ell}_6$ are compared with the experimental value obtained by NA7 and some phenomenological estimates ($\bar{\ell}_6$ determines the leading contribution in the chiral expansion of the charge radius). *Bottom panel: scalar form factor of the pion.* Lattice results for the scalar radius $\langle r^2 \rangle_S^\pi$ and the combination $\bar{\ell}_1 - \bar{\ell}_2$ of effective coupling constants are compared with the outcome of a dispersive calculation of these quantities [198] (the leading term in the chiral expansion of the scalar radius is determined by the coupling constant $\bar{\ell}_4$, for which the available information is collected in Tab. 12; the lattice estimate for $\bar{\ell}_1 - \bar{\ell}_2$ stems from an analysis of the momentum dependence of the vector and scalar form factors, based on the two-loop formulae of χ PT [234]).

these conditions might fail, the authors proposed a more general framework, referred to as "Generalized χ PT", which includes χ PT as a special case. The results found on the lattice demonstrate that QCD does satisfy both of the above conditions – in the context of QCD, the proposed generalization of the effective theory does not appear to be needed. There is a modified version, however, referred to as "Resummed χ PT" [258], which is motivated by the possibility that the Zweig rule violating couplings L_4 and L_6 might be larger than expected. The available lattice data do not exclude this possibility (see section 5.2.4).

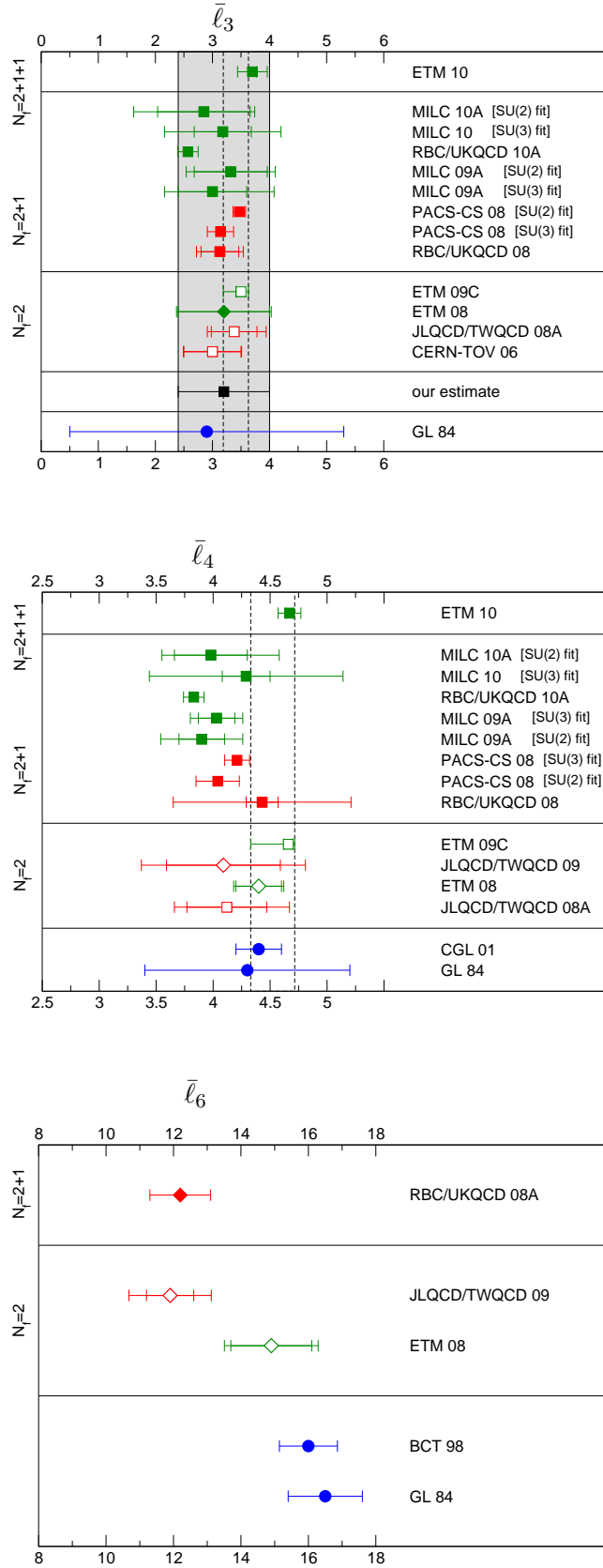


Figure 9: Summary of lattice results for the effective coupling constants $\bar{\ell}_3$, $\bar{\ell}_4$ and $\bar{\ell}_6$. The filled symbols refer to lattice calculations with $N_f = 2 + 1$, while the empty ones represent simulations with $N_f = 2$. Squares indicate determinations from correlators in the p -regime, diamonds refer to determinations from the pion form factor. The gray band represents our estimate of $\bar{\ell}_3$, whereas the dashed ones indicate the current $N_f = 2$ values of $\bar{\ell}_3$ and $\bar{\ell}_4$.

5.2 SU(3) Low-Energy Constants

5.2.1 Quark-mass dependence of pseudoscalar masses and decay constants

In the isospin limit, the relevant SU(3) formulae take the form [91]

$$\begin{aligned}
M_\pi^2 &\stackrel{\text{NLO}}{=} 2B_0 m_{ud} \left\{ 1 + \mu_\pi - \frac{1}{3}\mu_\eta + \frac{B_0}{F_0^2} \left[16m_{ud}(2L_8 - L_5) + 16(m_s + 2m_{ud})(2L_6 - L_4) \right] \right\}, \\
M_K^2 &\stackrel{\text{NLO}}{=} B_0(m_s + m_{ud}) \left\{ 1 + \frac{2}{3}\mu_\eta + \frac{B_0}{F_0^2} \left[8(m_s + m_{ud})(2L_8 - L_5) + 16(m_s + 2m_{ud})(2L_6 - L_4) \right] \right\}, \\
F_\pi &\stackrel{\text{NLO}}{=} F_0 \left\{ 1 - 2\mu_\pi - \mu_K + \frac{B_0}{F_0^2} \left[8m_{ud}L_5 + 8(m_s + 2m_{ud})L_4 \right] \right\}, \\
F_K &\stackrel{\text{NLO}}{=} F_0 \left\{ 1 - \frac{3}{4}\mu_\pi - \frac{3}{2}\mu_K - \frac{3}{4}\mu_\eta + \frac{B_0}{F_0^2} \left[4(m_s + m_{ud})L_5 + 8(m_s + 2m_{ud})L_4 \right] \right\},
\end{aligned} \tag{65}$$

where $B_0 = \Sigma_0/F_0^2$ and F_0 denote the condensate parameter and the pseudoscalar decay constant in the SU(3) chiral limit, respectively, and

$$\mu_P = \frac{M_P^2}{32\pi^2 F_0^2} \ln\left(\frac{M_P^2}{\mu^2}\right). \tag{66}$$

At the accuracy of these formulae, the quantities μ_π , μ_K , μ_η can equally well be evaluated with the leading order expressions for the masses,

$$M_\pi^2 \stackrel{\text{LO}}{=} 2B_0 m_{ud}, \quad M_K^2 \stackrel{\text{LO}}{=} B_0(m_s + m_{ud}), \quad M_\eta^2 \stackrel{\text{LO}}{=} \frac{2}{3}B_0(2m_s + m_{ud}). \tag{67}$$

Throughout, L_i denotes the renormalized low-energy constant/coupling (LEC) at scale μ . The normalization used for the decay constants is specified in footnote 13.

5.2.2 Charge radius

The SU(3) formula for the slope of the pion vector form factor reads [167]

$$\langle r^2 \rangle_{V,\pi\pi} \stackrel{\text{LO}}{=} -\frac{1}{32\pi^2 F_0^2} \left\{ 3 + 2 \ln\left(\frac{M_\pi^2}{\mu^2}\right) + \ln\left(\frac{M_K^2}{\mu^2}\right) \right\} + \frac{12L_9}{F_0^2}, \tag{68}$$

while the expression $\langle r^2 \rangle_{S,\text{oct}}$ for the octet part of the scalar radius does not contain any NLO low-energy constant at the 1-loop order [167].

5.2.3 Partially quenched formulae

The term ‘‘partially quenched QCD’’ is used in two ways. For heavy quarks (c , b and sometimes s) it usually means that these flavors are included in the valence sector, but not to the functional determinant. For the light quarks (u , d and sometimes s) it means that they are present in both the valence and the sea sector of the theory, but with different masses (e.g. a series of valence quark masses is evaluated on an ensemble with a fixed sea quark mass).

The program of extending the standard (unitary) SU(3) theory to the (second version of) ‘‘partially quenched QCD’’ has been completed at the 2-loop (NNLO) level for masses and decay constants [262]. These formulae tend to be complicated, with the consequence that a state-of-the-art analysis with $O(2000)$ bootstrap samples on $O(20)$ ensembles with $O(5)$ masses each [and hence $O(200'000)$ different fits] will require significant computational resources for the global fits. For an up-to-date summary of recent developments in Chiral Perturbation Theory relevant to lattice QCD we refer to [263].

Ref.	N_f	publication status	chiral extrapolation	continuum extrapolation	finite volume effects	renormalization	F_0 [MeV]	F/F_0	B/B_0	
JLQCD/TWQCD 10[240]	3	A	■	■	■	★	71(3)(8)			
MILC 10	[171]	2+1	C	●	★	★	●	80.3(2.5)(5.4)		
MILC 09A ²²	[59]	2+1	C	●	★	★	●	78.3(1.4)(2.9)	1.104(3)(41)	1.21(4)(⁺⁵ ₋₆)
MILC 09 ²²	[6]	2+1	A	●	★	★	●		1.15(5)(⁺¹³ ₋₃)	1.15(16)(⁺³⁹ ₋₁₃)
PACS-CS 08	[63]	2+1	A	★	■	■	■	83.8(6.4)	1.078(44)	1.089(15)
RBC/UKQCD 08	[108]	2+1	A	●	■	★	★	66.1(5.2)	1.229(59)	1.03(05)

Ref.	N_f	publication status	chiral extrapolation	continuum extrapolation	finite volume effects	renormalization	$\Sigma_0^{1/3}$ [GeV]	Σ/Σ_0	
JLQCD/TWQCD 10 [240]	3	A	■	■	■	★	0.214(6)(24)	1.31(13)(52)	
MILC 09A ²²	[59]	2+1	C	●	★	★	●	0.245(5)(4)(4)	1.48(9)(8)(10)
MILC 09 ²²	[6]	2+1	A	●	★	★	●	0.242(9)(⁺⁵ ₋₁₇)(4)	1.52(17)(⁺³⁸ ₋₁₅)
PACS-CS 08	[63]	2+1	A	★	■	■	■	0.290(15)	1.245(10)
RBC/UKQCD 08	[108]	2+1	A	●	■	★	★		1.55(21)

Table 14: Summary of lattice results for the low-energy constants F_0 , B_0 and $\Sigma_0 \equiv F_0^2 B_0$, which specify the effective SU(3) Lagrangian at leading order. The ratios F/F_0 , B/B_0 , Σ/Σ_0 , which compare these with their SU(2) counterparts, indicate the strength of the Zweig-rule violations in these quantities: in the large- N_c limit, they tend to unity. Numbers in slanted fonts are calculated by us, from the information given in the quoted references.

5.2.4 Recent lattice determinations

To date, there are three comprehensive papers with results based on lattice QCD with $N_f = 2+1$ dynamical flavors [6, 63, 108]. It is an open issue whether the data collected at $m_s \simeq m_s^{\text{phys}}$ allow for an unambiguous determination of SU(3) low-energy constants (cf. the discussion in [108]). So far only MILC has some data at considerably smaller m_s [6]. Furthermore, we are aware of a few papers with a result on one SU(3) low-energy constant each [176, 250, 264]. Some particulars of the comprehensive papers are shown in Tab. 14.

Results for the SU(3) low-energy constants of leading order are found in Tab. 14 and analogous results for some of the effective coupling constants that enter the chiral SU(3) Lagrangian at NLO are collected in Tab. 15. From PACS-CS [63] only those results are quoted which have been *corrected* for finite-size effects (misleadingly labeled “w/FSE” in their tables). For staggered data our “chiral” colour coding criterion is slightly ambiguous;

	Ref.	N_f		publication status	chiral extrapolation	continuum extrapolation	finite volume effects	$10^3 L_4$	$10^3 L_6$	$10^3(2L_6 - L_4)$
JLQCD/TWQCD 10	[240]	3	A	■	■	■			0.03(7)(17)	
MILC 10	[171]	2+1	C	●	★	★		-0.08(22)($^{+57}_{-33}$)	-0.02(16)($^{+33}_{-21}$)	0.03(24)($^{+32}_{-27}$)
MILC 09A ²²	[59]	2+1	C	●	★	★		0.04(13)(4)	0.07(10)(3)	0.10(12)(2)
MILC 09 ²²	[6]	2+1	A	●	★	★		0.1(3)($^{+3}_{-1}$)	0.2(2)($^{+2}_{-1}$)	0.3(1)($^{+2}_{-3}$)
PACS-CS 08	[63]	2+1	A	★	■	■		-0.06(10)(-)	0.02(5)(-)	0.10(2)(-)
RBC/UKQCD 08	[108]	2+1	A	●	■	★		0.14(8)(-)	0.07(6)(-)	0.00(4)(-)
Bijnens 09	[263]							0.0(-)(5)	0.0(-)(1)	0.0(-)(5)
GL 85	[91]							-0.3(5)	-0.2(3)	-0.1(8)

	Ref.	N_f		publication status	chiral extrapolation	continuum extrapolation	finite volume effects	$10^3 L_5$	$10^3 L_8$	$10^3(2L_8 - L_5)$
MILC 10	[171]	2+1	C	●	★	★		0.98(16)($^{+28}_{-41}$)	0.42(10)($^{+27}_{-23}$)	-0.15(11)($^{+45}_{-19}$)
MILC 09A ²²	[59]	2+1	C	●	★	★		0.84(12)(36)	0.36(5)(7)	-0.12(8)(21)
MILC 09 ²²	[6]	2+1	A	●	★	★		1.4(2)($^{+2}_{-1}$)	0.8(1)(1)	0.3(1)(1)
PACS-CS 08	[63]	2+1	A	★	■	■		1.45(7)(-)	0.62(4)(-)	-0.21(3)(-)
RBC/UKQCD 08	[108]	2+1	A	●	■	★		0.87(10)(-)	0.56(4)(-)	0.24(4)(-)
Bijnens 09	[263]							0.97(11)(-)	0.60(18)(-)	0.23(38)(-)
GL 85	[91]							1.4(5)	0.9(3)	0.4(8)

	Ref.	N_f		publication status	chiral extrapolation	continuum extrapolation	finite volume effects	$10^3 L_5$	$10^3 L_9$	$10^3 L_{10}$
JLQCD 08A	[264]	2	A	●	■	■				-5.2(2)($^{+5}_{-3}$)
RBC/UKQCD 08A	[250]	2+1	A	●	■	★			3.08(23)(51)	
NPLQCD 06	[176]	2+1	A	●	■	■		1.42(2)($^{+18}_{-54}$)		
Bijnens 09	[263]							0.97(11)(-)	5.93(43)(-)	
GL 85	[91]							1.4(5)	6.9(7)	-5.5(7)

Table 15: Summary of lattice results for some of the coupling constants that enter the effective SU(3) Lagrangian at NLO (running scale $\mu = 770$ MeV – the values in [6, 59, 91, 171] are evolved accordingly). The PACS-CS entry for L_6 is obtained from their results for $2L_6 - L_4$ and L_4 (and similarly for other entries in slanted fonts).

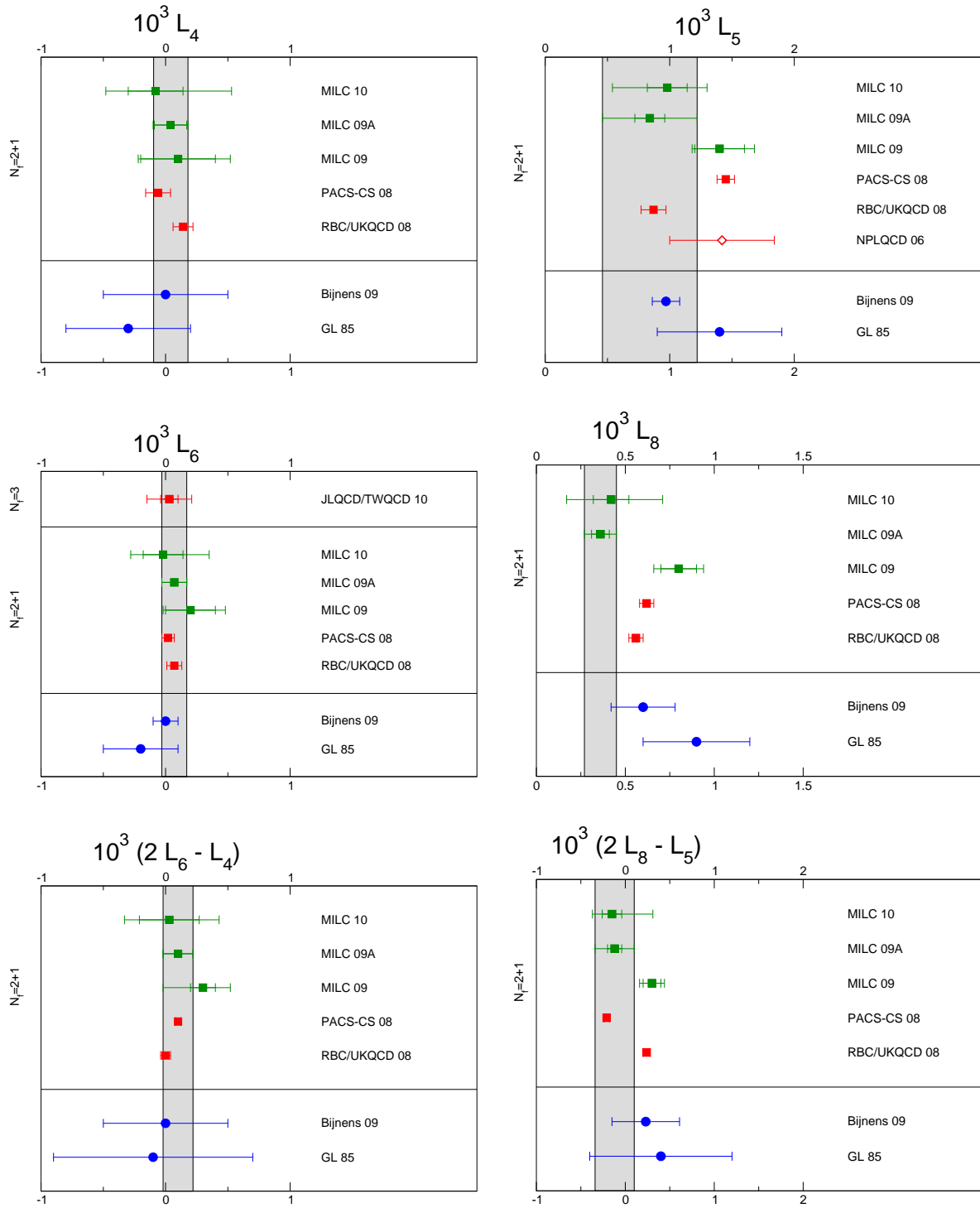


Figure 10: Summary of various lattice determinations of SU(3) low-energy constants.

we solve this issue pragmatically.²²

A graphical summary of the lattice results for the coupling constants L_4 , L_5 , L_6 and

²² The “chiral extrapolation” rating of [6] is based on the information on the RMS masses given in [59].

L_8 , which determine the masses and the decay constants of the pions and kaons at NLO of the chiral SU(3) expansion, is displayed in Fig. 10, along with the two phenomenological determinations quoted in the above tables. In general, there is a rather convincing overall consistency, although some of the lattice results possibly underestimate the theoretical error. Since only the calculation by the MILC collaboration is free of red tags, the gray bands in Fig. 10 mark their results.

In spite of this apparent consistency, there is a point which needs to be clarified as soon as possible. Some collaborations (RBC/UKQCD and PACS-CS) find that they are having difficulties in fitting their partially quenched data to the respective formulas for pion masses above $\simeq 400$ MeV. Evidently, this indicates that the data are stretching the regime of validity of these formulas. To date it is, however, not clear which subset of the data causes the troubles, whether it is the unitary part extending to too large values of the quark masses or whether it is due to $m^{\text{val}}/m^{\text{sea}}$ differing too much from one. In fact, little is known, in the framework of partially quenched χ PT, about the *shape* of the region of applicability in the m^{val} versus m^{sea} plane for fixed N_f .

In the large- N_c limit, the Zweig-rule becomes exact, but the quarks have $N_c = 3$. The work done on the lattice is ideally suited to disprove or confirm the approximate validity of this rule. Two of the coupling constants entering the effective SU(3) Lagrangian at NLO disappear when N_c is sent to infinity: L_4 and L_6 . The upper part of Tab. 15 and the left panels of Fig. 10 show that the lattice results for these are quite coherent. At the scale $\mu = M_\rho$, L_4 and L_6 are consistent with zero, indicating that these constants do approximately obey the Zweig-rule. As mentioned above, the ratios F/F_0 , B/B_0 and Σ/Σ_0 also test the validity of this rule. Their expansion in powers of m_s starts with unity and the contributions of first order in m_s are determined by the constants L_4 and L_6 , but they also contain terms of higher order. Quite apart from measuring the Zweig-rule violations, an accurate determination will thus also allow us to determine the range of m_s where the first few terms of the expansion represent an adequate approximation. Unfortunately, at present, the uncertainties in the lattice data on the ratios are too large to draw conclusions, both concerning the relative size of the subsequent terms in the chiral perturbation series and concerning the magnitude of the Zweig-rule violations. The data do appear to confirm the *paramagnetic inequalities* [257], which require $F/F_0 > 1$, $\Sigma/\Sigma_0 > 1$ and it appears that the ratio B/B_0 is also larger than unity, but the numerical results need to be improved before further conclusions can be drawn.

In principle, the matching formulae in [91] can be used to calculate the SU(2) couplings \bar{l}_i from the SU(3) couplings L_i .²³ This procedure, however, yields less accurate results than a direct determination within SU(2), as it relies on the expansion in powers of m_s , where the omitted higher order contributions generate comparatively large uncertainties. We plead with every collaboration performing $N_f = 2 + 1$ simulations to *directly* analyze their data in the SU(2) framework. In practice, lattice simulations are performed at values of m_s close to the physical value and the results are then corrected for the difference of m_s from its physical value. If simulations with more than one value of m_s have been performed, then this can be done by interpolation. Alternatively one can use the technique of *reweighting* (for a review see [5]), which applies an a posteriori correction to shift m_s into its physical value.

²³For instance, for the MILC data this yields $\bar{l}_3 = 3.32(64)(45)$ and $\bar{l}_4 = 4.03(16)(17)$ [59].

6 Kaon B -parameter B_K

6.1 Indirect CP-violation and ϵ_K

The mixing of neutral pseudoscalar mesons plays an important role in the understanding of the physics of CP-violation. In this section we will only focus on $K^0 - \bar{K}^0$ oscillations, which probe the physics of indirect CP-violation. We collect and comment the basic formulae; for extended reviews on the subject see, among others, refs. [265–267]. Indirect CP-violation arises in $K_L \rightarrow \pi\pi$ transitions through the decay of the CP = +1 component of K_L into two pions (which are also in a CP = +1 state). Its measure is defined as

$$\epsilon_K = \frac{\mathcal{A}[K_L \rightarrow (\pi\pi)_{I=0}]}{\mathcal{A}[K_S \rightarrow (\pi\pi)_{I=0}]}, \quad (69)$$

with the final state having total isospin zero. The parameter ϵ_K may also be expressed in terms of $K^0 - \bar{K}^0$ oscillations. In particular, to lowest order in the electroweak theory, the contribution to these oscillations arises from so-called box diagrams, in which two W -bosons and two “up-type” quarks (i.e. up, charm, top) are exchanged between the constituent down and strange quarks of the K -mesons. The loop integration of the box diagrams can be performed exactly. In the limit of vanishing external momenta and external quark masses, the result can be identified with an effective four-fermion interaction, expressed in terms of the “effective Hamiltonian”

$$\mathcal{H}_{\text{eff}}^{\Delta S=2} = \frac{G_F^2 M_W^2}{16\pi^2} \mathcal{F}^0 Q^{\Delta S=2} + \text{h.c.} . \quad (70)$$

In this expression, G_F is the Fermi coupling, M_W the W -boson mass, and

$$Q^{\Delta S=2} = [\bar{s}\gamma_\mu(1 - \gamma_5)d][\bar{s}\gamma_\mu(1 - \gamma_5)d] \equiv O_{\text{VV}+\text{AA}} - O_{\text{VA}+\text{AV}}, \quad (71)$$

is a dimension-six, four-fermion operator. The function \mathcal{F}^0 is given by

$$\mathcal{F}^0 = \lambda_c^2 S_0(x_c) + \lambda_t^2 S_0(x_t) + 2\lambda_c\lambda_t S_0(x_c, x_t), \quad (72)$$

where $\lambda_a = V_{as}^* V_{ad}$, and $a = c, t$ denotes a flavour index. The quantities $S_0(x_c)$, $S_0(x_t)$ and $S_0(x_c, x_t)$ with $x_c = m_c^2/M_W^2$, $x_t = m_t^2/M_W^2$ are the Inami-Lim functions [268], which express the basic electroweak loop contributions without QCD corrections. The contribution of the up quark, which is taken to be massless in this approach, has been taken into account by imposing the unitarity constraint $\lambda_u + \lambda_c + \lambda_t = 0$.

When strong interactions are included, $\Delta S = 2$ transitions can no longer be discussed at the quark level. Instead, the effective Hamiltonian must be considered between mesonic initial and final states. Since the strong coupling constant is large at typical hadronic scales, the resulting weak matrix element cannot be calculated in perturbation theory. The operator product expansion (OPE) does, however, factorize long- and short- distance effects. For energy scales below the charm threshold, the $K^0 - \bar{K}^0$ transition amplitude of the effective Hamiltonian can be expressed as

$$\begin{aligned} \langle \bar{K}^0 | \mathcal{H}_{\text{eff}}^{\Delta S=2} | K^0 \rangle &= \frac{G_F^2 M_W^2}{16\pi^2} \left[\lambda_c^2 S_0(x_c) \eta_1 + \lambda_t^2 S_0(x_t) \eta_2 + 2\lambda_c\lambda_t S_0(x_c, x_t) \eta_3 \right] \\ &\times \left(\frac{\bar{g}(\mu)^2}{4\pi} \right)^{-\gamma_0/(2\beta_0)} \left\{ 1 + \frac{\bar{g}(\mu)^2}{(4\pi)^2} \left[\frac{\beta_1\gamma_0 - \beta_0\gamma_1}{2\beta_0^2} \right] \right\} \langle \bar{K}^0 | Q_{\text{R}}^{\Delta S=2}(\mu) | K^0 \rangle + \text{h.c.}, \quad (73) \end{aligned}$$

where $\bar{g}(\mu)$ and $Q_{\text{R}}^{\Delta S=2}(\mu)$ are the renormalized gauge coupling and four-fermion operator in some renormalization scheme. The factors η_1, η_2 and η_3 depend on the renormalized coupling \bar{g} , evaluated at the various flavour thresholds m_t, m_b, m_c and M_{W} , as required by the OPE and RG-running procedure that separates high- and low-energy contributions. Explicit expressions can be found in [266] and references therein. We follow the same conventions for the RG-equations as in ref. [266]. Thus the Callan-Symanzik function and the anomalous dimension $\gamma(\bar{g})$ of $Q^{\Delta S=2}$ are defined by

$$\frac{d\bar{g}}{d\ln\mu} = \beta(\bar{g}), \quad \frac{dQ_{\text{R}}^{\Delta S=2}}{d\ln\mu} = -\gamma(\bar{g}) Q_{\text{R}}^{\Delta S=2}, \quad (74)$$

with perturbative expansions

$$\begin{aligned} \beta(g) &= -\beta_0 \frac{g^3}{(4\pi)^2} - \beta_1 \frac{g^5}{(4\pi)^4} - \dots \\ \gamma(g) &= \gamma_0 \frac{g^2}{(4\pi)^2} + \gamma_1 \frac{g^4}{(4\pi)^4} + \dots \end{aligned} \quad (75)$$

We stress that β_0, β_1 and γ_0 are universal, i.e. scheme-independent. $K^0 - \bar{K}^0$ mixing is usually considered in the naive dimensional regularization (NDR) scheme of $\overline{\text{MS}}$, and below we specify the perturbative coefficient γ_1 in that scheme:

$$\begin{aligned} \beta_0 &= \left\{ \frac{11}{3}N - \frac{2}{3}N_f \right\}, & \beta_1 &= \left\{ \frac{34}{3}N^2 - N_f \left(\frac{13}{3}N - \frac{1}{N} \right) \right\}, \\ \gamma_0 &= \frac{6(N-1)}{N}, & \gamma_1 &= \frac{N-1}{2N} \left\{ -21 + \frac{57}{N} - \frac{19}{3}N + \frac{4}{3}N_f \right\}. \end{aligned} \quad (76)$$

Note that for QCD the above expressions must be evaluated for $N = 3$ colours, while N_f denotes the number of active quark flavours. As already stated, eq. (73) is valid at scales below the charm threshold, after all heavier flavours have been integrated out, i.e. $N_f = 3$.

In eq. (73), the terms proportional to η_1, η_2 and η_3 , multiplied by the contributions containing $\bar{g}(\mu)^2$, correspond to the Wilson coefficient of the OPE, estimated at NLO in perturbation theory. Its dependence on the renormalization scheme and scale μ is cancelled by that of the weak matrix element $\langle \bar{K}^0 | Q_{\text{R}}^{\Delta S=2}(\mu) | K^0 \rangle$. The latter corresponds to the long-distance effects of the effective Hamiltonian and must be computed non-perturbatively. For historical, as well as technical reasons, it is convenient to express it in terms of the B -parameter B_K , defined as

$$B_K(\mu) = \frac{\langle \bar{K}^0 | Q_{\text{R}}^{\Delta S=2}(\mu) | K^0 \rangle}{\frac{8}{3}f_K^2 m_K^2}. \quad (77)$$

The four-quark operator $Q^{\Delta S=2}(\mu)$ is renormalized at scale μ in some regularization scheme, usually taken to be NDR. The renormalization group independent (RGI) B -parameter \hat{B}_K is related to $B_K(\mu)$ by the exact formula

$$\hat{B}_K = \left(\frac{\bar{g}(\mu)^2}{4\pi} \right)^{-\gamma_0/(2\beta_0)} \exp \left\{ \int_0^{\bar{g}(\mu)} dg \left(\frac{\gamma(g)}{\beta(g)} + \frac{\gamma_0}{\beta_0 g} \right) \right\} B_K(\mu). \quad (78)$$

At NLO in perturbation theory, the above reduces to

$$\hat{B}_K = \left(\frac{\bar{g}(\mu)^2}{4\pi} \right)^{-\gamma_0/(2\beta_0)} \left\{ 1 + \frac{\bar{g}(\mu)^2}{(4\pi)^2} \left[\frac{\beta_1 \gamma_0 - \beta_0 \gamma_1}{2\beta_0^2} \right] \right\} B_K(\mu), \quad (79)$$

which, to this order, is the scale-independent product of all μ -dependent quantities in eq. (73).

The implementation of non-perturbative renormalization in lattice calculations is based on the numerical evaluation of a non-perturbative matching condition between the bare operator matrix element and its counterpart in some intermediate renormalization scheme, where the latter has a controlled perturbative relation to continuum schemes such as $\overline{\text{MS}}$. Examples of intermediate schemes are the RI/MOM scheme [115] (also dubbed the ‘‘Rome-Southampton method’’) and the Schrödinger functional (SF) scheme [114]. Typical scales for the transition between lattice regularization and intermediate scheme are $\mu = \mathcal{O}(1 \text{ GeV})$. When applied to the case at hand, this implies that $B_K(\mu \approx 1 \text{ GeV})$ in the intermediate scheme must then be matched to the RGI B -parameter via eq. (79). Obviously, due to asymptotic freedom, the NLO relation provides a more reliable link if it is applied at scales far greater than $\mu = \mathcal{O}(1 \text{ GeV})$. Therefore, in order to remove any doubts about the use of perturbation theory at NLO when determining \hat{B}_K , it is advantageous to run non-perturbatively to larger values of μ , where eq. (79) provides an accurate matching relation. Indeed, neglecting higher orders in perturbation theory has been identified by the authors of [269] as one of the dominant systematic uncertainties in their result for \hat{B}_K . We note that the short-distance QCD corrections in eq. (73) are known in perturbation theory, to NLO for η_1, η_2 and to NNLO for η_3 [270]. This implies that an uncertainty of $\mathcal{O}(\alpha_s(m_c))$ pertains to the $K^0 - \bar{K}^0$ transition amplitude and ϵ_K , even if the computation of the kaon B -parameter is essentially free from perturbative effects. However, since η_1 and η_2 are currently being determined beyond NLO as well [271], the issue of eliminating systematic uncertainties arising from the use of perturbation theory in the matching procedure becomes more acute.

The ‘‘master formula’’, for ϵ_K , which connects the experimentally observable quantity ϵ_K to the matrix element of $\mathcal{H}_{\text{eff}}^{\Delta S=2}$, is [267, 272, 273]

$$\epsilon_K = \exp(i\phi_\epsilon) \sin(\phi_\epsilon) \left[\frac{\text{Im}[\langle \bar{K}^0 | \mathcal{H}_{\text{eff}}^{\Delta S=2} | K^0 \rangle]}{\Delta M_K} + \frac{\text{Im}(A_0)}{\text{Re}(A_0)} \right], \quad (80)$$

for λ_u real and positive; the phase of ϵ_K is given by

$$\phi_\epsilon = \arctan \frac{\Delta M_K}{\Delta \Gamma_K / 2}. \quad (81)$$

The quantities ΔM_K and $\Delta \Gamma_K$ are the mass- and decay width-differences between long- and short-lived neutral Kaons, while A_0 is the amplitude of the Kaon decay into an isospin-0 two pion state. Experimentally known values of the above quantities are:

$$\begin{aligned} |\epsilon_K| &= 2.280(13) \times 10^{-3}, \\ \phi_\epsilon &= 43.51(5)^\circ, \\ \Delta M_K &= 3.491(9) \times 10^{-12} \text{ MeV}, \\ \Delta \Gamma_K &= 7.335(4) \times 10^{-15} \text{ GeV}, \end{aligned} \quad (82)$$

while the last term in the square brackets of eq. (80) has been estimated in ref. [274]. Long distance contributions, omitted from the first term in the square brackets of eq. (80) have been recently discussed in ref. [275].

6.2 Lattice computation of B_K

The lattice calculation of B_K is affected by the same systematic effects, discussed in previous sections. However, the issue of renormalization merits special attention. The reason

is that the multiplicative renormalizability of the relevant operator $Q^{\Delta S=2}$ is lost, once the regularized QCD action ceases to be invariant under chiral transformations. With Wilson fermions, $Q^{\Delta S=2}$ mixes with four additional dimension-six operators which belong to different representations of the chiral group, with mixing coefficients that are finite functions of the gauge coupling. This complicated renormalization pattern is the main source of systematic error in computations of B_K with Wilson quarks. It can be bypassed via the implementation of specifically designed methods, which are either based on Ward identities [276] or on a modification of the Wilson quark action, known as twisted mass QCD [52, 277]. An advantage of staggered fermions is the presence of a remnant $U(1)$ chiral symmetry. However, at non-vanishing lattice spacing, the symmetry among the extra unphysical degrees of freedom (tastes) is broken. As a result, mixing with other dimension-six operators cannot be avoided in the staggered formulation, which complicates the determination of the B -parameter.

Fermionic lattice actions based on the Ginsparg-Wilson relation [278] are invariant under the chiral group, and hence four-quark operators such as $Q^{\Delta S=2}$ renormalize multiplicatively. However, depending on the particular formulation of Ginsparg-Wilson fermions, residual chiral symmetry breaking effects may be present in actual calculations. For instance, in the case of domain wall fermions, the finiteness of the extra 5th dimension implies that the decoupling of modes with different chirality is not exact, which produces a residual non-zero quark mass in the chiral limit. Whether or not a significant mixing with dimension-six operators is induced as well must be investigated on a case-by-case basis.

In this section we focus on recent results for B_K , obtained for $N_f = 2$ and $2 + 1$ flavours of dynamical quarks. A compilation of results is shown in Table 16 and Fig. 11. An overview of the quality of systematic error studies is represented by the colour coded entries in Table 16. In Appendix B.4 we gather the simulation details and results from different collaborations, the values of the most relevant lattice parameters, and comparative tables on the various estimates of systematic errors. Note that some references do not quote results for both B_K and \hat{B}_K . In this case we have performed the conversion ourselves by evaluating the proportionality factor in eq. (79) for $\mu = 2 \text{ GeV}$. This requires fixing the value of $\alpha_s(2 \text{ GeV})$ in the two- and three-flavour cases. For $N_f = 2$ we have inserted the non-perturbative result for the Λ -parameter by the ALPHA Collaboration [279], i.e. $\Lambda^{(2)} = 245(16)(16) \text{ MeV}$, into the NLO expression for α_s , neglecting the quoted error. This gives $\hat{B}_K/B_K = 1.412$, in accordance with ref. [280]. For $N_f = 3$ we use the value $\alpha_s(M_Z) = 0.1184$ [122] and run it across the quark thresholds down to $\mu = 2 \text{ GeV}$, using the four-loop RG β -function. We then obtain $\hat{B}_K/B_K = 1.368$ in the three-flavour theory.

At present four collaborations have reported estimates of B_K for $N_f = 2 + 1$. The RBC/UKQCD collaboration uses domain wall fermions, while the results by HPQCD/UKQCD are based on the configurations generated by MILC, using Asqtad improved, rooted staggered fermions. In Aubin 09 a mixed-action approach is adopted in which staggered sea quarks²⁴ are combined with HYP-smearred [289] domain wall fermions. The SWME result reported in [281] is also based on the Asqtad MILC ensembles, but uses HYP-smearred staggered quarks in the valence sector.

In view of our quality criteria we note that one main shortcoming of the results by HPQCD/UKQCD 06 [285] is that they are based on data obtained at a single lattice spacing. This is also true for the results of RBC/UKQCD 07A, 08 [108, 284], which, however, have recently been updated by including data at a second value of a (see RBC/UKQCD 10B

²⁴Aubin 09 also use configurations generated by MILC.

Collaboration	Ref.	N_f		publication status	continuum extrapolation	chiral extrapolation	finite volume	renormalization	running	B_K	\hat{B}_K
SWME 11	[281]	2+1	P	★	●	●	■	–	–	0.523(7)(26)	0.716(10)(35)
RBC/UKQCD 10B	[282]	2+1	P	●	●	★	★	<i>a</i>	–	0.549(5)(26)	0.749(7)(26)
SWME 10	[283]	2+1	A	★	●	●	■	–	–	0.529(9)(32)	0.724(12)(43)
Aubin 09	[269]	2+1	A	●	★ [□]	●	★	–	–	0.527(6)(21)	0.724(8)(29)
RBC/UKQCD 07A, 08	[108, 284]	2+1	A	■	●	★	★	–	–	0.524(10)(28)	0.720(13)(37)
HPQCD/UKQCD 06	[285]	2+1	A	■	●*	★	■	–	–	0.618(18)(135)	0.83(18)
ETM 10A	[286]	2	A	★	●	●	★	<i>b</i>	–	0.516(18)(12)	0.729(25)(17)
JLQCD 08	[280]	2	A	■	●	■	★	–	–	0.537(4)(40)	0.758(6)(71)
RBC 04	[287]	2	A	■	■	■ [†]	★	–	–	0.495(18)	0.699(25)
UKQCD 04	[288]	2	A	■	■	■ [†]	■	–	–	0.49(13)	0.69(18)

* This result has been obtained with only two “light” sea quark masses.

[†] These results have been obtained at $(M_\pi L)_{\min} > 4$ in a lattice box with a spatial extension $L < 2$ fm.

[□] In this mixed action computation, the lightest valence pion weighs ~ 230 MeV, while the lightest sea taste-pseudoscalar, used in the chiral fits, weighs ~ 370 MeV.

a B_K is renormalized non-perturbatively at a scale of 2 GeV in a couple of $N_f = 3$ RI/SMOM schemes. A careful study of perturbative matching uncertainties has been performed by comparing results in the two schemes in the region of 2 GeV to 3 GeV [282].

b B_K is renormalized non-perturbatively at scales $1/a \sim 2 \div 3$ GeV in the $N_f = 2$ RI/MOM scheme. In this scheme, non-perturbative and NLO running for the are shown to agree from 4 GeV down 2 GeV to better than 3% [102, 286].

Table 16: Results for the kaon B -parameter together with a summary of systematic errors. If information about non-perturbative running is available, this is indicated in the column “running”, with details given at the bottom of the table.

[282]). The good agreement between the earlier results and the latest update indicates that discretization effects for B_K , computed using domain wall fermions appear to be small at the present level of accuracy. Aubin09 have also data at two values of the lattice spacing, similar to those of RBC/UKQCD 10B, while the SWME 10 [283] and SWME 11 [281] results are obtained at three and four lattice spacings, respectively. Having two smaller lattice spacings at their disposal compared to other collaborations, SWME 10,11 have performed the most complete study of discretization effects for this quantity so far.

The determination of the renormalization factors merits special attention, owing to the fact that the renormalization and mixing patterns of four-quark operators such as $Q^{\Delta S=2}$ are typically much more complicated than for quark bilinears. The renormalization factors used by HPQCD/UKQCD 06 are based on perturbation theory at one loop, which is by far the biggest source of systematic uncertainty quoted by these authors. The same is true for the SWME 10,11 results [281, 283]: Here the estimated uncertainty in their latest estimate

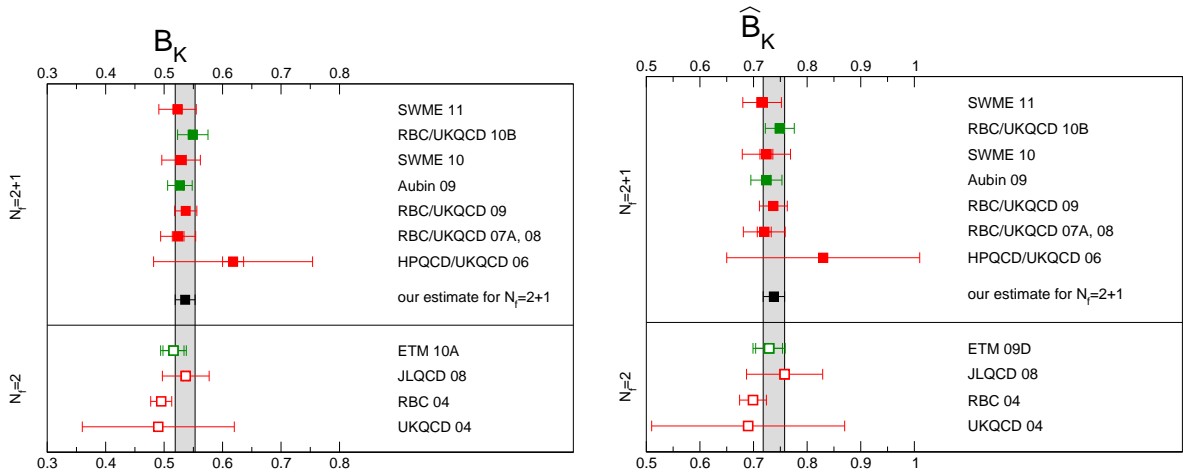


Figure 11: Recent unquenched lattice results for B_K ($\overline{\text{MS}}$ -scheme, scale $\mu = 2 \text{ GeV}$) and for the corresponding RGI parameter \hat{B}_K . The gray band indicates our estimate.

for B_K [281] arising from neglecting higher orders in perturbation theory amounts to 4.4%, which accounts for about 95% of the entire systematic error reported by this collaboration. The two other groups, RBC/UKQCD 07A, 08, 10B and Aubin 09, have both implemented a non-perturbative renormalization procedure based on the RI/MOM scheme. Nonetheless, Aubin 09 state that their biggest single systematic uncertainty of 3.2% in B_K (or 85% of the total systematic error) is still associated with the uncertainty in the renormalization factor which links the B -parameter of the bare operator to that in the $\overline{\text{MS}}$ -scheme at 2 GeV. RBC/UKQCD 10B [282] have investigated several different RI/MOM schemes, including so-called non-exceptional momenta. The resulting spread of results in different schemes is then included in the uncertainty for the renormalization factor. As observed in [282], this error can be significantly reduced if the conversion to the $\overline{\text{MS}}$ -scheme is performed at 3 GeV instead of the conventional choice, $\mu = 2 \text{ GeV}$. For this reason, the RBC/UKQCD collaboration prefers to quote $B_K^{\overline{\text{MS}}}(3 \text{ GeV})$, but also gives the value obtained at the conventional scale, for comparison with other results. All of the numbers listed in the first column of Table 16 refer to the conventional scale. In ref. [290] the RBC/UKQCD collaboration also investigated the effects of residual chiral symmetry breaking induced by the finite extent of the 5th dimension in the domain wall fermion formulation and found that the mixing of $Q^{\Delta S=2}$ with operators of opposite chirality was negligibly small.

The rules of section 2 stipulate that our averages only involve results which are free of red tags and are published in a refereed journal. Papers which, at the time of writing, are still unpublished but are obvious updates of earlier published results should also be taken into account. In view of the above, we combine the results of Aubin 09 and RBC/UKQCD 10B, by applying the following procedure: in a first step statistical and systematic errors are added in quadrature, in order to have an overall error for the result of a particular collaboration. In a second step the results from the two groups are combined in a weighted average. This yields

$$N_f = 2 + 1 : \quad B_K^{\overline{\text{MS}}}(2\text{GeV}) = 0.536(17) \quad \hat{B}_K = 0.738(20). \quad (83)$$

Here we have used the RBC/UKQCD 10B result at the scale of 2 GeV, in spite of the bigger uncertainty reported for the associated renormalization factor.

Due to the use of one-loop perturbation theory for the renormalization factor, the SWME results are assigned a red tag and are thus not included in the average. However it must be stressed that they are in excellent agreement with eq. (83). Also the earlier HPQCD/UKQCD estimate, albeit with bigger statistical and systematic errors, agrees with our average. The observation that independent calculations produce compatible results – despite the fact that according to the colour coding in Table 16 some systematic effects are not fully controlled – lends further confidence to the result quoted in eq. (83).

We now pass over to the results computed for $N_f = 2$ flavours of dynamical quarks. The UKQCD 04 result [288], computed with $O(a)$ improved Wilson fermions, is afflicted by many systematic errors and has a rather large overall error. Results by the JLQCD collaboration [280] are computed using overlap fermions in both the sea and valence quark sectors. Besides the usual systematic uncertainties listed in Table 16, they quote a 5% systematic error due to the uncertainty in the physical value of r_0 , which sets the scale in their simulation. They also quote a 1.4% systematic error, owing to the fact that they determine B_K on gauge configurations with a fixed value of the topological charge. In view of the high numerical cost of simulations with dynamical overlap quarks, it is not surprising that the lattice sizes of ref. [280] are smaller than those in present simulations with $N_f = 2 + 1$ flavours of dynamical staggered or domain wall fermions. Consequently, finite-volume effects are less well controlled in ref. [280]. The RBC 04 result [287] has been obtained using domain wall fermions at rather heavy pseudoscalar (pion) masses; otherwise it has similar systematics as the JLQCD 08 run. The result by ETM 09D [291] is based on a set of ensembles which allows for an extensive investigation of systematic uncertainties. In particular, it is so far the only $N_f = 2$ calculation involving data computed at three values of the lattice spacing. Being the only result without red tags, it is quoted as the currently best overall estimate for $N_f = 2$:

$$N_f = 2 : \quad B_K^{\overline{\text{MS}}}(2\text{GeV}) = 0.516(18)(12) \quad \hat{B}_K = 0.729(25)(17). \quad (84)$$

It is clear that with the present level of accuracy, any dependence of B_K on the number of dynamical quark flavours, N_f , is not visible.

It is interesting to compare these results to the best available quenched data, computed for large (valence) quark masses and with degenerate down and strange quarks. Avoiding a detailed discussion about the systematics, we show an (incomplete) compilation of indicative results in Tab. 17. We see that they agree with the ones obtained with $N_f = 2$ and $N_f = 2 + 1$ at the level of two standard deviations.

Collaboration	Ref.	N_f	B_K	\hat{B}_K
ALPHA 09	[292]	0	0.532(25)	0.73(3)
CP-PACS 08	[293]	0	0.565(6)	0.782(9)
ALPHA 07	[294]	0	0.534(52)	0.74(7)
JLQCD 97	[295]	0	0.628(42)	0.86(6)

Table 17: Quenched results for the B -parameter B_K from various collaborations. Errors have been combined in quadrature.

Acknowledgments

We wish to thank Sinya Aoki, Silas Beane, Claude Bernard, Joachim Brod, Petros Dimopoulos, Xining Du, Jürg Gasser, Peter Hasenfratz, Shoji Hashimoto, Gregorio Herdoiza, Matthias Jamin, Karl Jansen, Kim Maltman, Ferenc Niedermayer, Uli Nierste, Carlos Pena, Matts Roos, Gerrit Schierholz, Stephen Sharpe and André Walker-Loud for correspondence and useful comments. The Albert Einstein Center for Fundamental Physics at the University of Bern is supported by the “Innovations- und Kooperationsprojekt C-13” of the “Schweizerische Universitätskonferenz SUK/CRUS”. This work was partially supported by CNRS grants GDR n^o 2921 (Physique subatomique et calculs sur réseau) and PICS n^o 4707, by UK STFC grant ST/G000557/1, by the Helmholtz Association through the virtual institute “Spin and strong QCD” (VH-VI-231), by the Swiss National Science Foundation and by EU contract MRTN-CT-2006-035482 (Flavianet).

A Glossary

A.1 Lattice actions

In this appendix we give brief descriptions of the lattice actions used in the simulations and summarize their main features.

A.1.1 Gauge actions

The simplest and most widely used discretization of the Yang-Mills part of the QCD action is the Wilson plaquette action [296]:

$$S_G = \beta \sum_x \sum_{\mu < \nu} \left(1 - \frac{1}{3} \text{Re Tr } W_{\mu\nu}^{1 \times 1}(x) \right), \quad (85)$$

where the plaquette, $W_{\mu\nu}^{1 \times 1}(x)$, is the product of link variables around an elementary square of the lattice, i.e.

$$W_{\mu\nu}^{1 \times 1}(x) \equiv U_\mu(x) U_\nu(x + a\hat{\mu}) U_\mu(x + a\hat{\nu})^{-1} U_\nu(x)^{-1}. \quad (86)$$

This expression reproduces the Euclidean Yang-Mills action in the continuum up to corrections of order a^2 . There is a general formalism, known as the “Symanzik improvement programme” [18, 19], which is designed to cancel the leading lattice artifacts, such that observables have an accelerated rate of convergence to the continuum limit. The improvement programme is implemented by adding higher-dimensional operators, whose coefficients must be tuned appropriately in order to cancel the leading lattice artifacts. The effectiveness of this procedure depends largely on the method with which the coefficients are determined. The most widely applied methods (in ascending order of effectiveness) include perturbation theory, tadpole-improved (partially resummed) perturbation theory, renormalization group methods, and the non-perturbative evaluation of improvement conditions.

In the case of Yang-Mills theory, the simplest version of an improved lattice action is obtained by adding rectangular 1×2 loops to the plaquette action, i.e.

$$S_G^{\text{imp}} = \beta \sum_x \left\{ c_0 \sum_{\mu < \nu} \left(1 - \frac{1}{3} \text{Re Tr } W_{\mu\nu}^{1 \times 1}(x) \right) + c_1 \sum_{\mu, \nu} \left(1 - \frac{1}{3} \text{Re Tr } W_{\mu\nu}^{1 \times 2}(x) \right) \right\}, \quad (87)$$

where the coefficients c_0, c_1 satisfy the normalization condition $c_0 + 8c_1 = 1$. The *Symanzik-improved* [297], *Iwasaki* [298], and *DBW2* [299, 300] actions are all defined through eq. (87) via particular choices for c_0, c_1 . Details are listed in Table 18 together with the abbreviations used in the summary tables.

Abbrev.	c_1	Description
Wilson	0	Wilson plaquette action
tlSym	$-1/12$	tree-level Symanzik-improved gauge action
tadSym	variable	tadpole Symanzik-improved gauge action
Iwasaki	-0.331	Renormalization group improved (“Iwasaki”) action
DBW2	-1.4088	Renormalization group improved (“DBW2”) action

Table 18: Summary of lattice gauge actions. The leading lattice artifacts are $O(a^2)$ or better for all discretizations.

A.1.2 Quark actions

If one attempts to discretize the quark action, one is faced with the fermion doubling problem: the naive lattice transcription produces a 16-fold degeneracy of the fermion spectrum.

Wilson fermions

Wilson’s solution to the doubling problem is based on adding a dimension-5 operator which removes the doublers from the low-energy spectrum. The Wilson-Dirac operator for the massless case reads [296]

$$D_w = \frac{1}{2}\gamma_\mu(\nabla_\mu + \nabla_\mu^*) + a\nabla_\mu^*\nabla_\mu, \quad (88)$$

where ∇_μ, ∇_μ^* denote lattice versions of the covariant derivative. Adding the Wilson term, $a\nabla_\mu^*\nabla_\mu$, results in an explicit breaking of chiral symmetry even in the massless theory. Furthermore, the leading order lattice artifacts are of order a . With the help of the Symanzik improvement programme, the leading artifacts can be cancelled by adding the so-called “Clover” or Sheikholeslami-Wohlert (SW) term. The resulting expression in the massless case reads

$$D_{sw} = D_w + \frac{ia}{4}c_{sw}\sigma_{\mu\nu}\widehat{F}_{\mu\nu}, \quad (89)$$

where $\sigma_{\mu\nu} = \frac{i}{2}[\gamma_\mu, \gamma_\nu]$, and $\widehat{F}_{\mu\nu}$ is a lattice transcription of the gluon field strength tensor $F_{\mu\nu}$. Provided that the coefficient c_{sw} is suitably tuned, observables computed using D_{sw} will approach the continuum limit with a rate proportional to a^2 . Chiral symmetry remains broken, though. The coefficient c_{sw} can be determined perturbatively at tree-level (tree-level impr., $c_{sw} = 1$ or tlSW in short), via a mean field approach [301] (mean-field impr. or mfSW) or via a non-perturbative approach [302] (non-perturbatively impr. or npSW).

Finally, we mention “twisted mass QCD” as a method which was originally designed to address another problem of Wilson’s discretization: the Wilson-Dirac operator is not protected against the occurrence of unphysical zero modes, which manifest themselves as “exceptional” configurations. They occur with a certain frequency in numerical simulations with Wilson quarks and can lead to strong statistical fluctuations. The problem can be cured by introducing a so-called “chirally twisted” mass term, after which the fermionic part of the QCD action in the continuum assumes the form [52]

$$S_F^{\text{tm;cont}} = \int d^4x \bar{\psi}(x)(\gamma_\mu D_\mu + m + i\mu_q\gamma_5\tau^3)\psi(x). \quad (90)$$

Here, μ_q is the twisted mass parameter, and τ^3 is a Pauli matrix. The standard action in the continuum can be recovered via a global chiral field rotation. The lattice action of twisted mass QCD (tmWil) for $N_f = 2$ flavours is defined as

$$S_F^{\text{tm}}[U, \bar{\psi}, \psi] = a^4 \sum_{x \in \Lambda_E} \bar{\psi}(x)(D_w + m_0 + i\mu_q\gamma_5\tau^3)\psi(x). \quad (91)$$

Although this formulation breaks physical parity and flavour symmetries, it has a number of advantages over standard Wilson fermions. In particular, the presence of the twisted mass parameter μ_q protects the discretized theory against unphysical zero modes. Another attractive feature of twisted mass lattice QCD is the fact that the leading lattice artifacts are of order a^2 without the need to add the Sheikholeslami-Wohlert term [53]. Although the problem of

explicit chiral symmetry breaking remains, the twisted formulation is particularly useful to circumvent some of the problems that are encountered in connection with the renormalization of local operators on the lattice, such as those required to determine B_K .

Staggered fermions

An alternative procedure to deal with the doubling problem is based on so-called “staggered” or Kogut-Susskind (KS) fermions [303]. Here the degeneracy is only lifted partially, from 16 down to 4. It has become customary to refer to these residual doublers as “tastes” in order to distinguish them from physical flavours. At order a^2 different tastes can interact via gluon exchange, thereby generating large lattice artifacts. The improvement programme can be used to suppress taste-changing interactions, leading to “improved staggered fermions”, with the so-called “Asqtad” and “HISQ” actions as the most widely used versions [304, 305]. The standard procedure to remove the residual doubling of staggered quarks (“four tastes per flavour”) is to take fractional powers of the quark determinant in the QCD functional integral. This is usually referred to as the “fourth root trick”. The validity of this procedure has not been rigorously proven so far. In fact, it has been questioned by several authors, and the issue is still hotly debated (for both sides of the argument see the reviews in refs. [55–58, 306]).

Ginsparg-Wilson fermions

Fermionic lattice actions, which do not suffer from the doubling problem whilst preserving chiral symmetry go under the name of “Ginsparg-Wilson fermions”. In the continuum the massless Dirac operator anti-commutes with γ_5 . At non-zero lattice spacing chiral symmetry can be realized even if this condition is relaxed according to [307, 308]

$$\{D, \gamma_5\} = aD\gamma_5D, \quad (92)$$

which is now known as the Ginsparg-Wilson relation [278]. A lattice Dirac operator which satisfies eq. (92) can be constructed in several ways. The “domain wall” construction proceeds by introducing a fifth dimension of length N_5 and coupling the fermions to a mass defect (i.e. a negative mass term) [309]. The five-dimensional action can be constructed such that modes of opposite chirality are trapped at the four-dimensional boundaries in the limit of an infinite extent of the extra dimension [310]. In any real simulation, though, one has to work with a finite value of N_5 , so that the decoupling of chiral modes is not exact. This leads to a residual breaking of chiral symmetry, which, however, is exponentially suppressed. A doubler-free, (approximately) chirally symmetric quark action can thus be realized at the expense of simulating a five-dimensional theory.

The so-called “overlap” or Neuberger-Dirac operator can be derived from the domain wall formulation [311]. It acts in four space-time dimensions and is, in its simplest form, defined by

$$D_N = \frac{1}{\bar{a}} \left(1 - \frac{A}{\sqrt{A^\dagger A}} \right), \quad A = 1 + s - aD_w, \quad \bar{a} = \frac{a}{1+s}, \quad (93)$$

where D_w is the massless Wilson-Dirac operator, and $|s| < 1$ is a tunable parameter. The overlap operator D_N removes all doublers from the spectrum, and can easily be shown to satisfy the Ginsparg-Wilson relation. The occurrence of an inverse square root in D_N renders the application of D_N in a computer program potentially very costly, since it must be implemented using, for instance, a polynomial approximation.

The third example of an operator which satisfies the Ginsparg-Wilson relation is the so-called fixed-point action [312, 313]. This construction proceeds via a renormalization group

approach. A related formalism are the so-called “chirally improved” fermions [314].

Smearing

A simple modification which can help improve the action as well as the computational performance is the use of smeared gauge fields in the covariant derivatives of the fermionic action. Any smearing procedure is acceptable as long as it consists of only adding irrelevant (local) operators. Moreover, it can be combined with any discretization of the quark action. The “Asqtad” staggered quark action mentioned above [304] is an example which makes use of so-called “Asqtad” smeared (or “fat”) links. Another example is the use of n-HYP smeared [289, 315], n-stout smeared [316, 317] or n-HEX (hypercubic stout) smeared [318] gauge links in the tree-level clover improved discretization of the quark action, denoted by “n-HYP t1SW”, “n-stout t1SW” and “n-HEX t1SW” in the following.

In Table 19 we summarize the most widely used discretizations of the quark action and their main properties together with the abbreviations used in the summary tables. Note that in order to maintain the leading lattice artifacts of the actions as given in the table in non-spectral observables (like operator matrix elements) the corresponding non-spectral operators need to be improved as well.

A.2 Setting the scale

In simulations of lattice QCD quantities such as hadron masses and decay constants are obtained in “lattice units” i.e. as dimensionless numbers. In order to convert them into physical units they must be expressed in terms of some experimentally known, dimensionful reference quantity Q . This procedure is called “setting the scale”. It amounts to computing the non-perturbative relation between the bare gauge coupling g_0 (which is an input parameter in any lattice simulation) and the lattice spacing a expressed in physical units. To this end one chooses a value for g_0 and computes the value of the reference quantity in a simulation: This yields the dimensionless combination, $(aQ)|_{g_0}$, at the chosen value of g_0 . The calibration of the lattice spacing is then achieved via

$$a^{-1} [\text{MeV}] = \frac{Q|_{\text{exp}} [\text{MeV}]}{(aQ)|_{g_0}}, \quad (94)$$

where $Q|_{\text{exp}}$ denotes the experimentally known value of the reference quantity. Common choices for Q are the mass of the nucleon, the Ω baryon or the decay constants of the pion and the kaon. Vector mesons, such as the ρ or K^* -meson, are unstable and therefore their masses are not very well suited for setting the scale, despite the fact that they have been used over many years for that purpose.

Another widely used quantity to set the scale is the hadronic radius r_0 , which can be determined from the force between static quarks via the relation [319]

$$F(r_0)r_0^2 = 1.65. \quad (95)$$

If the force is derived from potential models describing heavy quarkonia, the above relation determines the value of r_0 as $r_0 \approx 0.5$ fm. A variant of this procedure is obtained [320] by using the definition $F(r_1)r_1^2 = 1.00$, which yields $r_1 \approx 0.32$ fm. It is important to realize that both r_0 and r_1 are not directly accessible in experiment, so that their values derived from phenomenological potentials are necessarily model-dependent. In spite of the inherent ambiguity

Abbrev.	Discretization	Leading lattice artifacts	Chiral symmetry	Remarks
Wilson	Wilson	$O(a)$	broken	
tmWil	Twisted Mass Wilson	$O(a^2)$ at maximal twist	broken	flavour symmetry breaking: $(M_{\text{PS}}^0)^2 - (M_{\text{PS}}^\pm)^2 \sim O(a^2)$
tISW	Sheikholeslami-Wohlert	$O(g^2 a)$	broken	tree-level impr., $c_{\text{sw}} = 1$
n-HYP tISW	Sheikholeslami-Wohlert	$O(g^2 a)$	broken	tree-level impr., $c_{\text{sw}} = 1$, n-HYP smeared gauge links
n-stout tISW	Sheikholeslami-Wohlert	$O(g^2 a)$	broken	tree-level impr., $c_{\text{sw}} = 1$, n-stout smeared gauge links
mfSW	Sheikholeslami-Wohlert	$O(g^2 a)$	broken	mean-field impr.
npSW	Sheikholeslami-Wohlert	$O(a^2)$	broken	non-perturbatively impr.
KS	Staggered	$O(a^2)$	$U(1) \otimes U(1)$ subgr. unbroken	rooting for $N_f < 4$
Asqtad	Staggered	$O(a^2)$	$U(1) \otimes U(1)$ subgr. unbroken	Asqtad smeared gauge links, rooting for $N_f < 4$
HISQ	Staggered	$O(a^2)$	$U(1) \otimes U(1)$ subgr. unbroken	HISQ smeared gauge links, rooting for $N_f < 4$
DW	Domain Wall	asymptotically $O(a^2)$	remnant breaking exponentially suppr.	exact chiral symmetry and $O(a)$ impr. only in the limit $L_s \rightarrow \infty$
overlap	Neuberger	$O(a^2)$	exact	

Table 19: The most widely used discretizations of the quark action and some of their properties. Note that in order to maintain the leading lattice artifacts of the action in non-spectral observables (like operator matrix elements) the corresponding non-spectral operators need to be improved as well.

whenever hadronic radii are used to calibrate the lattice spacing, they are very useful quantities for performing scaling tests and continuum extrapolations of lattice data. Furthermore, they can be easily computed with good statistical accuracy in lattice simulations.

A.3 Matching and running

The lattice formulation of QCD amounts to introducing a particular regularization scheme. Thus, in order to be useful for phenomenology, hadronic matrix elements computed in lattice simulations must be related to some continuum reference scheme, such as the $\overline{\text{MS}}$ -scheme of dimensional regularization. The matching to the continuum scheme usually involves running to some reference scale using the renormalization group.

In principle, the matching factors which relate lattice matrix elements to the $\overline{\text{MS}}$ -scheme, can be computed in perturbation theory formulated in terms of the bare coupling. It has been known for a long time, though, that the perturbative expansion is not under good control. Several techniques have been developed which allow for a non-perturbative matching between lattice regularization and continuum schemes, and are briefly introduced here.

Regularization-independent Momentum Subtraction

In the *Regularization-independent Momentum Subtraction* (“RI/MOM” or “RI”) scheme [115] a non-perturbative renormalization condition is formulated in terms of Green functions involving quark states in a fixed gauge (usually Landau gauge) at non-zero virtuality. In this way one relates operators in lattice regularization non-perturbatively to the RI scheme. In a second step one matches the operator in the RI scheme to its counterpart in the $\overline{\text{MS}}$ -scheme. The advantage of this procedure is that the latter relation involves perturbation theory formulated in the continuum theory. The uncontrolled use of lattice perturbation theory can thus be avoided. A technical complication is associated with the accessible momentum scales (i.e. virtualities), which must be large enough (typically several GeV) in order for the perturbative relation to $\overline{\text{MS}}$ to be reliable. The momentum scales in simulations must stay well below the cutoff scale (i.e. 2π over the lattice spacing), since otherwise large lattice artifacts are incurred. Thus, the applicability of the RI scheme traditionally relies on the existence of a “window” of momentum scales, which satisfy

$$\Lambda_{\text{QCD}} \lesssim p \lesssim 2\pi a^{-1}. \quad (96)$$

However, solutions for mitigating this limitation, which involve continuum limit, non-perturbative running to higher scales in the RI/MOM scheme, have recently been proposed and implemented [65, 105, 282, 321].

Schrödinger functional

Another example of a non-perturbative matching procedure is provided by the Schrödinger functional (SF) scheme [114]. It is based on the formulation of QCD in a finite volume. If all quark masses are set to zero the box length remains the only scale in the theory, such that observables like the coupling constant run with the box size L . The great advantage is that the RG running of scale-dependent quantities can be computed non-perturbatively using recursive finite-size scaling techniques. It is thus possible to run non-perturbatively up to scales of, say, 100 GeV, where one is sure that the perturbative relation between the SF and $\overline{\text{MS}}$ -schemes is controlled.

Perturbation theory

The third matching procedure is based on perturbation theory in which higher order are effectively resummed [301]. Although this procedure is easier to implement, it is hard to estimate the uncertainty associated with it.

In Table 20 we list the abbreviations used in the compilation of results together with a short description.

Abbrev.	Description
RI	Regularization-independent momentum subtraction scheme
SF	Schrödinger functional scheme
PT1 ℓ	matching/running computed in perturbation theory at one loop
PT2 ℓ	matching/running computed in perturbation theory at two loop

Table 20: The most widely used matching and running techniques.

A.4 Chiral extrapolation

As mentioned in section 1.1, Symanzik’s framework can be combined with Chiral Perturbation Theory. The well-known terms occurring in the chiral effective Lagrangian are then supplemented by contributions proportional to powers of the lattice spacing a . The additional terms are constrained by the symmetries of the lattice action and therefore depend on the specific choice of the discretization. The resulting effective theory can be used to analyze the a -dependence of the various quantities of interest – provided the quark masses and the momenta considered are in the range where the truncated chiral perturbation series yields an adequate approximation. Understanding the dependence on the lattice spacing is of central importance for a controlled extrapolation to the continuum limit.

For staggered fermions, this program has first been carried out for a single staggered flavor (a single staggered field) [24] at $O(a^2)$. In the following, this effective theory is denoted by $S\chi$ PT. It was later generalized to an arbitrary number of flavours [28, 30], and to next-to-leading order [33]. The corresponding theory is commonly called Rooted Staggered chiral perturbation theory and is denoted by $RS\chi$ PT.

For Wilson fermions, the effective theory has been developed in [23, 26, 31] and is called $W\chi$ PT, while the theory for Wilson twisted mass fermions [32, 34, 40] is termed $tmW\chi$ PT.

Another important approach is to consider theories in which the valence and sea quark masses are chosen to be different. These theories are called *partially quenched*. The acronym for the corresponding chiral effective theory is $PQ\chi$ PT [20–22, 25].

Finally, one can also consider theories where the fermion discretizations used for the sea and the valence quarks are different. The effective chiral theories for these “mixed action” theories are referred to as $MA\chi$ PT [27, 29, 35–39].

A.5 Summary of simulated lattice actions

In the following two tables we summarize the gauge and quark actions used in the various calculations. Abbreviations are explained in section [A.1.1](#) and [A.1.2](#), and summarized in tables [18](#) and [19](#).

Collab.	Ref.	N_f	gauge action	quark action
ALPHA 05	[98]	2	Wilson	npSW
CERN-TOV 06	[254]	2	Wilson	Wilson/npSW
CERN 08	[215]	2	Wilson	npSW
Bernardoni 10	[244]	2	Wilson	npSW [†]
CP-PACS 01	[101]	2	Iwasaki	mfSW
ETM 07, 07A, 08, 09, 09A-D, 10B, D	[49, 54, 94, 160, 161, 177, 235, 237, 246, 291]	2	tlSym	tmWil
HHS 08	[247]	2	tadSym	n-HYP tlSW
JLQCD 08	[280]	2	Iwasaki	overlap
JLQCD 02, 05	[100, 164]	2	Wilson	npSW
JLQCD/TWQCD 07, 08A, 10	[95, 240, 248]	2	Iwasaki	overlap
QCDSF 07	[162]	2	Wilson	npSW
QCDSF/UKQCD 04, 06, 06A, 07	[96, 99, 178, 260]	2	Wilson	npSW
RBC 07	[73]	2	DBW2	DW
RBC 04, 06	[163, 287]	2	DBW2	DW
SPQcdR 05	[97]	2	Wilson	Wilson
UKQCD 04, 07	[159, 288]	2	Wilson	npSW

[†] The calculation uses overlap fermions in the valence quark sector.

Table 21: Summary of simulated lattice actions with $N_f = 2$ quark flavours.

Collab.	Ref.	N_f	gauge action	quark action
Aubin 08, 09	[173, 269]	2 + 1	tadSym	Asqtad [†]
SWME 10, 11	[281, 283]	2 + 1	tadSym	Asqtad ⁺
Blum 10	[74]	2 + 1	Iwasaki	DW
BMW 10A-C	[65, 75, 105]	2 + 1	tlSym	2-HEX tlSW
BMW 10	[41]	2 + 1	tlSym	6-stout tlSW
CP-PACS/JLQCD 07	[109]	2 + 1	Iwasaki	npSW
ETM 10, 10E	[60, 170]	2 + 1 + 1	Iwasaki	tmWil
HPQCD 05	[110]	2 + 1	tadSym	Asqtad
HPQCD/UKQCD 06	[285]	2 + 1	tadSym	Asqtad
HPQCD/UKQCD 07	[175]	2 + 1	tadSym	Asqtad [*]
HPQCD/MILC/UKQCD 04	[111]	2 + 1	tadSym	Asqtad
JLQCD 09	[241]	2 + 1	Iwasaki	overlap
JLQCD/TWQCD 08B, 09A	[172, 243]	2 + 1	Iwasaki	overlap
JLQCD/TWQCD 10	[240]	2 + 1, 3	Iwasaki	overlap
LHP 04	[259]	2 + 1	tadSym	Asqtad [†]
MILC 04, 07, 09, 09A, 10, 10A	[6, 77, 103, 111, 171, 322]	2 + 1	tadSym	Asqtad
NPLQCD 06	[176]	2 + 1	tadSym	Asqtad [†]
PACS-CS 08, 08A, 09, 10	[42, 63, 64, 174]	2 + 1	Iwasaki	npSW
RBC/UKQCD 07, 08, 08A, 10, 10A-B	[106, 108, 158, 250, 282, 284]	2 + 1	Iwasaki	DW
TWQCD 08	[242]	2 + 1	Iwasaki	DW

[†] The calculation uses domain wall fermions in the valence quark sector.

^{*} The calculation uses HISQ staggered fermions in the valence quark sector.

⁺ The calculation uses HYP smeared improved staggered fermions in the valence quark sector.

Table 22: Summary of simulated lattice actions with $N_f = 2 + 1$ or $N_f = 2 + 1 + 1$ quark flavours.

B Notes

B.1 Notes to section 3 on quark masses

Collab.	Ref.	N_f	a [fm]	Description
PACS-CS 10	[64]	2+1	0.09	cf. PACS-CS 08
MILC 10A	[103]	2+1		cf. MILC 09, 09A
BMW 10A, 10B	[65, 105]	2+1	0.116,0.093,0.077, 0.065,0.054	Scale setting via M_π, M_K, M_Ω .
RBC/UKQCD 10A	[106]	2+1	0.114, 0.087	Scale set through M_Ω .
Blum 10	[74]	2+1	0.11	Relies on RBC/UKQCD 08 scale setting.
PACS-CS 09	[42]	2+1	0.09	Scale setting via M_Ω .
HPQCD 09, 10	[104, 107]	2+1		
MILC 09A, 09	[6, 59]	2+1	0.045, 0.06, 0.09	Scale set through r_1 and Υ and continuum extrapolation based on RS χ PT.
PACS-CS 08	[63]	2+1	0.09	Scale set through M_Ω . Non-perturbatively $O(a)$ -improved.
RBC/UKQCD 08	[108]	2+1	0.11	Scale set through M_Ω . Automatic $O(a)$ -improvement due to approximate chiral symmetry. $(\Lambda_{\text{QCD}}a)^2 \approx 4\%$ systematic error due to lattice artifacts added.
CP-PACS/JLQCD 07	[109]	2+1	0.07,0.10,0.12	Scale set through M_K or M_ϕ . Non-perturbatively $O(a)$ -improved.
HPQCD 05	[110]	2+1	0.09,0.12	Scale set through the $\Upsilon - \Upsilon'$ mass difference.
HPQCD/MILC/UKQCD 04, MILC 04	[77, 111]	2+1	0.09,0.12	Scale set through r_1 and Υ and continuum extrapolation based on RS χ PT.

Table 23: Continuum extrapolations/estimation of lattice artifacts in determinations of m_{ud} and m_s with $N_f = 2 + 1$ quark flavours.

Collab.	Ref.	N_f	a [fm]	Description
ETM 10B	[94]	2	0.098, 0.085, 0.067, 0.054	Scale set through F_π .
JLQCD/TWQCD 08A	[95]	2	0.12	Scale set through r_0 .
RBC 07	[73]	2	0.12	Scale set through M_ρ .
ETM 07	[49]	2	0.09	Scale set through F_π .
QCDSF/UKQCD 06	[96]	2	0.065–0.09	Scale set through r_0 .
SPQcdR 05	[97]	2	0.06,0.08	Scale set through M_{K^*} .
ALPHA 05	[98]	2	0.07-0.12	Scale set through r_0 .
QCDSF/UKQCD 04	[99]	2	0.07-0.12	Scale set through r_0 .
JLQCD 02	[100]	2	0.09	Scale set through M_ρ .
CP-PACS 01	[101]	2	0.11,0.16,0.22	Scale set through M_ρ .

Table 24: Continuum extrapolations/estimation of lattice artifacts in determinations of m_{ud} and m_s with $N_f = 2$ quark flavours.

Collab.	Ref.	N_f	$M_{\pi,\min}$ [MeV]	Description
PACS-CS 10	[64]	2+1		cf. PACS-CS 08
MILC 10A	[103]	2+1		NLO SU(2) S χ PT. Cf. also MILC 09A,09.
BMW 10A, 10B	[65, 105]	2+1	135	Interpolation to the physical point.
RBC/UKQCD 10A	[106]	2+1	290	
Blum 10	[74, 108]	2+1	242 (valence), 330 (sea)	Extrapolation done on the basis of PQ χ PT formulae with virtual photons.
PACS-CS 09	[42]	2+1	135	Physical point reached by reweighting technique, no chiral extrapolation needed.
HPQCD 09, 10	[104, 107]	2+1		
MILC 09A, 09	[6, 59]	2+1	177, 240	NLO SU(3) RS χ PT, continuum χ PT at NNLO and NNNLO and NNNNLO analytic terms. The lightest Nambu-Goldstone mass is 177 MeV (09A) and 224 MeV (09) (at $a=0.09\text{fm}$) and the lightest RMS mass is 258MeV (at $a=0.06\text{fm}$).
PACS-CS 08	[63]	2+1	156	NLO SU(2) χ PT and SU(3) (Wilson) χ PT.
RBC/UKQCD 08	[108]	2+1	242 (valence), 330 (sea)	SU(3) PQ χ PT and heavy kaon NLO SU(2) PQ χ PT fits.
CP-PACS/JLQCD 07	[109]	2+1	620	NLO Wilson χ PT fits to meson masses.
HPQCD 05	[110]	2+1	240	PQ RS χ PT fits.
HPQCD/MILC/UKQCD 04, MILC 04	[77, 111]	2+1	240	PQ RS χ PT fits.

Table 25: Chiral extrapolation/minimum pion mass in determinations of m_{ud} and m_s with $N_f = 2 + 1$ quark flavours.

Collab.	Ref.	N_f	$M_{\pi,\min}$ [MeV]	Description
ETM 10B	[94]	2	270	Fits based on NLO χ PT and Symanzik expansion up to $O(a^2)$
JLQCD/TWQCD 08A	[95]	2	290	NLO χ PT fits.
RBC 07	[73]	2	440	NLO fit including $O(\alpha)$ effects.
ETM 07	[49]	2	300	Polynomial and PQ χ PT fits.
QCDSF/UKQCD 06	[96]	2	520 (valence), 620 (sea)	NLO (PQ) χ PT fits.
SPQcdR 05	[97]	2	600	Polynomial fit.
ALPHA 05	[98]	2	560	LO χ PT fit.
QCDSF/UKQCD 04	[99]	2	520 (valence), 620 (sea)	NLO (PQ) χ PT fits.
JLQCD 02	[100]	2	560	Polynomial and χ PT fits.
CP-PACS 01	[101]	2	430	Polynomial fits.

Table 26: Chiral extrapolation/minimum pion mass in determinations of m_{ud} and m_s with $N_f = 2$ quark flavours.

Collab.	Ref.	N_f	L [fm]	$M_{\pi,\min}L$	Description
PACS-CS 10	[64]	2+1			cf. PACS-CS 08
MILC 10A	[103]	2+1			cf. MILC 09A,09
BMW 10A, 10B	[65, 105]	2+1	$\gtrsim 5.0$	$\gtrsim 4.0$	FS corrections below 5 per mil on the largest lattices.
RBC/UKQCD 10A	[106]	2+1	2.7	$\gtrsim 4.0$	
Blum 10	[74]	2+1	1.8, 2.7	—	Simulations done with dynamical photons; large finite volume effects analytically corrected for, but not related to $M_\pi L$.
PACS-CS 09	[42]	2+1	2.9	2.0	Only one volume.
HPQCD 09, 10	[104, 107]	2+1			
MILC 09A, 09	[6, 59]	2+1	2.5, 2.9, 3.4, 3.6, 3.8, 5.8	4.1, 3.8	
PACS-CS 08	[63]	2+1	2.9	2.3	Correction for FSE from χ PT using [323].
RBC/UKQCD 08	[108]	2+1	1.8, 2.7	4.6	Various volumes for comparison and correction for FSE from χ PT [194, 195, 323].
CP-PACS/JLQCD 07	[109]	2+1	2.0	6.0	Estimate based on the comparison to a $L = 1.6$ fm volume assuming powerlike dependence on L .
HPQCD 05	[110]	2+1	2.4, 2.9	3.5	
HPQCD/MILC/UKQCD 04, MILC 04	[77, 111]	2+1	2.4, 2.9	3.5	NLO S χ PT.

Table 27: Finite volume effects in determinations of m_{ud} and m_s with $N_f = 2 + 1$ quark flavours.

Collab.	Ref.	N_f	L [fm]	$M_{\pi, \min} L$	Description
ETM 10B	[94]	2	$\gtrsim 2.0$	3.5	One volume $L = 1.7$ fm at $m_\pi = 495$, $a = 0.054$ fm.
JLQCD/TWQCD 08A	[95]	2	1.9	2.8	Corrections for FSE based on NLO χ PT.
RBC 07	[73]	2	1.9	4.3	Estimate of FSE based on a model.
ETM 07	[49]	2	2.1	3.2	NLO PQ χ PT
QCDSF/UKQCD 06	[96]	2	1.4–1.9	4.7	
SPQcdR 05	[97]	2	1.0–1.5	4.3	Comparison between 1.0 and 1.5 fm.
ALPHA 05	[98]	2	2.6	7.4	
QCDSF/UKQCD 04	[99]	2	1.7–2.0	4.7	
JLQCD 02	[100]	2	1.8	5.1	Numerical study with three volumes.
CP-PACS 01	[101]	2	2.0–2.6	5.7	

Table 28: Finite volume effects in determinations of m_{ud} and m_s with $N_f = 2$ quark flavours.

Collab.	Ref.	N_f	Description
PACS-CS 10	[64]	2+1	Non-perturbative renormalization and running; Schrödinger functional method.
MILC 10A	[103]	2+1	cf. MILC 09A,09
BMW 10A, 10B	[65, 105]	2+1	Non-perturbative renormalization (tree-level improved RI-MOM), non-perturbative running.
RBC/UKQCD 10A	[106]	2+1	Non-perturbative renormalization (RI/SMOM).
Blum 10	[74]	2+1	Relies on non-perturbative renormalization factors calculated by RBC/UKQCD 08; no QED renormalization.
PACS-CS 09	[42]	2+1	Non-perturbative renormalization; Schrödinger functional method.
HPQCD 09, 10	[104, 107]	2+1	Lattice calculation of m_s/m_c : m_s derived from the perturbative determination of m_c .
MILC 09A, 09	[6, 59]	2+1	2-loop perturbative renormalization.
PACS-CS 08	[63]	2+1	1-loop perturbative renormalization.
RBC/UKQCD 08	[108]	2+1	Non-perturbative renormalization, 3-loop perturbative matching.
CP-PACS/JLQCD 07	[109]	2+1	1-loop perturbative renormalization, tadpole improved.
HPQCD 05	[110]	2+1	2-loop perturbative renormalization.
HPQCD/MILC/UKQCD 04, MILC 04	[77, 111]	2+1	1-loop perturbative renormalization.

Table 29: Renormalization in determinations of m_{ud} and m_s with $N_f = 2 + 1$ quark flavours.

Collab.	Ref.	N_f	Description
ETM 10B	[94]	2	Non-perturbative renormalization.
JLQCD/TWQCD 08A	[95]	2	Non-perturbative renormalization.
RBC 07	[73]	2	Non-perturbative renormalization.
ETM 07	[49]	2	Non-perturbative renormalization.
QCDSF/UKQCD 06	[96]	2	Non-perturbative renormalization.
SPQcdR 05	[97]	2	Non-perturbative renormalization.
ALPHA 05	[98]	2	Non-perturbative renormalization.
QCDSF/UKQCD 04	[99]	2	Non-perturbative renormalization.
JLQCD 02	[100]	2	1-loop perturbative renormalization.
CP-PACS 01	[101]	2	1-loop perturbative renormalization.

Table 30: Renormalization in determinations of m_{ud} and m_s with $N_f = 2$ quark flavours.

B.2 Notes to section 4 on $|V_{ud}|$ and $|V_{us}|$

Collab.	Ref.	N_f	a [fm]	Description
RBC/UKQCD 07,10	[158, 159]	2+1	0.114(2)	Scale fixed through Ω baryon mass. Add $(\Lambda_{\text{QCD}}a)^2 \approx 4\%$ systematic error for lattice artifacts. Fifth dimension with extension $L_s = 16$, therefore small residual chiral symmetry breaking and approximate $O(a)$ -improvement.
ETM 10D	[160]	2	0.054, 0.068, 0.086, 101	Scale set through F_π . Automatic $O(a)$ impr., flavour symmetry breaking: $(M_{PS}^0)^2 - (M_{PS}^\pm)^2 \sim O(a^2)$.
ETM 09A	[161]	2	0.069, 0.883(6), 0.103	Scale set through F_π . Automatic $O(a)$ impr., flavour symmetry breaking: $(M_{PS}^0)^2 - (M_{PS}^\pm)^2 \sim O(a^2)$. Three lattice spacings only for pion mass 470 MeV.
QCDSF 07	[162]	2	0.075	Scale set with r_0 . Non-perturbatively $O(a)$ -improved Wilson fermions, not clear whether currents improved.
RBC 06	[163]	2	0.12	Scale set through M_ρ . Automatic $O(a)$ -improvement due to approximate chiral symmetry of the action.
JLQCD 05	[164]	2	0.0887	Scale set through M_ρ . Non-perturbatively $O(a)$ -improved Wilson fermions.

Table 31: Continuum extrapolations/estimation of lattice artifacts in determinations of $f_+(0)$.

Collab.	Ref.	N_f	$M_{\pi,\min}$ [MeV]	Description
RBC/UKQCD 07,10	[158, 159]	2+1	330	NLO SU(3) χ PT with phenomenological ansatz for higher orders.
ETM 10D	[160]	2	260	NLO heavy kaon SU(2) χ PT and NLO SU(3) χ PT and phenomenological ansatz for higher orders. Average of $f_+(0)$ -fit and joint $f_+(0)$ - f_K/f_π -fit.
ETM 09A	[161]	2	260	NLO heavy kaon SU(2) χ PT and NLO SU(3) χ PT and phenomenological ansatz for higher orders.
QCDSF 07	[162]	2	591	Only one value for the pion mass.
RBC 06	[163]	2	490	NLO SU(3) χ PT and phenomenological ansatz for higher orders.
JLQCD 05	[164]	2	550	NLO SU(3) χ PT and phenomenological ansatz for higher orders.

Table 32: Chiral extrapolation/minimum pion mass in determinations of $f_+(0)$.

Collab.	Ref.	N_f	L [fm]	$M_{\pi,\min}L$	Description
RBC/UKQCD 07,10	[158, 159]	2+1	2.7	4.7	Two volumes for all but the lightest pion mass.
ETM 10D	[160]	2	1.7-2.8	3.7	
ETM 09A	[161]	2	2.1, 2.8	3.2	Two volumes at $M_\pi = 300$ MeV and χ PT-motivated estimate of the error due to FSE.
QCDSF 07	[162]	2	1.9	5.4	
RBC 06	[163]	2	1.9	4.7	
JLQCD 05	[164]	2	1.8	4.9	

Table 33: Finite volume effects in determinations of $f_+(0)$.

Collab.	Ref.	N_f	a [fm]	Description
ETM 10E	[170]	2+1+1	0.061, 0.078	Scale set through f_π/m_π . Two lattice spacings but a -dependence ignored in all fits. Finer lattice spacing from [249].
RBC/UKQCD 10A	[106]	2+1	0.114, 0.087	Scale set through M_Ω .
MILC 10	[171]	2+1	0.045 - 0.09	3 lattice spacings, continuum extrapolation by means of RS χ PT.
BMW 10	[41]	2+1	0.065, 0.083, 0.124	Scale set through $M_{\Omega,\Xi}$. Perturbative $O(a)$ -improvement.
JLQCD/TWQCD 08A	[95]	2+1	0.100(2)	Scale set through F_π . Automatic $O(a)$ -improvement due to chiral symmetry of action.
MILC 09A	[59]	2+1	0.045, 0.06, 0.09	Scale set through r_1 and Υ and continuum extrapolation based on RS χ PT.
MILC 09	[6]	2+1	0.045, 0.06, 0.09, 0.12	Scale set through r_1 and Υ and continuum extrapolation based on RS χ PT.
Aubin 08	[173]	2+1	0.09, 0.12	Scale set through r_1 and Υ and continuum extrapolation based on MA χ PT.
PACS-CS 08, 08A	[63, 174]	2+1	0.0907(13)	Scale set through M_Ω . Non-perturbatively $O(a)$ -improved.
HPQCD/UKQCD 07	[175]	2+1	0.06, 0.09, 0.15	Scale set through r_1 and Υ and continuum extrapolation on continuum- χ PT motivated ansatz. Taste breaking of sea quarks ignored.
RBC/UKQCD 08	[108]	2+1	0.114(2)	Scale set through M_Ω . Automatic $O(a)$ -improvement due to approximate chiral symmetry. $(\Lambda_{\text{QCD}}a)^2 \approx 4\%$ systematic error due to lattice artifacts added.
NPLQCD 06	[176]	2+1	0.125	Scale set through r_0 and F_π . Taste breaking of sea quarks ignored.
ETM 10D	[160]	2	0.054, 0.068, 0.086, 0.101	Scale set through F_π . Automatic $O(a)$ impr., flavour symmetry breaking: $(M_{PS}^0)^2 - (M_{PS}^\pm)^2 \sim O(a^2)$.
ETM 09	[177]	2	0.07, 0.09, 0.10	Scale set through F_π . Automatic $O(a)$ impr., flavour symmetry breaking: $(M_{PS}^0)^2 - (M_{PS}^\pm)^2 \sim O(a^2)$.
QCDSF/UKQCD 07	[178]	2	0.06, 0.07	Scale set through F_π . Non-perturbative $O(a)$ -improvement.

Table 34: Continuum extrapolations/estimation of lattice artifacts in determinations of f_K/f_π .

Collab.	Ref.	N_f	$M_{\pi,\min}$ [MeV]	Description
ETM 10E	[170]	2+1+1	265	Pion mass on finer lattice from [324].
RBC/UKQCD 10A	[106]	2+1	290	Results are based on heavy kaon NLO SU(2) PQ χ PT.
MILC 10	[171]	2+1	258	Lightest Nambu-Goldstone mass is 177 MeV (at 0.09 fm) and lightest RMS mass is 258 MeV (at 0.06 fm). NLO rS χ PT and NNLO χ PT.
BMW 10	[41]	2+1	190	Comparison of various fit-ansätze: SU(3) χ PT, heavy kaon SU(2) χ PT, polynomial.
JLQCD/TWQCD 08A	[95]	2+1	340	NNLO SU(3) χ PT.
MILC 09A	[59]	2+1	177	NLO SU(3) RS χ PT, continuum χ PT at NNLO and NNNLO and NNNNLO analytic terms and heavy kaon SU(2) RS χ PT with NNLO continuum chiral logs on a smaller sub-set of the lattices. The lightest Nambu-Goldstone mass is 177 MeV (at $a = 0.09$ fm) and the lightest RMS mass is 258 MeV (at $a = 0.06$ fm).
MILC 09	[6]	2+1	240	NLO SU(3) RS χ PT with continuum χ PT NNLO and NNNLO analytic terms added. According to [59] the lightest sea Nambu-Goldstone mass is 224 MeV and the lightest RMS mass is 258 MeV (at $a = 0.06$ fm).
Aubin 08	[173]	2+1	240	NLO MA χ PT. According to [59] the lightest sea Nambu-Goldstone mass is 246 MeV (at $a = 0.09$ fm) and the lightest RMS mass is 329 MeV (at $a = 0.09$ fm).
PACS-CS 08, 08A	[63, 174]	2+1	156	NLO SU(2) χ PT and SU(3) (Wilson) χ PT.
HPCD/UKQCD 07	[175]	2+1	240	NLO SU(3) chiral perturbation theory with NNLO and NNNLO analytic terms. The sea RMS mass for the employed lattices is heavier than 250 MeV.
RBC/UKQCD 08	[108]	2+1	330	While SU(3) PQ χ PT fits were studied, final results are based on heavy kaon NLO SU(2) PQ χ PT.
NPLQCD 06	[176]	2+1	300	NLO SU(3) χ PT and some NNLO terms. The sea RMS mass for the employed lattices is heavier.
ETM 10D	[160]	2	260	NLO SU(3) χ PT and phenomenological ansatz for higher orders. Joint $f_+(0)$ - f_K/f_π -fit.
ETM 09	[177]	2	270	NLO heavy meson SU(2) χ PT and NLO SU(3) χ PT.
QCDSF/UKQCD 07	[178]	2	300	Linear extrapolation of lattice data.

Table 35: Chiral extrapolation/minimum pion mass in determinations of f_K/f_π .

Collab.	Ref.	N_f	L [fm]	$M_{\pi, \min} L$	Description
ETM 10E	[170]	2+1+1	1.9 - 2.9	$\gtrsim 3.9$	Simulation parameters from [249, 324].
RBC/UKQCD 10A	[106]	2+1	2.7	$\gtrsim 4.0$	
MILC 10	[171]	2+1	2.52	4.11	$L \geq 2.9$ fm for the lighter masses.
BMW 10	[41]	2+1	2.0, 2.6, 2.7, 3.0, 4.0	4.0	Various volumes for comparison and correction for FSE from χ PT using [323].
JLQCD/TWQCD 08A	[95]	2+1	1.6	2.8	Estimate of FSE using χ PT [323, 325]
MILC 09A	[59]	2+1	2.5, 2.9, 3.4, 3.6, 3.8, 5.8	4.1	
MILC 09	[6]	2+1	2.4, 2.5, 2.9, 3.0, 3.4, 3.6, 3.8, 5.8	3.8	Various volumes for comparison and correction for FSEs from (RS) χ PT [323].
Aubin 08	[173]	2+1	2.4, 3.4	4.0	Correction for FSE from MA χ PT.
PACS-CS 08, 08A	[63, 174]	2+1	2.9	2.3	Correction for FSE from χ PT using [323].
HPCD/UKQCD 07	[175]	2+1	2.3, 2.4, 2.5, 2.9	3.8	Correction for FSE from χ PT using [323].
RBC/UKQCD 08	[108]	2+1	1.8, 2.7	4.6	Various volumes for comparison and correction for FSE from χ PT [194, 195, 323].
NPLQCD 06	[176]	2+1	2.5	3.8	Correction for FSE from S χ PT [28, 30]
ETM 10D	[160]	2	2.0-2.5	3.7	
ETM 09	[177]	2	2.0, 2.4, 2.7	3.3	Correction for FSE from χ PT [194, 195, 323].
QCDSF/UKQCD 07	[178]	2	1.4, ..., 2.6	4.2	Correction for FSE from χ PT

Table 36: Finite volume effects in determinations of f_K/f_π .

B.3 Notes to section 5 on Low-Energy Constants

Collab.	Ref.	N_f	a [fm]	Description
Bernardoni 10	[244]	2	0.0784(10)	Scale fixed through M_K . Non-perturbative $O(a)$ improvement. No estimate of systematic error.
JLQCD/TWQCD 10	[240]	2	0.11	One lattice spacing, scale fixed through r_0 . Estimate of 7% systematic error due to finite lattice spacing.
JLQCD/TWQCD 09	[252]	2	0.1184(21)	Automatic $O(a)$ impr., exact chiral symmetry. Scale fixed through r_0 . Scale ambiguity added as systematic error.
ETM 09B	[246]	2	0.063, 0.073	Automatic $O(a)$ impr. Estimate of lattice artifacts. (4% – 10% effect, not added in final result) by comparing two lattice spacings. $r_0 = 0.49$ fm used to convert results in physical units.
ETM 09C	[237]	2	0.051 - 0.1	Automatic $O(a)$ impr. Scale fixed through F_π . 4 lattice spacings, continuum extrapolation.
ETM 08	[235]	2	0.07-0.09	Automatic $O(a)$ impr. Discretization effects estimated by comparing two lattice spacings. Scale fixed through F_π .
JLQCD/TWQCD 08A JLQCD 08A	[95] [264]	2	0.1184(3)(21)	Automatic $O(a)$ impr., exact chiral symmetry. Scale fixed through r_0 . Scale ambiguity added as systematic error.
CERN 08	[215]	2	0.0784(10)	Scale fixed through M_K . Non-perturbative $O(a)$ improvement. No estimate of systematic error.
HHS 08	[247]	2	0.1153(5)	Tree level $O(a)$ improvement. Scale fixed through r_0 . Estimate of lattice artifacts via $W\chi$ PT in [326].
JLQCD/TWQCD 07	[248]	2	0.1111(24)	Automatic $O(a)$ impr., exact chiral symmetry. Scale fixed through r_0 . No estimate of lattice artifacts.
JLQCD/TWQCD 07A	[245]	2	$\simeq 0.12$	Automatic $O(a)$ impr., exact chiral symmetry. Scale fixed through r_0 . No estimate of lattice artifacts.
CERN-TOV 06	[254]	2	0.0717(15), 0.0521(7), 0.0784(10)	Scale fixed through M_K . The lattice with $a = 0.0784(10)$ is obtained with non-perturbative $O(a)$ improvement. No estimate of systematic error.
QCDSF/UKQCD 06A	[260]	2	0.07-0.115	5 lattice spacings. Non-perturbative $O(a)$ improvement. Scale fixed through r_0 .

Table 37: Continuum extrapolations/estimation of lattice artifacts in $N_f = 2$ determinations of the Low-Energy Constants.

Collab.	Ref.	N_f	a [fm]	Description
ETM 10	[60]	2+1+1	0.078, 0.086	Scale fixed through F_π/M_π . Systematic error taken into account by considering two lattice spacings.
MILC 10, 10A	[103, 171]	2+1	0.045 - 0.09	3 lattice spacings, continuum extrapolation by means of RS χ PT.
JLQCD/TWQCD 10	[240]	2+1, 3	0.11	One lattice spacing, scale fixed through m_Ω .
RBC/UKQCD 10A	[106]	2+1	0.1106(27), 0.0888(12)	Two lattice spacings. Data combined in global chiral-continuum fits.
JLQCD 09	[241]	2+1	0.1075(7)	Scale fixed through r_0 . Systematic error associated to lattice artifacts of order 7.4% estimated through mismatch of the lattice spacing obtained from different inputs.
MILC 09, 09A	[6, 59]	2+1	0.045 - 0.18	Total of 6 lattice spacings, continuum extrapolation by means of RS χ PT.
TWQCD 08	[242]	2+1	0.122(3)	Scale fixed through m_ρ, r_0 . No estimate of systematic effects.
JLQCD/TWQCD 08B	[243]	2+1	0.1075(7)	Scale fixed through r_0 . No estimate of systematic effects for the observable adopted in this work.
PACS-CS 08	[63]	2+1	0.0907	Only one lattice spacing, no attempt to estimate size of cut-off effects.
RBC/UKQCD 08	[108]	2+1	0.114	Only one lattice spacing, attempt to estimate size of cut-off effects via formal argument.
RBC/UKQCD 08A	[250]	2+1	0.114	Only one lattice spacing, attempt to estimate size of cut-off effects via formal argument.
NPLQCD 06	[176]	2+1	0.125	Only one lattice spacing, continuum χ PT used.
LHP 04	[259]	2+1	$\simeq 0.12$	Only one lattice spacing, mixed discretization approach.

Table 38: Continuum extrapolations/estimation of lattice artifacts in $N_f = 2+1$ and $2+1+1$ determinations of the Low-Energy Constants.

Collab.	Ref.	N_f	$M_{\pi,\min}$ [MeV]	Description
Bernardoni 10	[244]	2	297, 377, 426	NLO SU(2) fit of the topological susceptibility.
JLQCD/TWQCD 10	[240]	2	$m\Sigma V < 1$ (ϵ -reg.) $m \simeq m_s/6 - m_s$ (p -reg.)	Quark masses both in the p and in the ϵ -regime. NLO chiral fit of the spectral density interpolating the two regimes. ($+1.2\%$ / -1.8%) for $\Sigma^{1/3}$ associated to chiral fit.
JLQCD/TWQCD 09	[252]	2	290	LECs extracted from NNLO chiral fit of vector and scalar radii $\langle r^2 \rangle_{V,S}^\pi$.
ETM 09B	[246]	2	$\mu = m\Sigma V \simeq 0.11 - 0.35$	NLO SU(2) ϵ -regime fit.
ETM 09C	[237]	2	280	NNLO SU(2) fit. Systematic error estimated by performing a large set of different fits.
ETM 08	[235]	2	260	LECs extracted from pion form factor using NNLO χ PT and fixing the pion scalar radius to the experimental value.
JLQCD/TWQCD 08A JLQCD 08A	[95] [264]	2	290	NNLO SU(2) fit up to $M_\pi = 750$ MeV. Estimate of systematic error due to truncation of chiral series.
CERN 08	[215]	2	$m_{q,\min}=13$ MeV	NLO SU(2) fit for the mode number of the Dirac operator.
HHS 08	[247]	2	$\mu_1 = m\Sigma V_1 \simeq 0.7 - 2.9$ $\mu_2 = m\Sigma V_2 \simeq 2.1 - 5.0$	ϵ -regime: higher values might be too large to be considered in the ϵ -regime. NLO SU(2) ϵ -regime fit.
JLQCD/TWQCD 07	[248]	2	$\mu = m\Sigma V \simeq 0.556$	NLO SU(2) ϵ -regime fit.
JLQCD/TWQCD 07A	[245]	2	$m_{ud} = m_s/6 - m_s$	Quark condensate extracted from topological susceptibility, LO chiral fit.
CERN-TOV 06	[254]	2	403, 381, 377	NLO SU(2) fit up to $M_\pi \simeq 540$ MeV.
QCDSF/UKQCD 06A	[260]	2	400	Several fit functions to extrapolate the pion form factor.

Table 39: Chiral extrapolation/minimum pion mass in $N_f = 2$ determinations of the Low-Energy Constants.

Collab.	Ref.	N_f	$M_{\pi,\min}$ [MeV]	Description
ETM 10	[60]	2+1+1	270	SU(2) NLO and NNLO fits.
MILC 10, 10A	[103, 171]	2+1		Cf. MILC 09A.
JLQCD/TWQCD 10	[240]	2+1,3	$m_{ud}\Sigma V < 1$ (ϵ -reg) $m_{ud} = m_s/6 - m_s$ (p -reg.), $m_s \sim \text{phys.}$	For the $N_f = 2 + 1$ runs, light quark masses both in the ϵ - and in the p -regime. For the $N_f = 3$ runs, only masses in the p -regime. NLO chiral fit of the spectral density interpolating the two regimes. $(^{+2.2\%}_{-0.2\%})$ systematic error associated to $\Sigma^{1/3}$ and $\pm 8.7\%$ to $\Sigma_0^{1/3}$.
RBC/UKQCD 10A	[106]	2+1	290-420	The range is 225-420 MeV for partially quenched pions. NLO SU(2) χ PT fits are used.
JLQCD 09	[241]	2+1	$m_{ud}\Sigma V < 1$ (ϵ -reg) $m_{ud} = m_s/6 - m_s$ (p -reg.), $m_s \sim \text{phys.}$	Quark masses both in the ϵ and in the p -regime. NLO chiral fit of the spectral density interpolating the two regimes. $(^{+2.2\%}_{-0.7\%})$ % systematic error estimated by varying the fit range and using formulae for SU(2) versus SU(3) χ PT.
MILC 09	[6]	2+1	240	Value taken from text of [6]; according to [59] lightest Nambu-Goldstone mass is 224 MeV and lightest RMS mass is 258 MeV (at 0.06 fm).
MILC 09A	[59]	2+1	258	Lightest Nambu-Goldstone mass is 177 MeV (at 0.09 fm) and lightest RMS mass is 258 MeV (at 0.06 fm).
TWQCD 08	[242]	2+1	$m_{ud} = (m_s - 3m_s)/4$, $m_s \sim \text{phys.}$	Quark condensate extracted from topological susceptibility, LO chiral fit.
JLQCD/TWQCD 08B	[243]	2+1	$m_{ud} = m_s/6 - m_s$, $m_s \sim \text{phys.}$	Quark condensate extracted from topological susceptibility, LO chiral fit.
PACS-CS 08	[63]	2+1	156	To date, lightest published quark mass reached in a direct simulation.
RBC/UKQCD 08	[108]	2+1	330	Other unitary masses are 419, 557, 672 MeV, lightest non-unitary pion goes down to 242 MeV.
RBC/UKQCD 08A	[250]	2+1	330	Pion electromagnetic form factor computed at one pion mass. Low values of q^2 reached thanks to partially twisted boundary conditions. LECs determined from NLO χ PT fit in q^2 .
NPLQCD 06	[176]	2+1	460	Value refers to lightest RMS mass at $a = 0.125$ fm as quoted in [59].
LHP 04	[259]	2+1	318	Pion form factor extracted from vector meson dominance fit.

Table 40: Chiral extrapolation/minimum pion mass in $N_f = 2+1$ and $2+1+1$ determinations of the Low-Energy Constants.

Collab.	Ref.	N_f	L [fm]	$M_{\pi,\min}L$	Description
Bernardoni 10	[244]	2	1.88	2.8	Finite-volume effects included in the NLO chiral fit.
JLQCD/TWQCD 10	[240]	2	1.8-1.9		Finite volume effects estimated through differences between different topological sectors. Systematic error of 3.7% on $\Sigma^{1/3}$.
JLQCD/TWQCD 09	[252]	2	1.89	2.9	Finite-volume corrections for form factor estimated through NLO χ PT [327, 328]. Additional finite-volume effect for fixed topological charge [329].
ETM 09B	[246]	2	1.3, 1.5	ϵ -regime	Topology: not fixed. Comparison between 2 volumes, estimate of 8% systematic effect (not quoted in the final result). Volume might be too small for ϵ -expansion.
ETM 09C	[237]	2	2.0-2.5	4.4, 3.7, 3.2, 3.5	Several volumes. Finite-volume effects estimated through [323].
ETM 08	[235]	2	2.1, 2.8	3.4, 3.7	For pion form factor only data with $M_{\pi}L \gtrsim 4$ are considered in the final analysis. FSE for pion masses and decay constants are taken into account according to [323].
JLQCD/TWQCD 08A JLQCD 08A	[95] [264]	2	1.89	2.9	Finite-volume corrections estimates through [323]. Additional finite-volume effect for fixed topological charge [329].
CERN 08	[215]	2	1.88, 2.51	-	For the specific observable studied here the finite-volume effects $\propto e^{-M_{\Lambda}L/2}$, with $M_{\Lambda} \gg M_{\pi}$. Finite-volume effects checked by comparing 2 volumes.
HHS 08	[247]	2	1.84, 2.77	ϵ -regime	Topology: not fixed. Comparison between 2 volumes.
JLQCD/TWQCD 07	[248]	2	1.78	ϵ -regime	Topology: fixed to $\nu = 0$.
JLQCD/TWQCD 07A	[245]	2	1.92	-	Topology fixed to $\nu = 0$ gives finite-volume effects estimated through [329].
CERN-TOV 06	[254]	2	1.72, 1.67, 1.88	3.5, 3.2, 3.6	No estimate of finite-volume effects.
QCDSF/UKQCD 06A	[260]	2	1.4-2.0	3.8	Use NLO χ PT [327] to investigate finite-volume effects.

Table 41: Finite volume effects in $N_f = 2$ determinations of the Low-Energy Constants.

Collab.	Ref.	N_f	L [fm]	$M_{\pi, \min} L$	Description
ETM 10	[60]	2+1+1	1.9-2.8	3.0	Finite-size effects studied using [323]. LECs are extracted from data which satisfy $M_{\pi^+} L \gtrsim 4$, but $M_{\pi^0} L \sim 2$.
MILC 10, 10A	[103, 171]	2+1	2.52	4.11	$L \geq 2.9$ fm for the lighter masses.
JLQCD/TWQCD 10	[240]	2+1, 3	1.9, 2.7		Finite volume effects estimated by comparing with larger volume for a fixed quark mass. For F estimated to be 3%, for $\Sigma^{1/3}$ and $\Sigma_0^{1/3}$ ($+0.3\%$, -1.0%).
RBC/UKQCD 10A	[106]	2+1	2.7	$\simeq 4$	Finite-volume corrections included by means of χ PT.
JLQCD 09	[241]	2+1	1.72	ϵ/p -regime	Finite-volume effects estimated by comparing with larger volume ($L = 2.58$ fm) for a fixed m_{ud} , m_s .
MILC 09, 09A	[6, 59]	2+1	2.4/2.9	3.5/4.11	$L_{\min} = 2.4$ fm, but $L \geq 2.9$ fm for lighter masses; one coarse ensemble with $M_{\pi} L = 3.5$, all fine ones have $M_{\pi} L > 4.11$.
TWQCD 08	[242]	2+1	1.95	-	No estimate of finite-volume effects.
JLQCD/TWQCD 08B	[243]	2+1	1.72	-	Topology fixed to $\nu = 0$ gives finite-volume effects estimated through [329].
PACS-CS 08	[63]	2+1	2.9	2.3	Possible finite volume effects are the main concern of the authors.
RBC/UKQCD 08	[108]	2+1	2.74	4.6	Good setting to correct residual finite-volume effects by means of χ PT.
RBC/UKQCD 08A	[250]	2+1	2.74	4.6	Finite-size effects on the form factor and radius estimated to be $< 1\%$ using χ PT
NPLQCD 06	[176]	2+1	2.5	3.7	Value refers to lightest valence pion mass.
LHP 04	[259]	2+1	$\simeq 2.4$	3.97	Value refers to domain-wall valence pion mass.

Table 42: Finite volume effects in $N_f = 2 + 1$ and $2 + 1 + 1$ determinations of the Low-Energy Constants.

Collab.	Ref.	N_f	Description
ETM 10	[60]	2+1+1	Non-perturbative
JLQCD/TWQCD 10	[240]	2+1, 3	Non-perturbative
MILC 10, 10A	[103, 171]	2+1	2 loop
RBC/UKQCD 10A	[106]	2+1	Non-perturbative
JLQCD 09	[241]	2+1	Non-perturbative
MILC 09, 09A	[6, 59]	2+1	2 loop
TWQCD 08	[242]	2+1	Non-perturbative
JLQCD/TWQCD 08B	[243]	2+1	Non-perturbative
PACS-CS 08	[63]	2+1	1 loop
RBC/UKQCD 08, 08A	[108, 250]	2+1	Non-perturbative
NPLQCD 06	[176]	2+1	—
LHP 04	[259]	2+1	—
All collaborations		2	Non-perturbative

Table 43: Renormalization in determinations of the Low-Energy Constants.

B.4 Notes to section 6 on Kaon B_K -parameter B_K

In the following, we summarize the characteristics (lattice actions, pion masses, lattice spacings, etc.) of the recent $N_f = 2 + 1$ and $N_f = 2$ runs. We also provide brief descriptions of how systematic errors are estimated by the various authors.

Collab.	Ref.	N_f	a [fm]	Description
SWME 11	[281]	2+1	0.12, 0.09, 0.06, 0.04	Continuum extrapolation of results obtained at four lattice spacings; residual discretization error of 0.21% from difference to result at smallest lattice spacing.
RBC/UKQCD 10B	[282]	2+1	0.114, 0.087	Two lattice spacings. Combined chiral and continuum fits.
SWME 10	[283]	2+1	0.12, 0.09, 0.06	Continuum extrapolation of results obtained at four lattice spacings; residual discretization error of 0.21% from difference to result at smallest lattice spacing.
Aubin 09	[269]	2+1	0.09, 0.12	Two lattice spacings; quote 0.3% discretization error, estimated from various a^2 -terms in fit function
RBC/UKQCD 07A, 08	[108, 284]	2+1	0.114(2)	Single lattice spacing; quote 4% discretization error, estimated from the difference between computed and experimental values of f_π .
HPQCD/UKQCD 06	[285]	2+1	0.12	Single lattice spacing; 3% discretization error quoted without providing more details.
ETM 10A	[286]	2	0.07, 0.09, 0.1	Three lattice spacings; 1.2% error quoted.
JLQCD 08	[280]	2	0.118(1)	Single lattice spacing; no error quoted.
RBC 04	[287]	2	0.117(4)	Single lattice spacing; no error quoted.
UKQCD 04	[288]	2	0.10	Single lattice spacing; no error quoted.

Table 44: Continuum extrapolations/estimation of lattice artifacts in determinations of B_K .

Collab.	Ref.	N_f	$M_{\pi,\min}$ [MeV]	Description
SWME 11	[281]	2+1	309, 292, 275, 334	The $M_{\pi,\min}$ entries correspond to the four lattice spacings. Chiral extrapolations based on SU(2) staggered χ PT at NLO, including some analytic NNLO terms. Combined 1.1% error from various different variations in the fit procedure.
RBC/UKQCD 10B	[282]	2+1	327, 289	The $M_{\pi,\min}$ entries correspond to two lattice spacings. Combined chiral and continuum extrapolations.
SWME 10	[283]	2+1	309, 292, 275	The $M_{\pi,\min}$ entries correspond to the three lattice spacings. Chiral extrapolations based on SU(2) staggered χ PT at NLO, including some analytic NNLO terms. SU(3) staggered χ PT as cross-check. Combined 1.1% error from various different variations in the fit procedure.
Aubin 09	[269]	2+1	240/370	The $M_{\pi,\min}$ entries correspond to the smallest valence/sea quark masses. Chiral & continuum fits based on NLO mixed action χ PT at NLO, including a subset of NNLO terms. Systematic error estimated from spread arising from variations in the fit function. Relevant pion mass in the sea quark sector is the singlet pion mass of 370 MeV.
RBC/UKQCD 07A, 08[108, 284]		2+1	330	Fits based on SU(2) PQ χ PT at NLO. Effect of neglecting higher orders estimated at 6% via difference between fits based on LO and NLO expressions.
HPQCD/UKQCD 06	[285]	2+1	360	3% uncertainty from chiral extrapolation quoted, without giving further details.
ETM 10A	[286]	2	300, 270, 400	Each $M_{\pi,\min}$ entry corresponds to a different lattice spacing. Simultaneous chiral & continuum extrapolations, based on χ PT at NLO, are carried out. Systematic error from several sources, including lattice calibration, quark mass calibration, chiral and continuum extrapolation etc., estimated at 3.1%.
JLQCD 08	[280]	2	290	Fits based on NLO PQ χ PT. Range of validity investigated. Fit error included in statistical uncertainty.
RBC 04	[287]	2	490	Fits based on NLO PQ χ PT. Fit error included in statistical uncertainty.
UKQCD 04	[288]	2	780	Fits to continuum chiral behaviour at fixed sea quark mass. Separate extrapolation in sea quark mass. Fit error included in overall uncertainty.

Table 45: Chiral extrapolation/minimum pion mass in determinations of B_K .

Collab.	Ref.	N_f	L [fm]	$M_{\pi, \min} L$	Description
SWME 11	[281]	2+1	2.4/3.3, 2.4, 2.8, 2.8	$\gtrsim 3.5$	Each L -entry corresponds to a different lattice spacing, with two volumes at the coarsest lattice. Central value obtained via finite-volume staggered χ PT. Residual uncertainty of 0.6% from difference obtained using χ PT in infinite volume.
RBC/UKQCD 10B	[282]	2+1	2.7	$\gtrsim 4.0$	Finite-volume χ PT applied; residual finite-volume error estimated from the difference to fit to χ PT in infinite volume.
SWME 10	[283]	2+1	2.4/3.3, 2.4, 2.8	$\gtrsim 3.5$	Each L -entry corresponds to a different lattice spacing, with two volumes at the coarsest lattice. Finite-volume error of 0.9% estimated from difference obtained on two volumes at the coarsest lattice spacing.
Aubin 09	[269]	2+1	2.4, 3.4	3.5	Each L entry corresponds to a different lattice spacing. Keep $m_\pi L \gtrsim 3.5$; no comparison of results from different volumes; 0.6% error estimated from mixed action χ PT correction.
RBC/UKQCD 07A, 08	[108, 284]	2+1	1.83/2.74	4.60	Each L entry corresponds to a different volume at the same lattice spacing; 1% error from difference in results on two volumes.
HPQCD/UKQCD 06	[285]	2+1	2.46	4.49	Single volume; no error quoted.
ETM 10A	[286]	2	2.2, 2.2/2.9, 2.1	3.3, 3.3/4.3, 5	Each L entry corresponds to a different lattice spacing, with two volumes at the intermediate lattice spacing. Results from these two volumes at $M_\pi \sim 300$ MeV are compatible.
JLQCD 08	[280]	2	1.89	2.75	Single volume; data points with $m_{\text{val}} < m_{\text{sea}}$ excluded; 5% error quoted as upper bound of PQ χ PT estimate of the effect.
RBC 04	[287]	2	1.87	4.64	Single volume; no error quoted.
UKQCD 04	[288]	2	1.6	6.51	Single volume; no error quoted.

Table 46: Finite volume effects in determinations of B_K .

Collab.	Ref.	N_f	Ren.	running match.	Description
SWME 11	[281]	2+1	PT1 ℓ	PT1 ℓ	Uncertainty from neglecting higher orders estimated at 4.4% by identifying the unknown 2-loop coefficient with result at the smallest lattice spacing.
RBC/UKQCD 10B	[282]	2+1	RI	PT1 ℓ	Variety of different RI-MOM schemes including non-exceptional momenta. Residual uncertainty of 2% uncertainty in running & matching.
SWME 10	[283]	2+1	PT1 ℓ	PT1 ℓ	Uncertainty from neglecting higher orders estimated at 5.5% by identifying the unknown 2-loop coefficient with result at the smallest lattice spacing.
Aubin 09	[269]	2+1	RI	PT1 ℓ	Total uncertainty in matching & running of 3.3%, estimated from a number of sources, including chiral extrapolation fit ansatz for n.p. determination, strange sea quark mass dependence, residual chiral symmetry breaking, perturbative matching & running.
RBC/UKQCD 07A, 08	[108, 284]	2+1	RI	PT1 ℓ	Uncertainty from n.p. determination of ren. factor included in statistical error; 2% systematic error from perturbative matching to $\overline{\text{MS}}$ estimated via size of correction itself.
HPQCD/UKQCD 06	[285]	2+1	PT1 ℓ	PT1 ℓ	Uncertainty due to neglecting 2-loop order in perturbative matching and running estimated by multiplying result by α^2 .
ETM 10A	[286]	2	RI	PT1 ℓ	Uncertainty from RI renormalization estimated at 2.5%.
JLQCD 08	[280]	2	RI	PT1 ℓ	Uncertainty from n.p. determination of ren. factor included in statistical error; 2.3% systematic error from perturbative matching to $\overline{\text{MS}}$ estimated via size of correction itself.
RBC 04	[287]	2	RI	PT1 ℓ	Uncertainty from n.p. determination of ren. factor included.
UKQCD 04	[288]	2	PT1 ℓ	PT1 ℓ	No error quoted.

Table 47: Running and matching in determinations of B_K .

References

- [1] Flavianet Lattice Averaging Group (FLAG), *Review of lattice results concerning low energy particle physics*, <http://itpwiki.unibe.ch/flag>.
- [2] J. Laiho, E. Lunghi and R. Van de Water, *2+1 Flavor Lattice QCD Averages*, <http://krone.physik.unizh.ch/~lunghi/webpage/LatAves>.
- [3] J. Laiho, E. Lunghi, and R. S. Van de Water, *Lattice QCD inputs to the CKM unitarity triangle analysis*, *Phys. Rev.* **D81** (2010) 034503, [[arXiv:0910.2928](https://arxiv.org/abs/0910.2928)].
- [4] K. Jansen, *Lattice QCD: a critical status report*, *PoS LAT2008* (2008) 010, [[arXiv:0810.5634](https://arxiv.org/abs/0810.5634)].
- [5] C. Jung, *Status of dynamical ensemble generation*, *PoS LAT2009* (2009) 002, [[arXiv:1001.0941](https://arxiv.org/abs/1001.0941)].
- [6] [MILC 09], A. Bazavov, *et. al.*, *Full nonperturbative QCD simulations with 2+1 flavors of improved staggered quarks*, *Rev. Mod. Phys.* **82** (2010) 1349–1417, [[arXiv:0903.3598](https://arxiv.org/abs/0903.3598)].
- [7] M. Hasenbusch, *Speeding up the hybrid Monte Carlo algorithm for dynamical fermions*, *Phys.Lett.* **B519** (2001) 177–182, [[hep-lat/0107019](https://arxiv.org/abs/hep-lat/0107019)].
- [8] M. Lüscher, *Schwarz-preconditioned HMC algorithm for two-flavour lattice QCD*, *Comput. Phys. Commun.* **165** (2005) 199–220, [[hep-lat/0409106](https://arxiv.org/abs/hep-lat/0409106)].
- [9] C. Urbach, K. Jansen, A. Shindler, and U. Wenger, *HMC algorithm with multiple time scale integration and mass preconditioning*, *Comput. Phys. Commun.* **174** (2006) 87–98, [[hep-lat/0506011](https://arxiv.org/abs/hep-lat/0506011)].
- [10] M. A. Clark and A. D. Kennedy, *Accelerating Dynamical Fermion Computations using the Rational Hybrid Monte Carlo (RHMC) Algorithm with Multiple Pseudofermion Fields*, *Phys. Rev. Lett.* **98** (2007) 051601, [[hep-lat/0608015](https://arxiv.org/abs/hep-lat/0608015)].
- [11] K.-I. Ishikawa, *Recent algorithm and machine developments for lattice QCD*, *PoS LAT2008* (2008) 013, [[arXiv:0811.1661](https://arxiv.org/abs/0811.1661)].
- [12] [RBC 07A], D. J. Antonio, *et. al.*, *Localization and chiral symmetry in 3 flavor domain wall QCD*, *Phys. Rev.* **D77** (2008) 014509, [[arXiv:0705.2340](https://arxiv.org/abs/0705.2340)].
- [13] [MILC 10], A. Bazavov, *et. al.*, *Topological susceptibility with the asqtad action*, *Phys. Rev.* **D81** (2010) 114501, [[arXiv:1003.5695](https://arxiv.org/abs/1003.5695)].
- [14] S. Schaefer, R. Sommer, and F. Virotta, *Critical slowing down and error analysis in lattice QCD simulations*, [[arXiv:1009.5228](https://arxiv.org/abs/1009.5228)].
- [15] M. Lüscher, *Topology, the Wilson flow and the HMC algorithm*, [[arXiv:1009.5877](https://arxiv.org/abs/1009.5877)].
- [16] S. Schaefer, *Algorithms for lattice QCD: progress and challenges*, [[arXiv:1011.5641](https://arxiv.org/abs/1011.5641)].
- [17] [BMW 08], S. Dürr, *et. al.*, *Ab-initio determination of light hadron masses*, *Science* **322** (2008) 1224–1227, [[arXiv:0906.3599](https://arxiv.org/abs/0906.3599)].

- [18] K. Symanzik, *Continuum limit and improved action in lattice theories. 1. Principles and ϕ^4 theory*, *Nucl. Phys.* **B226** (1983) 187.
- [19] K. Symanzik, *Continuum limit and improved action in lattice theories. 2. $O(N)$ nonlinear sigma model in perturbation theory*, *Nucl. Phys.* **B226** (1983) 205.
- [20] C. W. Bernard and M. F. L. Golterman, *Partially quenched gauge theories and an application to staggered fermions*, *Phys. Rev.* **D49** (1994) 486–494, [[hep-lat/9306005](#)].
- [21] S. R. Sharpe, *Enhanced chiral logarithms in partially quenched QCD*, *Phys. Rev.* **D56** (1997) 7052–7058, [[hep-lat/9707018](#)]. Erratum: *Phys. Rev.* **D62** (2000) 099901.
- [22] M. F. L. Golterman and K.-C. Leung, *Applications of Partially Quenched Chiral Perturbation Theory*, *Phys. Rev.* **D57** (1998) 5703–5710, [[hep-lat/9711033](#)].
- [23] S. R. Sharpe and R. L. Singleton, Jr, *Spontaneous flavor and parity breaking with Wilson fermions*, *Phys. Rev.* **D58** (1998) 074501, [[hep-lat/9804028](#)].
- [24] W.-J. Lee and S. R. Sharpe, *Partial Flavor Symmetry Restoration for Chiral Staggered Fermions*, *Phys. Rev.* **D60** (1999) 114503, [[hep-lat/9905023](#)].
- [25] S. R. Sharpe and N. Shoresh, *Physical results from unphysical simulations*, *Phys. Rev.* **D62** (2000) 094503, [[hep-lat/0006017](#)].
- [26] G. Rupak and N. Shoresh, *Chiral perturbation theory for the Wilson lattice action*, *Phys. Rev.* **D66** (2002) 054503, [[hep-lat/0201019](#)].
- [27] O. Bär, G. Rupak, and N. Shoresh, *Simulations with different lattice Dirac operators for valence and sea quarks*, *Phys. Rev.* **D67** (2003) 114505, [[hep-lat/0210050](#)].
- [28] C. Aubin and C. Bernard, *Pion and kaon masses in staggered chiral perturbation theory*, *Phys.Rev.* **D68** (2003) 034014, [[hep-lat/0304014](#)].
- [29] O. Bär, G. Rupak, and N. Shoresh, *Chiral perturbation theory at $O(a^{**2})$ for lattice QCD*, *Phys. Rev.* **D70** (2004) 034508, [[hep-lat/0306021](#)].
- [30] C. Aubin and C. Bernard, *Pseudoscalar decay constants in staggered chiral perturbation theory*, *Phys.Rev.* **D68** (2003) 074011, [[hep-lat/0306026](#)].
- [31] S. Aoki, *Chiral perturbation theory with Wilson-type fermions including a^{**2} effects: $N(f) = 2$ degenerate case*, *Phys. Rev.* **D68** (2003) 054508, [[hep-lat/0306027](#)].
- [32] S. Aoki and O. Bär, *Twisted-mass QCD, $O(a)$ improvement and Wilson chiral perturbation theory*, *Phys. Rev.* **D70** (2004) 116011, [[hep-lat/0409006](#)].
- [33] S. R. Sharpe and R. S. Van de Water, *Staggered chiral perturbation theory at next-to-leading order*, *Phys. Rev.* **D71** (2005) 114505, [[hep-lat/0409018](#)].
- [34] S. R. Sharpe and J. M. S. Wu, *Twisted mass chiral perturbation theory at next-to-leading order*, *Phys. Rev.* **D71** (2005) 074501, [[hep-lat/0411021](#)].

- [35] O. Bär, C. Bernard, G. Rupak, and N. Shoresh, *Chiral perturbation theory for staggered sea quarks and Ginsparg-Wilson valence quarks*, *Phys. Rev.* **D72** (2005) 054502, [[hep-lat/0503009](#)].
- [36] M. Golterman, T. Izubuchi, and Y. Shamir, *The role of the double pole in lattice QCD with mixed actions*, *Phys. Rev.* **D71** (2005) 114508, [[hep-lat/0504013](#)].
- [37] J.-W. Chen, D. O’Connell, and A. Walker-Loud, *Two meson systems with Ginsparg-Wilson valence quarks*, *Phys. Rev.* **D75** (2007) 054501, [[hep-lat/0611003](#)].
- [38] J.-W. Chen, D. O’Connell, and A. Walker-Loud, *Universality of Mixed Action Extrapolation Formulae*, *JHEP* **04** (2009) 090, [[arXiv:0706.0035](#)].
- [39] J.-W. Chen, M. Golterman, D. O’Connell, and A. Walker-Loud, *Mixed Action Effective Field Theory: an Addendum*, *Phys. Rev.* **D79** (2009) 117502, [[arXiv:0905.2566](#)].
- [40] O. Bär, *Chiral logs in twisted mass lattice QCD with large isospin breaking*, [arXiv:1008.0784](#).
- [41] [BMW 10], S. Dürr, *et. al.*, *The ratio F_K/F_π in QCD*, *Phys. Rev.* **D81** (2010) 054507, [[arXiv:1001.4692](#)].
- [42] [PACS-CS 09], S. Aoki, *et. al.*, *Physical point simulation in 2+1 flavor lattice QCD*, *Phys. Rev.* **D81** (2010) 074503, [[arXiv:0911.2561](#)].
- [43] J. Bijnens, G. Colangelo, and G. Ecker, *Double chiral logs*, *Phys. Lett.* **B441** (1998) 437–446, [[hep-ph/9808421](#)].
- [44] G. Ecker, P. Masjuan, and H. Neufeld, *Chiral extrapolation of lattice data*, *Phys. Lett.* **B692** (2010) 184–188, [[arXiv:1004.3422](#)].
- [45] G. Ecker, *Chiral extrapolation of $SU(3)$ amplitudes*, [arXiv:1012.1522](#).
- [46] [QCDSF/UKQCD 10], W. Bietenholz, *et. al.*, *Tuning the strange quark mass in lattice simulations*, *Phys. Lett.* **B690** (2010) 436–441, [[arXiv:1003.1114](#)].
- [47] [QCDSF/UKQCD 10A], W. Bietenholz, *et. al.*, *Flavour symmetry breaking and tuning the strange quark mass for 2+1 quark flavours*, *PoS LAT2010* (2010) 122, [[arXiv:1012.4371](#)].
- [48] A. Manohar and C. T. Sachrajda, *Quark masses*, in *Review of Particle Physics*, *J. Phys.* **G37** (2010) 075021, p. 583.
- [49] [ETM 07], B. Blossier, *et. al.*, *Light quark masses and pseudoscalar decay constants from $N_f = 2$ Lattice QCD with twisted mass fermions*, *JHEP* **04** (2008) 020, [[arXiv:0709.4574](#)].
- [50] J. C. Hardy and I. S. Towner, *Superallowed $0^+ \rightarrow 0^+$ nuclear β decays: A new survey with precision tests of the conserved vector current hypothesis and the Standard Model*, *Phys. Rev.* **C79** (2009) 055502, [[arXiv:0812.1202](#)].

- [51] C. Pena, *Twisted mass QCD for weak matrix elements*, *PoS LAT2006* (2006) 019, [[hep-lat/0610109](#)]. This is, to the best of our knowledge, the first time colour coding was used. It does not appear in the proceedings but in the slides, see <http://www.physics.utah.edu/lat06/abstracts/sessions/plenary.html>.
- [52] [ALPHA 01], R. Frezzotti, P. A. Grassi, S. Sint, and P. Weisz, *Lattice QCD with a chirally twisted mass term*, *JHEP* **08** (2001) 058, [[hep-lat/0101001](#)].
- [53] R. Frezzotti and G. C. Rossi, *Chirally improving Wilson fermions. I: $O(a)$ improvement*, *JHEP* **08** (2004) 007, [[hep-lat/0306014](#)].
- [54] [ETM 07A], P. Boucaud, *et. al.*, *Dynamical twisted mass fermions with light quarks*, *Phys. Lett.* **B650** (2007) 304–311, [[hep-lat/0701012](#)].
- [55] S. Dürr, *Theoretical issues with staggered fermion simulations*, *PoS LAT2005* (2006) 021, [[hep-lat/0509026](#)].
- [56] S. R. Sharpe, *Rooted staggered fermions: good, bad or ugly?*, *PoS LAT2006* (2006) 022, [[hep-lat/0610094](#)].
- [57] A. S. Kronfeld, *Lattice gauge theory with staggered fermions: how, where, and why (not)*, *PoS LAT2007* (2007) 016, [[arXiv:0711.0699](#)].
- [58] M. Golterman, *QCD with rooted staggered fermions*, *PoS CONFINEMENT8* (2008) 014, [[arXiv:0812.3110](#)].
- [59] [MILC 09A], A. Bazavov, *et. al.*, *MILC results for light pseudoscalars*, *PoS CD09* (2009) 007, [[arXiv:0910.2966](#)].
- [60] [ETM 10], R. Baron, P. Boucaud, J. Carbonell, A. Deuzeman, V. Drach, *et. al.*, *Light hadrons from lattice QCD with light (u, d), strange and charm dynamical quarks*, *JHEP* **1006** (2010) 111, [[arXiv:1004.5284](#)].
- [61] L. Lellouch, *Kaon physics: a lattice perspective*, *PoS LAT2008* (2009) 015, [[arXiv:0902.4545](#)].
- [62] M. Gell-Mann, R. J. Oakes, and B. Renner, *Behavior of current divergences under $SU(3) \times SU(3)$* , *Phys. Rev.* **175** (1968) 2195–2199.
- [63] [PACS-CS 08], S. Aoki, *et. al.*, *2+1 Flavor lattice QCD toward the physical point*, *Phys. Rev.* **D79** (2009) 034503, [[arXiv:0807.1661](#)].
- [64] [PACS-CS 10], S. Aoki, *et. al.*, *Non-perturbative renormalization of quark mass in $N_f = 2 + 1$ QCD with the Schroedinger functional scheme*, *JHEP* **08** (2010) 101, [[arXiv:1006.1164](#)].
- [65] [BMW 10A], S. Dürr, *et. al.*, *Lattice QCD at the physical point: light quark masses*, [[arXiv:1011.2403](#)].
- [66] B. Bloch-Devaux, *Results from NA48/2 on $\pi\pi$ scattering lengths measurements in $K^\pm \rightarrow \pi^+\pi^-e^\pm\nu$ and $K^\pm \rightarrow \pi^0\pi^0\pi^\pm$ decays*, *PoS CONFINEMENT8* (2008) 029.

- [67] J. Gasser, A. Rusetsky, and I. Scimemi, *Electromagnetic corrections in hadronic processes*, *Eur. Phys. J.* **C32** (2003) 97–114, [[hep-ph/0305260](#)].
- [68] A. Rusetsky, *Isospin symmetry breaking*, *PoS CD09* (2009) 071, [[arXiv:0910.5151](#)].
- [69] J. Gasser, *Theoretical progress on cusp effect and $K_{\ell 4}$ decays*, *PoS KAON* (2008) 033, [[arXiv:0710.3048](#)].
- [70] H. Leutwyler, *Light quark masses*, *PoS CD09* (2009) 005, [[arXiv:0911.1416](#)].
- [71] R. F. Dashen, *Chiral $SU(3)\times SU(3)$ as a symmetry of the strong interactions*, *Phys. Rev.* **183** (1969) 1245–1260.
- [72] A. Duncan, E. Eichten, and H. Thacker, *Electromagnetic splittings and light quark masses in lattice QCD*, *Phys. Rev. Lett.* **76** (1996) 3894–3897, [[hep-lat/9602005](#)].
- [73] [RBC 07], T. Blum, T. Doi, M. Hayakawa, T. Izubuchi, and N. Yamada, *Determination of light quark masses from the electromagnetic splitting of pseudoscalar meson masses computed with two flavors of domain wall fermions*, *Phys. Rev.* **D76** (2007) 114508, [[arXiv:0708.0484](#)].
- [74] [Blum 10], T. Blum, *et. al.*, *Electromagnetic mass splittings of the low lying hadrons and quark masses from 2+1 flavor lattice QCD+QED*, *Phys. Rev.* **D82** (2010) 094508, [[arXiv:1006.1311](#)].
- [75] [BMW 10C], A. Portelli, *et. al.*, *Electromagnetic corrections to light hadron masses*, *PoS LAT2010* (2010) 121, [[arXiv:1011.4189](#)].
- [76] [MILC 04A], C. Aubin, *et. al.*, *Results for light pseudoscalars from three-flavor simulations*, *Nucl. Phys. Proc. Suppl.* **140** (2005) 231–233, [[hep-lat/0409041](#)].
- [77] [MILC 04], C. Aubin, *et. al.*, *Light pseudoscalar decay constants, quark masses, and low energy constants from three-flavor lattice QCD*, *Phys. Rev.* **D70** (2004) 114501, [[hep-lat/0407028](#)].
- [78] J. Bijnens and J. Prades, *Electromagnetic corrections for pions and kaons: masses and polarizabilities*, *Nucl. Phys.* **B490** (1997) 239–271, [[hep-ph/9610360](#)].
- [79] J. F. Donoghue and A. F. Perez, *The electromagnetic mass differences of pions and kaons*, *Phys. Rev.* **D55** (1997) 7075–7092, [[hep-ph/9611331](#)].
- [80] [MILC 08], S. Basak, *et. al.*, *Electromagnetic splittings of hadrons from improved staggered quarks in full QCD*, *PoS LAT2008* (2008) 127, [[arXiv:0812.4486](#)].
- [81] C. Bernard and E. D. Freeland, *Electromagnetic corrections in staggered chiral perturbation theory*, *PoS LAT2010* (2010) 084, [[arXiv:1011.3994](#)].
- [82] R. Urech, *Virtual photons in chiral perturbation theory*, *Nucl. Phys.* **B433** (1995) 234–254, [[hep-ph/9405341](#)].
- [83] R. Baur and R. Urech, *On the corrections to Dashen’s theorem*, *Phys. Rev.* **D53** (1996) 6552–6557, [[hep-ph/9508393](#)].

- [84] R. Baur and R. Urech, *Resonance contributions to the electromagnetic low energy constants of chiral perturbation theory*, *Nucl. Phys.* **B499** (1997) 319–348, [[hep-ph/9612328](#)].
- [85] B. Moussallam, *A sum rule approach to the violation of Dashen’s theorem*, *Nucl. Phys.* **B504** (1997) 381–414, [[hep-ph/9701400](#)].
- [86] W. Cottingham,, *The neutron proton mass difference and electron scattering experiments*, *Ann. of Phys.* **25** (1963) 424.
- [87] R. H. Socolow, *Departures from the Eightfold Way. 3. Pseudoscalar-meson electromagnetic masses*, *Phys. Rev.* **137** (1965) B1221–B1228.
- [88] D. J. Gross, S. B. Treiman, and F. Wilczek, *Light quark masses and isospin violation*, *Phys. Rev.* **D19** (1979) 2188.
- [89] J. Gasser and H. Leutwyler, *Quark masses*, *Phys. Rept.* **87** (1982) 77–169.
- [90] T. Das, G. S. Guralnik, V. S. Mathur, F. E. Low, and J. E. Young, *Electromagnetic mass difference of pions*, *Phys. Rev. Lett.* **18** (1967) 759–761.
- [91] [GL 85], J. Gasser, and H. Leutwyler, *Chiral perturbation theory: expansions in the mass of the strange quark*, *Nucl. Phys.* **B250** (1985) 465.
- [92] G. Amoros, J. Bijnens, and P. Talavera, *QCD isospin breaking in meson masses, decay constants and quark mass ratios*, *Nucl. Phys.* **B602** (2001) 87–108, [[hep-ph/0101127](#)].
- [93] [GL 84], J. Gasser, and H. Leutwyler, *Chiral perturbation theory to one loop*, *Ann. Phys.* **158** (1984) 142.
- [94] [ETM 10B], B. Blossier, *et. al.*, *Average up/down, strange and charm quark masses with $N_f = 2$ twisted mass lattice QCD*, *Phys. Rev.* **D82** (2010) 114513, [[arXiv:1010.3659](#)].
- [95] [JLQCD/TWQCD 08A], J. Noaki, *et. al.*, *Convergence of the chiral expansion in two-flavor lattice QCD*, *Phys. Rev. Lett.* **101** (2008) 202004, [[arXiv:0806.0894](#)].
- [96] [QCDSF/UKQCD 06], M. Göckeler, *et. al.*, *Estimating the unquenched strange quark mass from the lattice axial Ward identity*, *Phys. Rev.* **D73** (2006) 054508, [[hep-lat/0601004](#)].
- [97] [SPQcdR 05], D. Becirevic, *et. al.*, *Non-perturbatively renormalised light quark masses from a lattice simulation with $N_f = 2$* , *Nucl. Phys.* **B734** (2006) 138–155, [[hep-lat/0510014](#)].
- [98] [ALPHA 05], M. Della Morte, *et. al.*, *Non-perturbative quark mass renormalization in two-flavor QCD*, *Nucl. Phys.* **B729** (2005) 117–134, [[hep-lat/0507035](#)].
- [99] [QCDSF/UKQCD 04], M. Göckeler, *et. al.*, *Determination of light and strange quark masses from full lattice QCD*, *Phys. Lett.* **B639** (2006) 307–311, [[hep-ph/0409312](#)].
- [100] [JLQCD 02], S. Aoki, *et. al.*, *Light hadron spectroscopy with two flavors of $O(a)$ -improved dynamical quarks*, *Phys. Rev.* **D68** (2003) 054502, [[hep-lat/0212039](#)].

- [101] [CP-PACS 01], A. Ali Khan, *et. al.*, *Light hadron spectroscopy with two flavors of dynamical quarks on the lattice*, *Phys. Rev.* **D65** (2002) 054505, [[hep-lat/0105015](#)].
Erratum: *Phys. Rev.* **D66** (2003) 059901.
- [102] [ETM 10C], M. Constantinou, *et. al.*, *Non-perturbative renormalization of quark bilinear operators with $N_f=2$ (tmQCD) Wilson fermions and the tree-level improved gauge action*, *JHEP* **08** (2010) 068, [[arXiv:1004.1115](#)].
- [103] [MILC 10A], A. Bazavov, *et. al.*, *Staggered chiral perturbation theory in the two-flavor case and $SU(2)$ analysis of the MILC data*, *PoS LAT2010* (2010) 083, [[arXiv:1011.1792](#)].
- [104] [HPQCD 10], C. McNeile, C. T. H. Davies, E. Follana, K. Hornbostel, and G. P. Lepage, *High-Precision c and b Masses, and QCD Coupling from Current-Current Correlators in Lattice and Continuum QCD*, *Phys. Rev.* **D82** (2010) 034512, [[arXiv:1004.4285](#)].
- [105] [BMW 10B], S. Dürr, *et. al.*, *Lattice QCD at the physical point: Simulation and analysis details*, [arXiv:1011.2711](#).
- [106] [RBC/UKQCD 10A], Y. Aoki, *et. al.*, *Continuum Limit Physics from 2+1 Flavor Domain Wall QCD*, [arXiv:1011.0892](#).
- [107] [HPQCD 09], C. T. H. Davies, *et. al.*, *Precise charm to strange mass ratio and light quark masses from full lattice QCD*, *Phys. Rev. Lett.* **104** (2010) 132003, [[arXiv:0910.3102](#)].
- [108] [RBC/UKQCD 08], C. Allton, *et. al.*, *Physical results from 2+1 flavor domain wall QCD and $SU(2)$ chiral perturbation theory*, *Phys. Rev.* **D78** (2008) 114509, [[arXiv:0804.0473](#)].
- [109] [CP-PACS/JLQCD 07], T. Ishikawa, *et. al.*, *Light quark masses from unquenched lattice QCD*, *Phys. Rev.* **D78** (2008) 011502, [[arXiv:0704.1937](#)].
- [110] [HPQCD 05], Q. Mason, H. D. Trottier, R. Horgan, C. T. H. Davies, and G. P. Lepage, *High-precision determination of the light-quark masses from realistic lattice QCD*, *Phys. Rev.* **D73** (2006) 114501, [[hep-ph/0511160](#)].
- [111] [HPQCD/MILC/UKQCD 04], C. Aubin, *et. al.*, *First determination of the strange and light quark masses from full lattice QCD*, *Phys. Rev.* **D70** (2004) 031504, [[hep-lat/0405022](#)].
- [112] [ALPHA 99], J. Garden, J. Heitger, R. Sommer, and H. Wittig, *Precision computation of the strange quark's mass in quenched QCD*, *Nucl. Phys.* **B571** (2000) 237–256, [[hep-lat/9906013](#)].
- [113] A. T. Lytle, *Non-perturbative calculation of Z_m using Asqtad fermions*, *PoS LAT2009* (2009) 202, [[arXiv:0910.3721](#)].
- [114] M. Lüscher, R. Narayanan, P. Weisz, and U. Wolff, *The Schrödinger functional: a renormalizable probe for non-Abelian gauge theories*, *Nucl. Phys.* **B384** (1992) 168–228, [[hep-lat/9207009](#)].

- [115] G. Martinelli, C. Pittori, C. T. Sachrajda, M. Testa, and A. Vladikas, *A general method for nonperturbative renormalization of lattice operators*, *Nucl. Phys.* **B445** (1995) 81–108, [[hep-lat/9411010](#)].
- [116] [HPQCD 08], I. Allison, *et. al.*, *High-precision charm-quark mass from current-current correlators in lattice and continuum QCD*, *Phys. Rev.* **D78** (2008) 054513, [[arXiv:0805.2999](#)].
- [117] A. I. Vainshtein *et. al.*, *Sum rules for light quarks in Quantum Chromodynamics*, *Sov. J. Nucl. Phys.* **27** (1978) 274.
- [118] S. Narison, *Strange quark mass from e^+e^- revisited and present status of light quark masses*, *Phys. Rev.* **D74** (2006) 034013, [[hep-ph/0510108](#)].
- [119] M. Jamin, J. A. Oller, and A. Pich, *Scalar $K\pi$ form factor and light quark masses*, *Phys. Rev.* **D74** (2006) 074009, [[hep-ph/0605095](#)].
- [120] K. G. Chetyrkin and A. Khodjamirian, *Strange quark mass from pseudoscalar sum rule with $O(\alpha_s^4)$ accuracy*, *Eur. Phys. J.* **C46** (2006) 721–728, [[hep-ph/0512295](#)].
- [121] C. A. Dominguez, N. F. Nasrallah, R. Röntschi, and K. Schilcher, *Light quark masses from QCD sum rules with minimal hadronic bias*, *Nucl. Phys. Proc. Suppl.* **186** (2009) 133–136, [[arXiv:0808.3909](#)].
- [122] [PDG 10], K. Nakamura, *et. al.*, *Review of particle physics*, *J. Phys.* **G37** (2010) 075021.
- [123] K. Maltman and J. Kambor, *$m_u + m_d$ from isovector pseudoscalar sum rules*, *Phys. Lett.* **B517** (2001) 332–338, [[hep-ph/0107060](#)].
- [124] T. van Ritbergen, J. A. M. Vermaseren, and S. A. Larin, *The four-loop β -function in Quantum Chromodynamics*, *Phys. Lett.* **B400** (1997) 379–384, [[hep-ph/9701390](#)].
- [125] K. G. Chetyrkin, B. A. Kniehl, and M. Steinhauser, *Strong coupling constant with flavour thresholds at four loops in the $\overline{\text{MS}}$ scheme*, *Phys. Rev. Lett.* **79** (1997) 2184–2187, [[hep-ph/9706430](#)].
- [126] K. G. Chetyrkin and A. Retey, *Renormalization and running of quark mass and field in the regularization invariant and $\overline{\text{MS}}$ schemes at three and four loops*, *Nucl. Phys.* **B583** (2000) 3–34, [[hep-ph/9910332](#)].
- [127] S. Bethke, *The 2009 World Average of $\alpha_s(M_Z)$* , *Eur. Phys. J.* **C64** (2009) 689–703, [[arXiv:0908.1135](#)].
- [128] S. Weinberg, *The problem of mass*, *Trans. New York Acad. Sci.* **38** (1977) 185–201.
- [129] H. Leutwyler, *The ratios of the light quark masses*, *Phys. Lett.* **B378** (1996) 313–318, [[hep-ph/9602366](#)].
- [130] R. Kaiser, *The η and the η' at large N_c , diploma work, University of Bern* (1997); H. Leutwyler, *On the $1/N$ -expansion in chiral perturbation theory*, *Nucl. Phys. Proc. Suppl.* **64** (1998) 223–231, [[hep-ph/9709408](#)].

- [131] J. A. Oller and L. Roca, *Non-perturbative study of the light pseudoscalar masses in chiral dynamics*, *Eur. Phys. J.* **A34** (2007) 371–386, [[hep-ph/0608290](#)].
- [132] J. Gasser and H. Leutwyler, $\eta \rightarrow 3\pi$ to one loop, *Nucl. Phys.* **B250** (1985) 539.
- [133] J. Kambor, C. Wiesendanger, and D. Wyler, *Final state interactions and Khuri-Treiman equations in $\eta \rightarrow 3\pi$ decays*, *Nucl. Phys.* **B465** (1996) 215–266, [[hep-ph/9509374](#)].
- [134] A. V. Anisovich and H. Leutwyler, *Dispersive analysis of the decay $\eta \rightarrow 3\pi$* , *Phys. Lett.* **B375** (1996) 335–342, [[hep-ph/9601237](#)].
- [135] C. Ditsche, B. Kubis, and U.-G. Meissner, *Electromagnetic corrections in $\eta \rightarrow 3\pi$ decays*, *Eur. Phys. J.* **C60** (2009) 83–105, [[arXiv:0812.0344](#)].
- [136] G. Colangelo, S. Lanz, and E. Passemar, *A new dispersive analysis of $\eta \rightarrow 3\pi$* , *PoS CD09* (2009) 047, [[arXiv:0910.0765](#)].
- [137] J. Bijnens and K. Ghorbani, $\eta \rightarrow 3\pi$ at two loops in chiral perturbation theory, *JHEP* **11** (2007) 030, [[arXiv:0709.0230](#)].
- [138] M. Antonelli *et. al.*, *An evaluation of $|V_{us}|$ and precise tests of the Standard Model from world data on leptonic and semileptonic kaon decays*, *Eur. Phys. J.* **C69** (2010) 399–424, [[arXiv:1005.2323](#)].
- [139] J. Gasser and G. R. S. Zarnauskas, *On the pion decay constant*, *Phys. Lett.* **B693** (2010) 122–128, [[arXiv:1008.3479](#)].
- [140] J. L. Rosner and S. Stone, *Decay constants of charged pseudoscalar mesons*, in *Review of Particle Physics*, *J. Phys.* **G37** (2010) 075021, p. 861.
- [141] V. Cirigliano and H. Neufeld, *A note on isospin violation in $P_{l2(\gamma)}$ decays*, [[arXiv:1102.0563](#)].
- [142] I. S. Towner and J. C. Hardy, *An improved calculation of the isospin-symmetry-breaking corrections to superallowed Fermi beta decay*, *Phys. Rev.* **C77** (2008) 025501, [[arXiv:0710.3181](#)].
- [143] G. A. Miller and A. Schwenk, *Isospin-symmetry-breaking corrections to superallowed Fermi beta decay: formalism and schematic models*, *Phys. Rev.* **C78** (2008) 035501, [[arXiv:0805.0603](#)].
- [144] N. Auerbach, *Coulomb corrections to superallowed beta decay in nuclei*, *Phys. Rev.* **C79** (2009) 035502, [[arXiv:0811.4742](#)].
- [145] H. Liang, N. Van Giai, and J. Meng, *Isospin corrections for superallowed Fermi beta decay in self-consistent relativistic random-phase approximation approaches*, *Phys. Rev.* **C79** (2009) 064316, [[arXiv:0904.3673](#)].
- [146] G. A. Miller and A. Schwenk, *Isospin-symmetry-breaking corrections to superallowed Fermi beta decay: radial excitations*, *Phys. Rev.* **C80** (2009) 064319, [[arXiv:0910.2790](#)].

- [147] I. S. Towner and J. C. Hardy, *Comparative tests of isospin-symmetry-breaking corrections to superallowed $0^+ \rightarrow 0^+$ nuclear beta decay*, [arXiv:1007.5343](#).
- [148] E. Gamiz, M. Jamin, A. Pich, J. Prades, and F. Schwab, *Determination of m_s and $|V_{us}|$ from hadronic tau decays*, *JHEP* **01** (2003) 060, [[hep-ph/0212230](#)].
- [149] E. Gamiz, M. Jamin, A. Pich, J. Prades, and F. Schwab, *V_{us} and m_s from hadronic τ decays*, *Phys. Rev. Lett.* **94** (2005) 011803, [[hep-ph/0408044](#)].
- [150] K. Maltman, *A mixed τ -electroproduction sum rule for V_{us}* , *Phys. Lett.* **B672** (2009) 257–263, [[arXiv:0811.1590](#)].
- [151] A. Pich and R. Kass, talks given at CKM 08, Rome, Italy, 2008, <http://ckm2008.roma1.infn.it>.
- [152] E. Gamiz, M. Jamin, A. Pich, J. Prades, and F. Schwab, *Theoretical progress on the V_{us} determination from τ decays*, *PoS KAON* (2008) 008, [[arXiv:0709.0282](#)].
- [153] K. Maltman, C. E. Wolfe, S. Banerjee, J. M. Roney, and I. Nugent, *Status of the hadronic τ determination of V_{us}* , *Int. J. Mod. Phys.* **A23** (2008) 3191–3195, [[arXiv:0807.3195](#)].
- [154] K. Maltman, C. E. Wolfe, S. Banerjee, I. M. Nugent, and J. M. Roney, *Status of the hadronic τ decay determination of $|V_{us}|$* , *Nucl. Phys. Proc. Suppl.* **189** (2009) 175–180, [[arXiv:0906.1386](#)].
- [155] M. Beneke and M. Jamin, *α_s and the τ hadronic width: fixed-order, contour-improved and higher-order perturbation theory*, *JHEP* **09** (2008) 044, [[arXiv:0806.3156](#)].
- [156] I. Caprini and J. Fischer, *α_s from τ decays: contour-improved versus fixed-order summation in a new QCD perturbation expansion*, *Eur. Phys. J.* **C64** (2009) 35–45, [[arXiv:0906.5211](#)].
- [157] S. Menke, *On the determination of α_s from hadronic τ decays with contour-improved, fixed order and renormalon-chain perturbation theory*, [arXiv:0904.1796](#).
- [158] [RBC/UKQCD 10], P. A. Boyle, *et. al.*, *$K \rightarrow \pi$ form factors with reduced model dependence*, *Eur. Phys. J.* **C69** (2010) 159–167, [[arXiv:1004.0886](#)].
- [159] [RBC/UKQCD 07], P. A. Boyle, *et. al.*, *K_{l3} semileptonic form factor from 2+1 flavour lattice QCD*, *Phys. Rev. Lett.* **100** (2008) 141601, [[arXiv:0710.5136](#)].
- [160] [ETM 10D], V. Lubicz, F. Mescia, L. Orifici, S. Simula, and C. Tarantino, *Improved analysis of the scalar and vector form factors of kaon semileptonic decays with $N_f = 2$ twisted-mass fermions*, *PoS LAT2010* (2010) 316, [[arXiv:1012.3573](#)].
- [161] [ETM 09A], V. Lubicz, F. Mescia, S. Simula, and C. Tarantino, *$K \rightarrow \pi \ell \nu$ semileptonic form factors from two-flavor lattice QCD*, *Phys. Rev.* **D80** (2009) 111502, [[arXiv:0906.4728](#)].
- [162] [QCDSF 07], D. Brömmel, *et. al.*, *Kaon semileptonic decay form factors from $N_f = 2$ non-perturbatively $O(a)$ -improved Wilson fermions*, *PoS LAT2007* (2007) 364, [[arXiv:0710.2100](#)].

- [163] [RBC 06], C. Dawson, T. Izubuchi, T. Kaneko, S. Sasaki, and A. Soni, *Vector form factor in K_{l3} semileptonic decay with two flavors of dynamical domain-wall quarks*, *Phys. Rev.* **D74** (2006) 114502, [[hep-ph/0607162](#)].
- [164] [JLQCD 05], N. Tsutsui, *et. al.*, *Kaon semileptonic decay form factors in two-flavor QCD*, *PoS LAT2005* (2006) 357, [[hep-lat/0510068](#)].
- [165] M. Ademollo and R. Gatto, *Nonrenormalization theorem for the strangeness violating vector currents*, *Phys. Rev. Lett.* **13** (1964) 264–265.
- [166] G. Furlan, F. Lannoy, C. Rossetti, and G. Segré, *Symmetry-breaking corrections to weak vector currents*, *Nuovo Cim.* **38** (1965) 1747.
- [167] J. Gasser and H. Leutwyler, *Low-energy expansion of meson form factors*, *Nucl. Phys.* **B250** (1985) 517–538.
- [168] D. Becirevic, G. Martinelli, and G. Villadoro, *The Ademollo-Gatto theorem for lattice semileptonic decays*, *Phys. Lett.* **B633** (2006) 84–88, [[hep-lat/0508013](#)].
- [169] [RBC 08], J. M. Flynn, and C. T. Sachrajda, *$SU(2)$ chiral perturbation theory for $Kl3$ decay amplitudes*, *Nucl. Phys.* **B812** (2009) 64–80, [[arXiv:0809.1229](#)].
- [170] [ETM 10E], F. Farchioni, G. Herdoiza, K. Jansen, M. Petschlies, C. Urbach, *et. al.*, *Pseudoscalar decay constants from $N_f = 2 + 1 + 1$ twisted mass lattice QCD*, *PoS LAT2010* (2010) 128, [[arXiv:1012.0200](#)].
- [171] [MILC 10], A. Bazavov, *et. al.*, *Results for light pseudoscalar mesons*, *PoS LAT2010* (2010) 074, [[arXiv:1012.0868](#)].
- [172] [JLQCD/TWQCD 09A], J. Noaki, *et. al.*, *Chiral properties of light mesons with $N_f = 2 + 1$ overlap fermions*, *PoS LAT2009* (2009) 096, [[arXiv:0910.5532](#)].
- [173] [Aubin 08], C. Aubin, J. Laiho, and R. S. Van de Water, *Light pseudoscalar meson masses and decay constants from mixed action lattice QCD*, *PoS LAT2008* (2008) 105, [[arXiv:0810.4328](#)].
- [174] [PACS-CS 08A] and Y. Kuramashi, *PACS-CS results for 2+1 flavor lattice QCD simulation on and off the physical point*, *PoS LAT2008* (2008) 018, [[arXiv:0811.2630](#)].
- [175] [HPQCD/UKQCD 07], E. Follana, C. T. H. Davies, G. P. Lepage, and J. Shigemitsu, *High precision determination of the π , K , D and D_s decay constants from lattice QCD*, *Phys. Rev. Lett.* **100** (2008) 062002, [[arXiv:0706.1726](#)].
- [176] [NPLQCD 06], S. R. Beane, P. F. Bedaque, K. Orginos, and M. J. Savage, *f_K/f_π in full QCD with domain wall valence quarks*, *Phys. Rev.* **D75** (2007) 094501, [[hep-lat/0606023](#)].
- [177] [ETM 09], B. Blossier, *et. al.*, *Pseudoscalar decay constants of kaon and D -mesons from $N_f = 2$ twisted mass Lattice QCD*, *JHEP* **07** (2009) 043, [[arXiv:0904.0954](#)].

- [178] [QCDSF/UKQCD 07], G. Schierholz et al., *Probing the chiral limit with clover fermions I: The meson sector, talk given at Lattice 2007, Regensburg, Germany*, PoS **LAT2007**, 133, <http://www.physik.uni-regensburg.de/lat07/hevea/schierholz.pdf>.
- [179] [LR 84], H. Leutwyler, and M. Roos, *Determination of the elements V_{us} and V_{ud} of the Kobayashi-Maskawa matrix*, *Z. Phys.* **C25** (1984) 91.
- [180] P. Post and K. Schilcher, *K_{l3} form factors at order p^6 in chiral perturbation theory*, *Eur. Phys. J.* **C25** (2002) 427–443, [[hep-ph/0112352](#)].
- [181] J. Bijnens and P. Talavera, *K_{l3} decays in chiral perturbation theory*, *Nucl. Phys.* **B669** (2003) 341–362, [[hep-ph/0303103](#)].
- [182] M. Jamin, J. A. Oller, and A. Pich, *Order p^6 chiral couplings from the scalar $K\pi$ form factor*, *JHEP* **02** (2004) 047, [[hep-ph/0401080](#)].
- [183] V. Cirigliano et. al., *The Green function and $SU(3)$ breaking in K_{l3} decays*, *JHEP* **04** (2005) 006, [[hep-ph/0503108](#)].
- [184] A. Kastner and H. Neufeld, *The K_{l3} scalar form factors in the Standard Model*, *Eur. Phys. J.* **C57** (2008) 541–556, [[arXiv:0805.2222](#)].
- [185] V. Bernard, M. Oertel, E. Passemar, and J. Stern, *Dispersive representation and shape of the $K_{\ell 3}$ form factors: robustness*, *Phys. Rev.* **D80** (2009) 034034, [[arXiv:0903.1654](#)].
- [186] V. Bernard and E. Passemar, *Chiral extrapolation of the strangeness changing $K\pi$ form factor*, *JHEP* **04** (2010) 001, [[arXiv:0912.3792](#)].
- [187] E. Passemar, *Dispersive approach to $K_{\ell 3}$ form factors*, *NA62 Physics Handbook Workshop, CERN 2009* (2009).
- [188] E. Passemar, *Precision SM calculations and theoretical interests beyond the SM in $K_{\ell 2}$ and $K_{\ell 3}$ decays*, *PoS KAON09* (2009) 024, [[arXiv:1003.4696](#)].
- [189] S. Di Vita et. al., *Vector and scalar form factors for K - and D -meson semileptonic decays from twisted mass fermions with $N_f = 2$* , *PoS LAT2009* (2009) 257, [[arXiv:0910.4845](#)].
- [190] [SPQcdR 04], D. Becirevic, et. al., *The $K \rightarrow \pi$ vector form factor at zero momentum transfer on the lattice*, *Nucl. Phys.* **B705** (2005) 339–362, [[hep-ph/0403217](#)].
- [191] R. Kowalewski and T. Mannel, *Determination of V_{cb} and V_{ub}* , in *Review of Particle Physics*, *J. Phys.* **G37** (2010) 075021, p. 1014.
- [192] M. E. Fisher and V. Privman, *First-order transitions breaking $O(n)$ symmetry: Finite-size scaling*, *Phys. Rev.* **B32** (1985) 447–464.
- [193] E. Brezin and J. Zinn-Justin, *Finite size effects in phase transitions*, *Nucl. Phys.* **B257** (1985) 867.

- [194] J. Gasser and H. Leutwyler, *Light quarks at low temperatures*, *Phys. Lett.* **B184** (1987) 83.
- [195] J. Gasser and H. Leutwyler, *Thermodynamics of chiral symmetry*, *Phys. Lett.* **B188** (1987) 477.
- [196] J. Gasser and H. Leutwyler, *Spontaneously Broken Symmetries: Effective Lagrangians at Finite Volume*, *Nucl. Phys.* **B307** (1988) 763.
- [197] P. Hasenfratz and H. Leutwyler, *Goldstone boson related finite size effects in field theory and critical phenomena with $O(N)$ symmetry*, *Nucl. Phys.* **B343** (1990) 241–284.
- [198] [CGL 01], G. Colangelo, J. Gasser, and H. Leutwyler, *$\pi\pi$ scattering*, *Nucl. Phys.* **B603** (2001) 125–179, [[hep-ph/0103088](#)].
- [199] F. C. Hansen, *Finite size effects in spontaneously broken $SU(N)\times SU(N)$ theories*, *Nucl. Phys.* **B345** (1990) 685–708.
- [200] F. C. Hansen and H. Leutwyler, *Charge correlations and topological susceptibility in QCD*, *Nucl. Phys.* **B350** (1991) 201–227.
- [201] H. Leutwyler and A. V. Smilga, *Spectrum of Dirac operator and role of winding number in QCD*, *Phys. Rev.* **D46** (1992) 5607–5632.
- [202] P. H. Damgaard, M. C. Diamantini, P. Hernandez, and K. Jansen, *Finite-size scaling of meson propagators*, *Nucl. Phys.* **B629** (2002) 445–478, [[hep-lat/0112016](#)].
- [203] P. H. Damgaard, P. Hernandez, K. Jansen, M. Laine, and L. Lellouch, *Finite-size scaling of vector and axial current correlators*, *Nucl. Phys.* **B656** (2003) 226–238, [[hep-lat/0211020](#)].
- [204] S. Aoki and H. Fukaya, *Chiral perturbation theory in a theta vacuum*, *Phys. Rev.* **D81** (2010) 034022, [[arXiv:0906.4852](#)].
- [205] F. Bernardoni, P. H. Damgaard, H. Fukaya, and P. Hernandez, *Finite volume scaling of Pseudo Nambu-Goldstone Bosons in QCD*, *JHEP* **10** (2008) 008, [[arXiv:0808.1986](#)].
- [206] P. H. Damgaard and H. Fukaya, *The chiral condensate in a finite volume*, *JHEP* **01** (2009) 052, [[arXiv:0812.2797](#)].
- [207] H. Leutwyler, *Energy levels of light quarks confined to a box*, *Phys. Lett.* **B189** (1987) 197.
- [208] P. Hasenfratz, *The QCD rotator in the chiral limit*, *Nucl. Phys.* **B828** (2010) 201–214, [[arXiv:0909.3419](#)].
- [209] F. Niedermayer and C. Weiermann, *The rotator spectrum in the δ -regime of the $O(n)$ effective field theory in 3 and 4 dimensions*, *Nucl. Phys.* **B842** (2011) 248–263, [[arXiv:1006.5855](#)].

- [210] M. Weingart, *The QCD rotator with a light quark mass*, [arXiv:1006.5076](#).
- [211] A. Hasenfratz, P. Hasenfratz, F. Niedermayer, D. Hierl, and A. Schafer, *First results in QCD with 2+1 light flavors using the fixed-point action*, *PoS LAT2006* (2006) 178, [[hep-lat/0610096](#)].
- [212] [QCDSF 10], W. Bietenholz, *et. al.*, *Pion in a box*, *Phys. Lett.* **B687** (2010) 410–414, [[arXiv:1002.1696](#)].
- [213] P. Di Vecchia and G. Veneziano, *Chiral dynamics in the large N limit*, *Nucl. Phys.* **B171** (1980) 253.
- [214] [TWQCD 09], Y.-Y. Mao, and T.-W. Chiu, *Topological susceptibility to the one-loop order in chiral perturbation theory*, *Phys. Rev.* **D80** (2009) 034502, [[arXiv:0903.2146](#)].
- [215] [CERN 08], L. Giusti, and M. Lüscher, *Chiral symmetry breaking and the Banks–Casher relation in lattice QCD with Wilson quarks*, *JHEP* **03** (2009) 013, [[arXiv:0812.3638](#)].
- [216] T. Banks and A. Casher, *Chiral symmetry breaking in confining theories*, *Nucl. Phys.* **B169** (1980) 103.
- [217] E. V. Shuryak and J. J. M. Verbaarschot, *Random matrix theory and spectral sum rules for the Dirac operator in QCD*, *Nucl. Phys.* **A560** (1993) 306–320, [[hep-th/9212088](#)].
- [218] J. J. M. Verbaarschot and I. Zahed, *Spectral density of the QCD Dirac operator near zero virtuality*, *Phys. Rev. Lett.* **70** (1993) 3852–3855, [[hep-th/9303012](#)].
- [219] J. J. M. Verbaarschot, *The spectrum of the QCD Dirac operator and chiral random matrix theory: the threefold way*, *Phys. Rev. Lett.* **72** (1994) 2531–2533, [[hep-th/9401059](#)].
- [220] J. J. M. Verbaarschot and T. Wettig, *Random matrix theory and chiral symmetry in QCD*, *Ann. Rev. Nucl. Part. Sci.* **50** (2000) 343–410, [[hep-ph/0003017](#)].
- [221] S. M. Nishigaki, P. H. Damgaard, and T. Wettig, *Smallest Dirac eigenvalue distribution from random matrix theory*, *Phys. Rev.* **D58** (1998) 087704, [[hep-th/9803007](#)].
- [222] P. H. Damgaard and S. M. Nishigaki, *Distribution of the k-th smallest Dirac operator eigenvalue*, *Phys. Rev.* **D63** (2001) 045012, [[hep-th/0006111](#)].
- [223] F. Basile and G. Akemann, *Equivalence of QCD in the epsilon-regime and chiral random matrix theory with or without chemical potential*, *JHEP* **12** (2007) 043, [[arXiv:0710.0376](#)].
- [224] G. Akemann, P. H. Damgaard, J. C. Osborn, and K. Splittorff, *A new chiral two-matrix theory for Dirac spectra with imaginary chemical potential*, *Nucl. Phys.* **B766** (2007) 34–67, [[hep-th/0609059](#)].

- [225] C. Lehner, S. Hashimoto, and T. Wettig, *The epsilon expansion at next-to-next-to-leading order with small imaginary chemical potential*, *JHEP* **06** (2010) 028, [[arXiv:1004.5584](#)].
- [226] C. Lehner, J. Bloch, S. Hashimoto, and T. Wettig, *Geometry dependence of RMT-based methods to extract the low-energy constants Sigma and F*, [arXiv:1101.5576](#).
- [227] [CERN-TOV 05], L. Del Debbio, L. Giusti, M. Lüscher, R. Petronzio, and N. Tantalo, *Stability of lattice QCD simulations and the thermodynamic limit*, *JHEP* **02** (2006) 011, [[hep-lat/0512021](#)].
- [228] H. Fukaya *et. al.*, *Two-flavor lattice QCD in the epsilon-regime and chiral random matrix theory*, *Phys. Rev.* **D76** (2007) 054503, [[arXiv:0705.3322](#)].
- [229] C. B. Lang, P. Majumdar, and W. Ortner, *The condensate for two dynamical chirally improved quarks in QCD*, *Phys. Lett.* **B649** (2007) 225–229, [[hep-lat/0611010](#)].
- [230] T. DeGrand, Z. Liu, and S. Schaefer, *Quark condensate in two-flavor QCD*, *Phys. Rev.* **D74** (2006) 094504, [[hep-lat/0608019](#)].
- [231] P. Hasenfratz *et. al.*, *2+1 Flavor QCD simulated in the epsilon-regime in different topological sectors*, *JHEP* **11** (2009) 100, [[arXiv:0707.0071](#)].
- [232] T. DeGrand and S. Schaefer, *Parameters of the lowest order chiral Lagrangian from fermion eigenvalues*, *Phys. Rev.* **D76** (2007) 094509, [[arXiv:0708.1731](#)].
- [233] J. F. Donoghue, J. Gasser, and H. Leutwyler, *The decay of a light Higgs boson*, *Nucl. Phys.* **B343** (1990) 341–368.
- [234] [BCT 98], J. Bijnens, G. Colangelo, and P. Talavera, *The vector and scalar form factors of the pion to two loops*, *JHEP* **05** (1998) 014, [[hep-ph/9805389](#)].
- [235] [ETM 08], R. Frezzotti, V. Lubicz, and S. Simula, *Electromagnetic form factor of the pion from twisted-mass lattice QCD at $N_f = 2$* , *Phys. Rev.* **D79** (2009) 074506, [[arXiv:0812.4042](#)].
- [236] [JLQCD/TWQCD 08], T. Kaneko, *et. al.*, *Pion vector and scalar form factors with dynamical overlap quarks*, *PoS LAT2008* (2008) 158, [[arXiv:0810.2590](#)].
- [237] [ETM 09C], R. Baron, *et. al.*, *Light meson physics from maximally twisted mass lattice QCD*, *JHEP* **08** (2010) 097, [[arXiv:0911.5061](#)].
- [238] J. Gasser, C. Haefeli, M. A. Ivanov, and M. Schmid, *Integrating out strange quarks in ChPT*, *Phys. Lett.* **B652** (2007) 21–26, [[arXiv:0706.0955](#)].
- [239] J. Gasser, C. Haefeli, M. A. Ivanov, and M. Schmid, *Integrating out strange quarks in ChPT: terms at order p^6* , *Phys. Lett.* **B675** (2009) 49–53, [[arXiv:0903.0801](#)].
- [240] **JLQCD and TWQCD** Collaboration, [JLQCD/TWQCD 10], H. Fukaya, *et. al.*, *Determination of the chiral condensate from QCD Dirac spectrum on the lattice*, *Phys. Rev.* **D83** (2011) 074501, [[arXiv:1012.4052](#)].

- [241] [JLQCD 09], H. Fukaya, *et. al.*, *Determination of the chiral condensate from 2+1-flavor lattice QCD*, *Phys. Rev. Lett.* **104** (2010) 122002, [[arXiv:0911.5555](#)].
- [242] [TWQCD 08], T.-W. Chiu, T.-H. Hsieh, and P.-K. Tseng, *Topological susceptibility in 2+1 flavors lattice QCD with domain-wall fermions*, *Phys. Lett.* **B671** (2009) 135–138, [[arXiv:0810.3406](#)].
- [243] [JLQCD/TWQCD 08B], T. W. Chiu, *et. al.*, *Topological susceptibility in (2+1)-flavor lattice QCD with overlap fermion*, *PoS LAT2008* (2008) 072, [[arXiv:0810.0085](#)].
- [244] [Bernardoni 10], F. Bernardoni, P. Hernandez, N. Garron, S. Necco, and C. Pena, *Probing the chiral regime of $N_f = 2$ QCD with mixed actions*, *Phys. Rev.* **D83** (2011) 054503, [[arXiv:1008.1870](#)].
- [245] [JLQCD/TWQCD 07A], S. Aoki, *et. al.*, *Topological susceptibility in two-flavor lattice QCD with exact chiral symmetry*, *Phys. Lett.* **B665** (2008) 294–297, [[arXiv:0710.1130](#)].
- [246] [ETM 09B], K. Jansen, and A. Shindler, *The epsilon regime of chiral perturbation theory with Wilson-type fermions*, *PoS LAT2009* (2009) 070, [[arXiv:0911.1931](#)].
- [247] [HHS 08], A. Hasenfratz, R. Hoffmann, and S. Schaefer, *Low energy chiral constants from epsilon-regime simulations with improved Wilson fermions*, *Phys. Rev.* **D78** (2008) 054511, [[arXiv:0806.4586](#)].
- [248] [JLQCD/TWQCD 07], H. Fukaya, *et. al.*, *Lattice study of meson correlators in the epsilon-regime of two-flavor QCD*, *Phys. Rev.* **D77** (2008) 074503, [[arXiv:0711.4965](#)].
- [249] [ETM 11], R. Baron, *et. al.*, *Light hadrons from $N_f = 2 + 1 + 1$ dynamical twisted mass fermions*, *PoS LAT2010* (2010) 123, [[arXiv:1101.0518](#)].
- [250] [RBC/UKQCD 08A], P. A. Boyle, *et. al.*, *The pion’s electromagnetic form factor at small momentum transfer in full lattice QCD*, *JHEP* **07** (2008) 112, [[arXiv:0804.3971](#)].
- [251] [CD 03], G. Colangelo, and S. Dürr, *The pion mass in finite volume*, *Eur. Phys. J.* **C33** (2004) 543–553, [[hep-lat/0311023](#)].
- [252] [JLQCD/TWQCD 09], S. Aoki, *et. al.*, *Pion form factors from two-flavor lattice QCD with exact chiral symmetry*, *Phys. Rev.* **D80** (2009) 034508, [[arXiv:0905.2465](#)].
- [253] S. Dürr, M_π^2 versus m_q : *Comparing CP-PACS and UKQCD data to chiral perturbation theory*, *Eur. Phys. J.* **C29** (2003) 383–395, [[hep-lat/0208051](#)].
- [254] [CERN-TOV 06], L. Del Debbio, L. Giusti, M. Lüscher, R. Petronzio, and N. Tantalo, *QCD with light Wilson quarks on fine lattices (I): first experiences and physics results*, *JHEP* **02** (2007) 056, [[hep-lat/0610059](#)].
- [255] N. H. Fuchs, H. Sazdjian, and J. Stern, *How to probe the scale of (anti- q q) in chiral perturbation theory*, *Phys. Lett.* **B269** (1991) 183–188.
- [256] J. Stern, H. Sazdjian, and N. H. Fuchs, *What π - π scattering tells us about chiral perturbation theory*, *Phys. Rev.* **D47** (1993) 3814–3838, [[hep-ph/9301244](#)].

- [257] S. Descotes-Genon, L. Girlanda, and J. Stern, *Paramagnetic effect of light quark loops on chiral symmetry breaking*, *JHEP* **01** (2000) 041, [[hep-ph/9910537](#)].
- [258] V. Bernard, S. Descotes-Genon, and G. Toucas, *Chiral dynamics with strange quarks in the light of recent lattice simulations*, [arXiv:1009.5066](#).
- [259] [LHP 04], F. D. R. Bonnet, R. G. Edwards, G. T. Fleming, R. Lewis, and D. G. Richards, *Lattice computations of the pion form factor*, *Phys. Rev.* **D72** (2005) 054506, [[hep-lat/0411028](#)].
- [260] [QCDSF/UKQCD 06A], D. Brommel, *et. al.*, *The pion form factor from lattice QCD with two dynamical flavours*, *Eur. Phys. J.* **C51** (2007) 335–345, [[hep-lat/0608021](#)].
- [261] S. R. Amendolia *et. al.*, *A measurement of the space - like pion electromagnetic form factor*, *Nucl. Phys.* **B277** (1986) 168.
- [262] J. Bijnens, N. Danielsson, and T. A. Lähde, *Three-flavor partially quenched chiral perturbation theory at NNLO for meson masses and decay constants*, *Phys. Rev.* **D73** (2006) 074509, [[hep-lat/0602003](#)].
- [263] J. Bijnens, *Status of strong ChPT*, *PoS EFT09* (2009) 022, [[arXiv:0904.3713](#)].
- [264] [JLQCD 08A], E. Shintani, *et. al.*, *S-parameter and pseudo-Nambu-Goldstone boson mass from lattice QCD*, *Phys. Rev. Lett.* **101** (2008) 242001, [[arXiv:0806.4222](#)].
- [265] G. C. Branco, L. Lavoura, and J. P. Silva, *CP violation*, *Int. Ser. Monogr. Phys.* **103** (1999) 1–536.
- [266] G. Buchalla, A. J. Buras, and M. E. Lautenbacher, *Weak decays beyond leading logarithms*, *Rev. Mod. Phys.* **68** (1996) 1125–1144, [[hep-ph/9512380](#)].
- [267] A. J. Buras, *Weak Hamiltonian, CP violation and rare decays*, [hep-ph/9806471](#).
Published in *Les Houches 1997, Probing the standard model of particle interactions*, Pt. 1, 281-539.
- [268] T. Inami and C. S. Lim, *Effects of superheavy quarks and leptons in low-energy weak processes $K_L \rightarrow \mu\bar{\mu}$, $K^+ \rightarrow \pi^+\nu\bar{\nu}$ and $K^0 \leftrightarrow \bar{K}^0$* , *Prog. Theor. Phys.* **65** (1981) 297.
- [269] [Aubin 09], C. Aubin, J. Laiho, and R. S. Van de Water, *The neutral kaon mixing parameter B_K from unquenched mixed-action lattice QCD*, *Phys. Rev.* **D81** (2010) 014507, [[arXiv:0905.3947](#)].
- [270] J. Brod and M. Gorbahn, *ϵ_K at Next-to-Next-to-Leading Order: The Charm-Top-Quark Contribution*, *Phys. Rev.* **D82** (2010) 094026, [[arXiv:1007.0684](#)].
- [271] U. Nierste *private communication* (2010).
- [272] K. Anikeev *et. al.*, *B physics at the Tevatron: Run II and beyond*, [hep-ph/0201071](#).
- [273] U. Nierste, *Three lectures on meson mixing and CKM phenomenology, published in Dubna 2008, Heavy Quark Physics (HQP08), pp. 1-39*, [arXiv:0904.1869](#).

- [274] A. J. Buras and D. Guadagnoli, *Correlations among new CP violating effects in $\Delta F = 2$ observables*, *Phys. Rev.* **D78** (2008) 033005, [[arXiv:0805.3887](#)].
- [275] A. J. Buras, D. Guadagnoli, and G. Isidori, *On ϵ_K beyond lowest order in the operator product expansion*, *Phys. Lett.* **B688** (2010) 309–313, [[arXiv:1002.3612](#)].
- [276] D. Becirevic *et. al.*, *$K^0\bar{K}^0$ mixing with Wilson fermions without subtractions*, *Phys. Lett.* **B487** (2000) 74–80, [[hep-lat/0005013](#)].
- [277] [ALPHA 06], P. Dimopoulos, *et. al.*, *A precise determination of B_K in quenched QCD*, *Nucl. Phys.* **B749** (2006) 69–108, [[hep-ph/0601002](#)].
- [278] P. H. Ginsparg and K. G. Wilson, *A remnant of chiral symmetry on the lattice*, *Phys. Rev.* **D25** (1982) 2649.
- [279] [ALPHA 04], M. Della Morte, *et. al.*, *Computation of the strong coupling in QCD with two dynamical flavours*, *Nucl. Phys.* **B713** (2005) 378–406, [[hep-lat/0411025](#)].
- [280] [JLQCD 08], S. Aoki, *et. al.*, *B_K with two flavors of dynamical overlap fermions*, *Phys. Rev.* **D77** (2008) 094503, [[arXiv:0801.4186](#)].
- [281] [SWME 11], J. Kim, C. Jung, H.-J. Kim, W. Lee, and S. R. Sharpe, *Finite volume effects in B_K with improved staggered fermions*, [[arXiv:1101.2685](#)].
- [282] [RBC/UKQCD 10B], Y. Aoki, *et. al.*, *Continuum Limit of B_K from 2+1 Flavor Domain Wall QCD*, [[arXiv:1012.4178](#)].
- [283] [SWME 10], T. Bae, *et. al.*, *B_K using HYP-smearred staggered fermions in $N_f = 2 + 1$ unquenched QCD*, *Phys. Rev.* **D82** (2010) 114509, [[arXiv:1008.5179](#)].
- [284] [RBC/UKQCD 07A], D. J. Antonio, *et. al.*, *Neutral kaon mixing from 2+1 flavor domain wall QCD*, *Phys. Rev. Lett.* **100** (2008) 032001, [[hep-ph/0702042](#)].
- [285] [HPQCD/UKQCD 06], E. Gamiz, *et. al.*, *Unquenched determination of the kaon parameter B_K from improved staggered fermions*, *Phys. Rev.* **D73** (2006) 114502, [[hep-lat/0603023](#)].
- [286] [ETM 10A], M. Constantinou, *et. al.*, *BK -parameter from $N_f = 2$ twisted mass lattice QCD*, *Phys. Rev.* **D83** (2011) 014505, [[arXiv:1009.5606](#)].
- [287] [RBC 04], Y. Aoki, *et. al.*, *Lattice QCD with two dynamical flavors of domain wall fermions*, *Phys. Rev.* **D72** (2005) 114505, [[hep-lat/0411006](#)].
- [288] [UKQCD 04], J. M. Flynn, F. Mescia, and A. S. B. Tariq, *Sea quark effects in B_K from $N_f = 2$ clover-improved Wilson fermions*, *JHEP* **11** (2004) 049, [[hep-lat/0406013](#)].
- [289] A. Hasenfratz and F. Knechtli, *Flavor symmetry and the static potential with hypercubic blocking*, *Phys. Rev.* **D64** (2001) 034504, [[hep-lat/0103029](#)].
- [290] Y. Aoki *et. al.*, *Non-perturbative renormalization of quark bilinear operators and B_K using domain wall fermions*, *Phys. Rev.* **D78** (2008) 054510, [[arXiv:0712.1061](#)].

- [291] [ETM 09D], V. Bertone, *et. al.*, *Kaon oscillations in the Standard Model and beyond using $N_f = 2$ dynamical quarks*, *PoS LAT2009* (2009) 258, [[arXiv:0910.4838](#)].
- [292] [ALPHA 09], P. Dimopoulos, H. Simma, and A. Vladikas, *Quenched B_K -parameter from Osterwalder-Seiler $tmQCD$ quarks and mass-splitting discretization effects*, *JHEP* **07** (2009) 007, [[arXiv:0902.1074](#)].
- [293] [CP-PACS 08], Y. Nakamura, S. Aoki, Y. Taniguchi, and T. Yoshie, *Precise determination of B_K and light quark masses in quenched domain-wall QCD*, *Phys. Rev.* **D78** (2008) 034502, [[arXiv:0803.2569](#)].
- [294] [ALPHA 07], P. Dimopoulos, *et. al.*, *Flavour symmetry restoration and kaon weak matrix elements in quenched twisted mass QCD*, *Nucl. Phys.* **B776** (2007) 258–285, [[hep-lat/0702017](#)].
- [295] [JLQCD 97], S. Aoki, *et. al.*, *Kaon B parameter from quenched lattice QCD*, *Phys. Rev. Lett.* **80** (1998) 5271–5274, [[hep-lat/9710073](#)].
- [296] K. G. Wilson, *Confinement of quarks*, *Phys. Rev.* **D10** (1974) 2445–2459.
- [297] M. Lüscher and P. Weisz, *On-shell improved lattice gauge theories*, *Commun. Math. Phys.* **97** (1985) 59.
- [298] Y. Iwasaki, *Renormalization group analysis of lattice theories and improved lattice action: two-dimensional nonlinear $O(N)$ sigma model*, *Nucl. Phys.* **B258** (1985) 141–156.
- [299] T. Takaishi, *Heavy quark potential and effective actions on blocked configurations*, *Phys. Rev.* **D54** (1996) 1050–1053.
- [300] P. de Forcrand *et. al.*, *Renormalization group flow of $SU(3)$ lattice gauge theory: numerical studies in a two coupling space*, *Nucl. Phys.* **B577** (2000) 263–278, [[hep-lat/9911033](#)].
- [301] G. P. Lepage and P. B. Mackenzie, *On the viability of lattice perturbation theory*, *Phys. Rev.* **D48** (1993) 2250–2264, [[hep-lat/9209022](#)].
- [302] M. Lüscher, S. Sint, R. Sommer, P. Weisz, and U. Wolff, *Non-perturbative $O(a)$ improvement of lattice QCD*, *Nucl. Phys.* **B491** (1997) 323–343, [[hep-lat/9609035](#)].
- [303] L. Susskind, *Lattice fermions*, *Phys. Rev.* **D16** (1977) 3031–3039.
- [304] [MILC 99], K. Orginos, D. Toussaint, and R. L. Sugar, *Variants of fattening and flavor symmetry restoration*, *Phys. Rev.* **D60** (1999) 054503, [[hep-lat/9903032](#)].
- [305] [HPQCD 06], E. Follana, *et. al.*, *Highly Improved Staggered Quarks on the Lattice, with Applications to Charm Physics*, *Phys. Rev.* **D75** (2007) 054502, [[hep-lat/0610092](#)].
- [306] M. Creutz, *Why rooting fails*, *PoS LAT2007* (2007) 007, [[arXiv:0708.1295](#)].
- [307] P. Hasenfratz, V. Laliena, and F. Niedermayer, *The index theorem in QCD with a finite cut-off*, *Phys. Lett.* **B427** (1998) 125–131, [[hep-lat/9801021](#)].

- [308] M. Lüscher, *Exact chiral symmetry on the lattice and the Ginsparg-Wilson relation*, *Phys. Lett.* **B428** (1998) 342–345, [[hep-lat/9802011](#)].
- [309] D. B. Kaplan, *A Method for simulating chiral fermions on the lattice*, *Phys. Lett.* **B288** (1992) 342–347, [[hep-lat/9206013](#)].
- [310] V. Furman and Y. Shamir, *Axial symmetries in lattice QCD with Kaplan fermions*, *Nucl. Phys.* **B439** (1995) 54–78, [[hep-lat/9405004](#)].
- [311] H. Neuberger, *Exactly massless quarks on the lattice*, *Phys. Lett.* **B417** (1998) 141–144, [[hep-lat/9707022](#)].
- [312] P. Hasenfratz *et. al.*, *The construction of generalized Dirac operators on the lattice*, *Int. J. Mod. Phys.* **C12** (2001) 691–708, [[hep-lat/0003013](#)].
- [313] P. Hasenfratz, S. Hauswirth, T. Jorg, F. Niedermayer, and K. Holland, *Testing the fixed-point QCD action and the construction of chiral currents*, *Nucl. Phys.* **B643** (2002) 280–320, [[hep-lat/0205010](#)].
- [314] C. Gattringer, *A new approach to Ginsparg-Wilson fermions*, *Phys. Rev.* **D63** (2001) 114501, [[hep-lat/0003005](#)].
- [315] A. Hasenfratz, R. Hoffmann, and S. Schaefer, *Hypercubic smeared links for dynamical fermions*, *JHEP* **05** (2007) 029, [[hep-lat/0702028](#)].
- [316] C. Morningstar and M. J. Peardon, *Analytic smearing of SU(3) link variables in lattice QCD*, *Phys. Rev.* **D69** (2004) 054501, [[hep-lat/0311018](#)].
- [317] [BMW 08A], S. Dürr, *et. al.*, *Scaling study of dynamical smeared-link clover fermions*, *Phys. Rev.* **D79** (2009) 014501, [[arXiv:0802.2706](#)].
- [318] S. Capitani, S. Dürr, and C. Hoelbling, *Rationale for UV-filtered clover fermions*, *JHEP* **11** (2006) 028, [[hep-lat/0607006](#)].
- [319] R. Sommer, *A new way to set the energy scale in lattice gauge theories and its applications to the static force and α_s in SU(2) Yang-Mills theory*, *Nucl. Phys.* **B411** (1994) 839–854, [[hep-lat/9310022](#)].
- [320] C. W. Bernard *et. al.*, *The static quark potential in three flavor QCD*, *Phys. Rev.* **D62** (2000) 034503, [[hep-lat/0002028](#)].
- [321] **RBC** Collaboration, R. Arthur and P. A. Boyle, *Step Scaling with off-shell renormalisation*, [[arXiv:1006.0422](#)].
- [322] [MILC 07], C. Bernard, *et. al.*, *Status of the MILC light pseudoscalar meson project*, *PoS LAT2007* (2007) 090, [[arXiv:0710.1118](#)].
- [323] [CDH 05], G. Colangelo, S. Dürr, and C. Haefeli, *Finite volume effects for meson masses and decay constants*, *Nucl. Phys.* **B721** (2005) 136–174, [[hep-lat/0503014](#)].
- [324] G. Herdoiza *private communication* (2011).

- [325] R. Brower, S. Chandrasekharan, J. W. Negele, and U. Wiese, *QCD at fixed topology*, *Phys.Lett.* **B560** (2003) 64–74, [[hep-lat/0302005](#)].
- [326] O. Bär, S. Necco, and S. Schaefer, *The epsilon regime with Wilson fermions*, *JHEP* **03** (2009) 006, [[arXiv:0812.2403](#)].
- [327] T. Bunton, F.-J. Jiang, and B. Tiburzi, *Extrapolations of Lattice Meson Form Factors*, *Phys.Rev.* **D74** (2006) 034514, [[hep-lat/0607001](#)].
- [328] B. Borasoy and R. Lewis, *Volume dependences from lattice chiral perturbation theory*, *Phys.Rev.* **D71** (2005) 014033, [[hep-lat/0410042](#)].
- [329] S. Aoki, H. Fukaya, S. Hashimoto, and T. Onogi, *Finite volume QCD at fixed topological charge*, *Phys. Rev.* **D76** (2007) 054508, [[arXiv:0707.0396](#)].